DISSERTATION

The Oncostatin M receptor expression in epithelial cells
promotes intestinal inflammation

Die Expression des Oncostatin-M-Rezeptors in Epithelzellen
fördert die Entzündung des Darms

zur Erlangung des akademischen Grades
Doctor of Philosophy (PhD)

vorgelegt der Medizinischen Fakultät
Charité – Universitätsmedizin Berlin

von

Roodline Cineus

Erstbetreuer: Prof. Dr. Dr. Ahmed N. Hegazy
Datum der Promotion: 23. März 2024

Table of Contents

Abbreviations

ACD	Advanced cell diagnostics
AMPs	Antimicrobial peptides
APCs	Antigen-presenting cells
BSA	Bovine serum albumin
CD	Crohn's disease
DAMP	Damage-Associated Molecular Pattern
DAPI	4',6-Diamidino-2-Phenylindole
DC	Dendritic Cell
DSS	Dextran sulfate sodium
DSS	Dextran Sulfate Sodium
DTT	1,4-Dithiothreitol
EDTA	ethylenediaminetetraacetic acid
ELISA	Enzyme-Linked Immunosorbent Assay
Eomes	Eomesodermin
ERK	Extracellular signal-regulated kinases
FACS	Fluorescence-Activated Cell Sorting
FCS	Fetal calf serum
Foxp3	Forkhead Box P3
GALT	Gut-Associated Lymphoid Tissue
GATA3	GATA binding protein 3
GF	Germ Free
GFR	Growth factor reduced
GI	Gastrointestinal
GM-CSF	Granulocyte macrophage-colony stimulating factor
Gp130	Glycoprotein-130
GWAS	Genome-wide association study
HBSS	Hanks' Balanced Salt Solution
Hh	Helicobacter hepaticus
I.P.	Intraperitoneal
IBD	Inflammatory bowel disease
IEC	Intestinal epithelial cell
IESCs	Pluripotent intestinal epithelial stem cells
IFN-γ	Interferon-γ

Ig	Immunoglobulin
IL	Interleukin
ILCs	Innate lymphoid cells
ISH	*in situ* hybridization
JAK	Janus kinase
JNK	c-Jun N-terminal kinase
LGR5	Leu-rich repeat-containing G protein-coupled receptor 5
LIF	Leukemia inhibitory factor
LIFR	Leukemia inhibitory factor receptor
LP	Lamina Propria
LPMC	Lamina propria mononuclear cells
LTi	Lymphoid tissue inducer
mAb	Monoclonal Antibody
MHC	Major histocompatibility complex
NK	Natural killer
NOD2	Nucleotide-binding oligomerization domain-containing protein 2
OSM	Oncostatin M
OSMR	Oncostatin M receptor
PAMP	Pathogen-Associated Molecular Pattern
PBS	Phosphate-buffered saline
PI	Propidium iodide
PI3K	Phosphatidylinositol-3-kinase
PP	Peyer's patches
PRR	Pattern Recognition Receptor
PVDF	Polyvinylidene fluoride
RNA	Ribonucleic acid
RORα	RAR Related Orphan Recep
RORγt	RAR-related orphan receptor-γ
SCFA	Short-chain fatty acid
SDS-PAGE	Sodium dodecyl sulfate–polyacrylamide gel electrophoresis
SOCS3	Suppressor of Cytokine Signaling-3
STAT	Signal transducer and activator of transcription
T-bet	T-box expressed in T cells
TBST	Tris-buffered saline with Tween20
TCR	T cell receptor

TF	Transcription factor
TNFα	Tumor necrosis factor α
UC	Ulcerative colitis
UMAP	Uniform manifold approximation and projection
ZO1	Zonula occludens-1

List of figures

Zusammenfassung

Die intestinale Homöostase hängt vom Zusammenspiel zwischen der Darmmikrobiota, dem Epithel und den Immunzellen ab. Kürzlich wurde eine neue Rolle von Oncostatin M (OSM), einem entzündungsfördernden Zytokin, bei Entzündungen im Darm von Mäusen und Menschen entdeckt. Frühere Studien haben gezeigt, dass OSM ein entscheidender Faktor für chronische Entzündungen bei Anti-TNF-α-refraktärer Kolitis ist. Die bemerkenswerten Unterschiede in den Signal- und Verteilungsprofilen von OSM und OSMR erfordern weitere Untersuchungen in verschiedenen Zelltypen, um ihr klinisches und therapeutisches Potenzial zu bewerten. Daher wurde in dieser Arbeit die Rolle von OSM und OSMR bei der Darmentzündung durch die Kombination von In-vitro- und In-vivo-Techniken untersucht. Für die In-vivo-Modellierung der Krankheit wurde das *Helicobacter hepaticus* (*H.h.*) Colitis-Modell verwendet, da es sowohl immun- als auch dysbiosebedingte Aspekte der IBD vereint. So konnten wir die Expression von OSM und OSMR als Reaktion auf die Entzündung und in bestimmten Organen und Zelluntergruppen messen. Darüber hinaus zeigte diese Arbeit, dass die OSM-OSMR-Achse in Darmepithelzellen (IECs) während einer chronischen Darmentzündung von Bedeutung ist. In-vitro-Untersuchungen zeigten, dass IL-22 das zentrale Zytokin ist, das die OSMR in IECs induziert und aufrechterhält. Darüber hinaus zeigten In-vivo-Experimente mit *Il22*-defizienten Mäusen, *Villin^{creERT}* x *Il22ra1^{fl/fl}* -Mäusen sowie die Blockade von IL-22 eine erhebliche Verringerung der OSMR in Epithelzellen während der Kolitis und eine geringere Pathologie. Darüber hinaus ist die OSMR-Signalübertragung in IECs während der Entzündung von Bedeutung, da ihre Auslöschung die Darmentzündung reduziert. Darüber hinaus führen Dysregulationen des OSM-OSMR-Signalwegs bei entzündlichen Darmerkrankungen (IBD) zu verstärkter Leukozytenrekrutierung und -aktivierung, Geweberetention und Gewebeumbau. Insgesamt hat diese Arbeit gezeigt, dass der OSM-OSMR-Signalweg unterschiedliche transkriptionelle Reaktionen in IECs auslöst und dass eine

differenzierte Ausrichtung auf den OSMR-Signalweg ein potenzieller therapeutischer Ansatz bei IBD sein könnte.

Abstract

Intestinal homeostasis depends on the interplay between the gut microbiota, epithelium, and immune cells. A novel role of Oncostatin M (OSM), a pro-inflammatory cytokine, has recently been identified in mouse and human intestinal inflammation. Previous studies have shown OSM as a critical driver of chronic inflammation in anti-TNF-α-refractory colitis. The notable differences in the signaling and distribution profiles of OSM and OSMR required further investigation in different cell types to evaluate their clinical and therapeutic potential. Therefore, this work evaluated the role of OSM and OSMR in intestinal inflammation by combining *in vitro* and *in vivo* techniques. For *in vivo* modeling of the disease, the *Helicobacter hepaticus (H.h)* colitis model was used, as it combines both immune and dysbiosis-driven aspects of IBD. This allowed us to measure OSM and OSMR expression in response to inflammation and within specific organs and cell subsets. Furthermore, this work showed that the OSM-OSMR axis is relevant in intestinal epithelial cells (IECs) during chronic intestinal inflammation. *In vitro* investigations showed that IL-22 is the central cytokine inducing and maintaining the OSMR in IECs. Moreover, *in vivo* experiments using *Il22* deficient mice, *Villin^{creERT}* x *Il22ra1^{fl/fl}* mice, as well as blockade of IL-22 showed a substantial reduction of OSMR in epithelial cells during colitis and decreased pathology. Furthermore, OSMR signaling is relevant in IECs during inflammation, as eradicating it reduces intestinal inflammation. Additionally, dysregulations of the OSM-OSMR pathway in inflammatory bowel disease (IBD) lead to enhanced leukocyte recruitment and activation, tissue retention, and tissue remodeling. Collectively, this work showed that the OSM-OSMR pathway drives distinct transcriptional responses in IECs, and differential targeting of the OSMR might be a potential therapeutic approach in IBD.

1 Introduction

1.1 The immune system

All life forms must defend against microbial assaults to survive. Therefore, highly effective strategies were designed to limit microorganisms' invasion of the host. The immune system, a complex system regulated by multifaceted and intricate networks, was developed to target explicit microbial invaders directly. The immune system is composed of different cells and molecules that defend the host against infections and prevents collateral damage to the host while promoting wound healing, tissue homeostasis, and regeneration[1-3].

The immune system is divided into two main types of responses to invading pathogens. The first response is the innate immune response, which provides the hosts with immediate defense and uses innate lymphoid cells (ILCs), natural killer cells, phagocytic cells such as monocytes, neutrophils, and macrophages, as well as cells that release inflammatory mediators such as mast cells, basophils, and eosinophils[4, 5]. The innate immune system also composes of various molecular components such as complements, acute-phase proteins, and cytokines. The adaptive immune system provides the host with a precise response and memory to respond to subsequent exposure rapidly and vigorously. The adaptive immune responses involve antigen-specific B and T cells and specialized cells, known as antigen-presenting cells (APCs) that display the antigen to lymphocytes. The B lymphocytes secrete immunoglobulins, which are antigen-specific antibodies responsible for eliminating extracellular microorganisms[4-6].

Studies have shown that innate immunity instructs adaptive immunity by interacting with antigen-presenting cells and T cells. This interaction is an important process that occurs at several stages throughout the immune response and is essential for the restoration of homeostasis. Consequently, if not adequately balanced, an overproduction of immunoregulatory mediators may be deleterious to the host, while an underproduction of these immunoregulators will leave the host susceptible to infections[7-12].

1.1.1 The intestinal immune system

The gastrointestinal tract is a major site for immunological processes. It is characterized by copious dietary and bacterial antigens. The intestine contains a significant number of immune cells compared to other tissues in the body. It is also one of the most challenged as it is continually exposed to a variety of antigens and prospective immune stimuli. Notably, the intestine of a healthy host is home to various commensals that are indispensable for digestive processes and immunological functions[13-17]. Remarkably, the intestine has an efficiently regulated immune response that effectively promotes the appropriate protection and tolerance towards commensals and pathogens. However, upon dysfunction, the host is subjected to an inappropriate and injurious activation of the immune response that is represented by the inflammatory bowel diseases, such as ulcerative colitis, Crohn's disease, as well as celiac disease and the enterocolitides characterizing many rare immunological and genetic disorders[14, 16].

1.1.2 The anatomy and function of the intestines

The intestines consist of different segments that have distinct endoscopic appearances. The large and small intestines are in a continuous tube lined by one single layer of columnar epithelium[15, 18]. Combined, they stretch from the lower aperture of the stomach to the anus. The small intestine is separated into different segments: the duodenum, nearest to the stomach; the jejunum; and the ileum. The duodenum and the jejunum have long villi covered by surface epithelium with extensive brush borders comprised of microvilli embedded with digestive enzymes, which aid in the digestion and absorption of metabolites from the diet. These two segments are responsible for most of the digestive processes. Thus, these segments' damage contributes to celiac disease and leads to malnutrition, malabsorption, and protein leakage[15, 18-20]. The ileum consists of shorter villi and has lower levels of brush border enzymes. The ileum is responsible for the absorption of vitamin B12 and bile salts[19].

The large intestine, also known as the colon, begins at the cecum, which is labeled as the entry point. The remainder of the colon is divided into the ascending (proximal) colon,

the transverse colon, the descending (distal) colon, and the sigmoid colon[21]. Unlike the small intestine, the cecum does not contain any villi and functions as a reservoir for commensals involved in the fermentative digestion of complex carbohydrates indigestible in the small intestines[22, 23]. Of note, the villi are also absent from the different segments of the large intestine. The ascending and transverse colon are responsible for absorbing water and other vital nutrients from the indigestible material from the small intestine and the formation and solidification of stool[24, 25.] The primary function of the descending colon is to store feces, while the sigmoid colon contracts to aid in the movement of the stool into the rectum.

Moreover, the intestines can be divided into distinct cellular compartments involved in different physiological functions. The mucosa of the intestines comprises the epithelium (described further in section 1.3), lamina propria (LP), and muscularis mucosa[26]. These cellular compartments contain most immune cells and are predominantly responsible for immune response. Furthermore, the immune responses are initiated in gut-associated lymphoid tissue (GALT), which are organized structures such as Peyer's Patches, isolated lymphoid follicles, and crypto patches[27, 28]. Additionally, the GALT is the inductive site for initiating adaptive immune responses[27, 28].

1.1.3 The intestinal microbiota

The intestinal microbiota refers to the diverse community of microorganisms, including protozoa, fungi, viruses, archaea, and bacteria found in the colon[29, 30]. The adult human colon contains an incredible number of organisms, including ~10^{14} bacteria as well as viral and fungal species, resulting in a metagenome >100 larger than the host genome[30-33]. Importantly, the gut microbiota plays a vital role in the intestine's protection, development, and homeostasis. Exemplarily, commensal bacteria are recognized as essential for the breakdown, absorption, and storage of nutrients, modulation of immune responses, regulation of gut maturation and integrity, and the prevention of pathogenic bacterial growth[17, 29, 30, 32, 34]. Studies have demonstrated that in the absence of the microbiota, germ-free (GF) mice demonstrate abnormal development of the GALT and

multiple immune compartments, including LP T-cell populations[30, 35-37]. Therefore, preserving the relationship between the host and the gut microbiota is crucial for mucosal development and health, as perturbations to the microbiota-host interactions may lead to dysbiosis, which influences the pathophysiology of an increasing list of diseases, including inflammatory bowel disease[13, 38, 39].

1.2 Inflammatory bowel disease

Inflammatory bowel disease (IBD) is a term that refers to a group of complicated chronic and relapsing inflammatory diseases that destruct the gastrointestinal tract (GI)[40, 41]. IBDs such as Crohn's disease (CD) and ulcerative colitis (UC) are found predominantly in clinically immunocompetent individuals whose symptoms arise from a robust, cytokine-driven inflammation of the gut[40, 41]. Studies have shown that Crohn's disease can affect any part of the gastrointestinal tract; however, it more commonly affects the small bowel and colon with discontinuous ulceration. In addition, ulcerative colitis primarily affects the colon and rectum, with continuous mucosa inflammation[41, 42]. Previous data insinuated that Crohn's disease was a modified T-helper-1 (Th1) and Th17 disease with cytokines such as interleukin-6 (IL-6), IL-12, IL-17, IL-23, tumor necrosis factor (TNF), and gamma-interferon (IFN-γ)[40, 43-52]. Moreover, ulcerative colitis was described as Th2 driven with cytokines, IL-4 and IL-13, and the innate immune products TNF, IL-1β, IL-6, and chemokines[40, 43-52]. The commonality of both diseases is epithelial barrier dysfunction, resulting in luminal contents entering the lamina propria[26, 53-57]. Subsequently, this leads to dendritic cells activating the different inflammatory T cell types listed above and macrophages producing proinflammatory cytokines, which activate natural killer (NK) cells[40, 43-52, 26, 53-57]. All in all, these events result in the perpetuation of intestinal inflammation. To date, as the modulation of intestinal inflammation remains to be elucidated, single-cell technology is being used to discover novel cell types and their involvements in IBD[33, 58, 59]. Exemplarily, using Single-cell RNA-sequencing, Lee *et al.* showed that CD8+ T cell signature was associated with increased disease severity by transcriptionally profiling circulating T cells isolated from patients with IBD[60].

IBD is vastly prevalent in western countries; however, an accelerated increase in its incidence has been reported in Asia. IBD is gradually emerging and spreading in both developed and developing countries[44, 61]. Though the exact cause of IBD is unknown, a combination of genetics, environmental factors, and the immune system is believed to be the triggers for the inflammation in the GI tract[40, 44, 61, 62]. Of note, the family aggregation has been recognized as a factor found predominantly in Crohn's disease rather than ulcerative colitis. In Crohn's disease, first-degree relatives of individuals affected are found to be approximately five folds or higher at risk of being affected[52, 62-64]. In addition, genome-wide association (GWA) studies for IBD susceptibility loci have identified a few genes that contribute to disease susceptibility. Specific mutations in the nucleotide-binding oligomerization domain-containing protein 2 (NOD2) gene, also labeled CARD15 and IBD1, were identified and associated with increased susceptibility to Crohn's disease[44, 65]. While the NOD2 gene does not increase the risk of ulcerative colitis, GWA studies have shown that some epithelial barrier genes, such as LAMB1, ECM1, HNF4A, CDH1, and GNA12, are explicitly associated with ulcerative colitis[44, 66-70].

1.2.1 Treatments for inflammatory bowel disease

Though IBD is a multifactorial disorder with unknown etiology, it is clear that immune dysregulation contributes strongly towards inflammation. Although there are currently no curative therapies for IBD, conventional treatments are aimed at reducing inflammation. Small molecules such as aminosalicylates decrease the inflammation of the inner wall, while corticosteroids, which are non-selective systemic anti-inflammatory therapies, are used to reduce the aberrant production of cytokines[71-76]. Both therapeutic strategies effectively suppress acute intestinal inflammation and resolve symptoms; however, they cannot reduce IBD long-term or promote mucosal healing after damage[71-76].

One of the newer treatments of IBD that has yielded some successful outcomes is the anti–TNF-α antibodies which target the general inflammatory cytokine, TNF-α[65, 77, 78].

Though this therapy has aided in controlling IBD, it is essential to note that the loss of efficacy limits the therapy, and a specific subset of patients is refractory. Studies have shown that patients with IBD have a clear breakdown of the symbiotic relationship between their intestinal commensal microflora and their mucosal immune system[77]. In addition, one of the characteristics of IBD is the defect of the epithelial barrier. The mucin-producing cells known as goblet cells have reportedly been depleted in both forms of IBD[54, 55, 57, 79, 80]. Notably, proinflammatory cytokine signaling furthers the breaking of the epithelial layer, which promotes and enhances the perpetuation of inflammation. A complete remission of IBD requires both the disappearance of inflammation and the repair of the damaged epithelium. Therefore, it is crucial for emerging therapies for IBD to not only focus on significant effector cytokines but also to consider the regeneration of the intestinal epithelium.

1.2.2 Models to study inflammatory bowel disease

A lot of the progresses in the understanding of different etiological factors and mechanisms regulating intestinal homeostasis and inflammation has been achieved through the usage of various animal models. In the case of IBD, a variety of models can be used to recapitulate some clinical aspects of the disease in humans[81, 82]. While these models represent a crucial source of information about biological systems, they do not fully represent the complexity of IBD in humans. Nevertheless, they are essential for understanding underlying mechanisms involved in the initiation and perpetuation of intestinal inflammation, as well as the validity of emerging therapeutics[82]. These models are classified into different groups: there are the chemically induced models (e.g., DSS (dextran sulfate sodium) or TNBS (trinitrobenzene sulfonic acid) colitis), the spontaneous models (IL-10 deficiency), the cell-transfer model (e.g., T cell transfer), and infection models (e.g., *Citrobacter rodentium, Helicobacter hepaticus*)[81-88]. In this thesis I used the *Helicobacter hepaticus* model of colitis.

1.2.3 *Helicobacter Hepaticus* model of colitis

Helicobacter hepaticus (*H.h*), a microaerobic gram-negative spiral bacterium, was first isolatedin the early 1900s in the liver of A/JCr mice[89, 90]. The primary colonization sites of *H.h* is the cecum and proximal colon. Though *H.h* can colonize wild-type mice without causing inflammation, it can induce chronic typhlitis, colitis, and rectal prolapse in immunodeficient strains such as *129Rag^-/-* and *Rag^-/-* mice[86, 87, 91]. Thus, *H.h* is a provocateur for inflammatory reactions against endogenous microbiota. Though *H.h* leads to typhlocolitis in IL-10-deficient mice[87, 91], this model takes several months to manifest colitis, making it unsuitable for large-scale studies. Interestingly, oral infection of C57BL/6 mice with *H.h* did not cause inflammation, and mono-colonization of germ-free IL-10-deficient mice does not induce intestinal inflammation, highlighting that different flora components are required for disease induction[92,93]. In 2006, Kullberg *et al.* demonstrated that infection of C57BL/6 mice with *H.h* and concurrent blockade of IL-10 signals with a monoclonal antibody against IL-10R lead to chronic intestinal inflammation[87]. The authors showed that the inflammation in this model was driven by IL-23 and not IL-12 for the development of maximal pathology[87]. Notably, the inflammation is characterized by increased IL-17A and IFN-γ in the mucosal[87, 94]. Importantly, histological assessment of this model depicts goblet cell depletion, leukocyte infiltration, epithelial cell hyperplasia, submucosal immune cell infiltration, and edema (**Figure 1**).

This model of colitis allows the study of effector pathways as it occurs in mice with normal innate and adaptive cells. However, there are evident difficulties in dissecting the role of specific cellular populations. Therefore, the cell conditional genetic knockouts or antibody-mediated ablation of cell types should be combined to understand fundamental pathways involved in disease development.

A
Steady state

B
H. hepaticus + αIL-10R

Epithelial hyperplasia + globlet cell depletion

LP infiltration

Crypt abscess

Submucosal inflamation

Magnification:10x
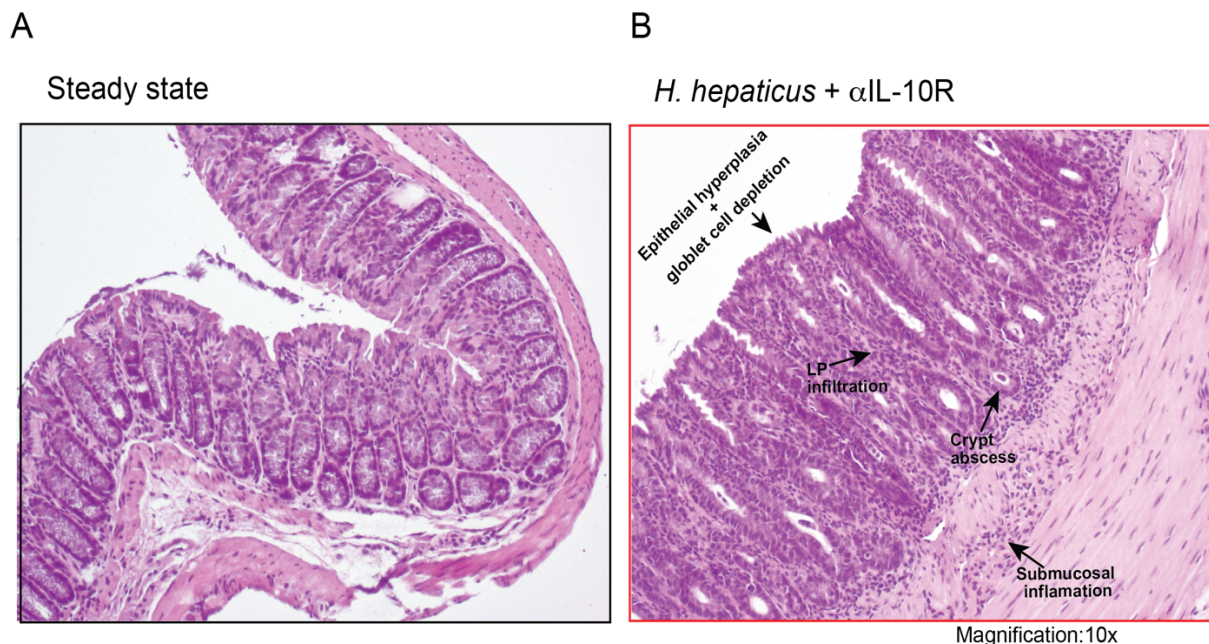
Figure 1: Representative hematoxylin/eosin (H&E)-stained sections of the colon. (A) C57BL/6 wild-type mice at steady state with an intact epithelium. (B) C57BL/6 wild-type after 14 days of H.h + α-IL10R induced colitis. Arrows mark submucosal inflammatory cell infiltrates, LP infiltration, crypt abscess, epithelial hyperplasia, and goblet cell depletion. Original magnification 10X. Pictures originate from the experiments carried out in this thesis.

1.3 The intestinal epithelium

The intestinal epithelium is lined by a single layer of columnar intestinal epithelial cells (IECs) that forms a physical barrier between the intestinal lumen and connective tissue[26, 95]. The main functions of the epithelium are to filter luminal contents and allow for their translocation into the circulation and to maintain and regulate the interaction of commensal or pathogenic microbial communities and mucosal immune by forming a barrier[10-14]. Moreover, IECs can sense and respond to microbial stimuli by secreting a variety of antimicrobial peptides to reinforce the barrier function and aid in the coordination of immune responses.

The IECs are continuously replaced/renewed every 4-5 days by pluripotent intestinal epithelial stem cells (pluripotent IESCs) that reside in the base of crypts[15, 16]. These stem cells are long-lived Leu-rich repeat-containing G protein-coupled receptor 5 (Lgr5)

positive stem cells[15, 16]. They give rise to transit-amplifying cells known as progenitors that differentiate into mature IECs types. Each of these differentiated epithelial cell subtypes holds specific functions in maintaining homeostasis; these include absorptive enterocytes, goblet cells, enteroendocrine cells, paneth cells (of the small intestine), tuft cells, and microfold cells (M cells)[54, 57].

These IECs have distinct functions within the epithelium. Exemplarily, the secretory IECs consist of enteroendocrine, goblet, and paneth cells. The enteroendocrine cells are essential to link the central and enteric neuroendocrine systems by secreting various hormone regulators for digestive functions. The goblet and paneth cells are involved in the luminal secretion of mucins and antimicrobial proteins (AMPs) to generate and maintain a physical and biochemical barrier to microbial contact with the epithelial surface and underlying immune cells[10, 12, 13, 17, 18]. Tuft cells serve as a sensor for lumenal contents, while M cells are responsible for the delivery of antigens directly to intraepithelial lymphocytes and the subepithelial lymphoid tissues[10, 12, 13, 17, 18].

1.3.1 The intestinal barrier

The first physical barrier pathogens encounter is the mucus layer. This layer is a hydrated mucus gel that covers the mucosal surface and protects the epithelial cells against digestive enzymes, microbial, and mechanical insults[10, 12, 13]. This layer protects the gastrointestinal tract by minimizing the interactions between the epithelium and commensal bacteria. The mucus layer is formed through the production of mucin glycoproteins produced by goblet cells, primarily by mucin 2 (MUC2)[26, 35, 96-99]. Of note, MUC2 is the most abundant of the mucins and is crucial in the organization of the intestinal mucous layers at the epithelial surface of the colon. Interestingly, studies have shown that MUC2-deficient mice develop spontaneous colitis and are predisposed to inflammation-induced colorectal cancers[100-102].

Furthermore, the protective mucus layer contains not only AMPs but also secretory IgA that aids in forming a matrix to prevent penetration of the barrier by intestinal microbes[18, 27, 35, 36]. In addition, the IECs express pattern recognition receptions (PRRs) that allow

the direct sensing of microbes. These PRRs include Toll-like receptors (TLRs) and nuclear oligomerization domain (NOD)-like receptors (NLRs) that recognize pathogen-associated molecular patterns (PAMPs) such as lipopolysaccharide, flagella, peptidoglycans, and microbial nucleic acids, as well as damage-associated molecular patterns (DAMPs) release in response to tissue injury or stress[35, 37-39]. These signals are essential for the IECs, as defects in the PRRs or PRR signaling lead to bacterial translocation and altered microbiota composition, which alter intestinal homeostasis.

Moreover, the intestinal barrier is made of a single layer of polarized IECs which creates a physical barrier. The adjacent epithelial cells are joined together by the apical junction complex (AJC), consisting of tight junctions (TJ) and adherens junctions[79, 103]. The tight junctions are the most apical structure of the apical complex and consist of various integral proteins such as claudins, occludins, and zonula occludens (ZO-1, ZO-2)[104, 105]. The TJ is responsible for maintaining the integrity of the epithelial barrier by regulating the paracellular transport of ions, metabolites, and macromolecules and thus controlling the flux of the intestinal elements[95, 99, 103-105].

1.3.2 The repair mechanism of the epithelium

It is evident that the IECs are barraged with stressful factors such as, cytotoxic and pathogenic stresses. These stresses often trigger apoptotic and cell death pathways, which consequently lead to gut barrier damage and inflammatory responses. Moreover, the ability of the intestinal epithelium to maintain a functional barrier is crucial in preserving host homeostasis. The IECs must be able to rapidly reestablish the sealing of the epithelial barrier following physiological damages to prevent extensive destruction that may lead to uncontrolled immunological responses.

The epithelial repair response can be divided into three main steps[35, 54, 55, 106]. Firstly, in the acute phase, the adjacent epithelial cells migrate to the site of injury to cover the affected area. This is known as the restitution phase and does not require cell proliferation. In this phase, the epithelial cells that migrate into the open area of the injury or ulcer dedifferentiate, reorganize their cytoskeleton and re-distribute to restore the

barrier integrity. The restoration phase is the most rapid response after injury and is modulated by various factors, including cytokines[55, 107], cell adhesion molecules[55], and growth factors[55, 108]. Secondly, after the restitution phase, epithelial cell proliferation is essential for replenishing the epithelium[107-109]. In this phase, the crypts' elongation and division near the injury are observed. The proliferation of the epithelial cells is promoted by various growth factors secreted from the mesenchymal cells and the local epithelial cells[55, 106]. The proliferation phase is crucial for progenitor cells' efficient and rapid expansion. Lastly, following the expansion/ proliferation phase, the appropriate lineage decision and maturation of the epithelial cells are needed to maintain the numerous functional activities of the mucosal epithelium[55, 106].

Collectively, it is evident that precise regulation of barrier function is a prerequisite for a healthy host. IECs have diverse functions which protect the host from infections and exposure to stimuli. However, in various diseases such as IBD, damage and impairment of the intestinal barrier occurs as recruited leukocytes interact directly with the epithelium, releasing inflammatory mediators and furthering the damage. This highlights the rancorous cycle between barrier dysfunction and inflammatory effects, which contributes to the perpetuation and aggravation of chronic inflammation in the intestines[17, 26, 54, 55, 57, 80, 110]. Recent evidence suggests that some inflammatory cytokines, such as IL-22, associated with barrier function can paradoxically contribute to intestinal inflammation and further induce barrier damage. Thus, furthering our knowledge in understanding the mechanisms that promote or prevent epithelial damage will help in the development of therapies to improve barrier function and mucosal healing in IBD.

1.3.3 Intestinal organoids as *in vitro* model

The advancement of all biosciences must have reliable and acute *in vitro* and *in vivo* models. Culturing primary intestinal epithelial cells has been challenging in recent years as IECs would undergo anoikis (a form of programed cell death) rapidly following isolation. In 2009, Sato *et al*. established a platform that simplified the process of growing and maintaining intestinal crypt cultures known as organoids[111]. Organoids are defined

as miniature organs grown *in vitro*, originating from stem cells. They can self-organize in 3D clusters and maintain the originating organ's functionality and molecular and cellular heterogeneity. Intestinal organoids, also known as mini-gut, are derived by culturing crypt-like domains consisting of intestinal stem cells (ISCs)-expressing Lgr5 (**Figure 2A**)[111, 112]. Remarkably, intestinal organoids have the capability to mimic the structure and cellular composition of a functional intestinal epithelium.
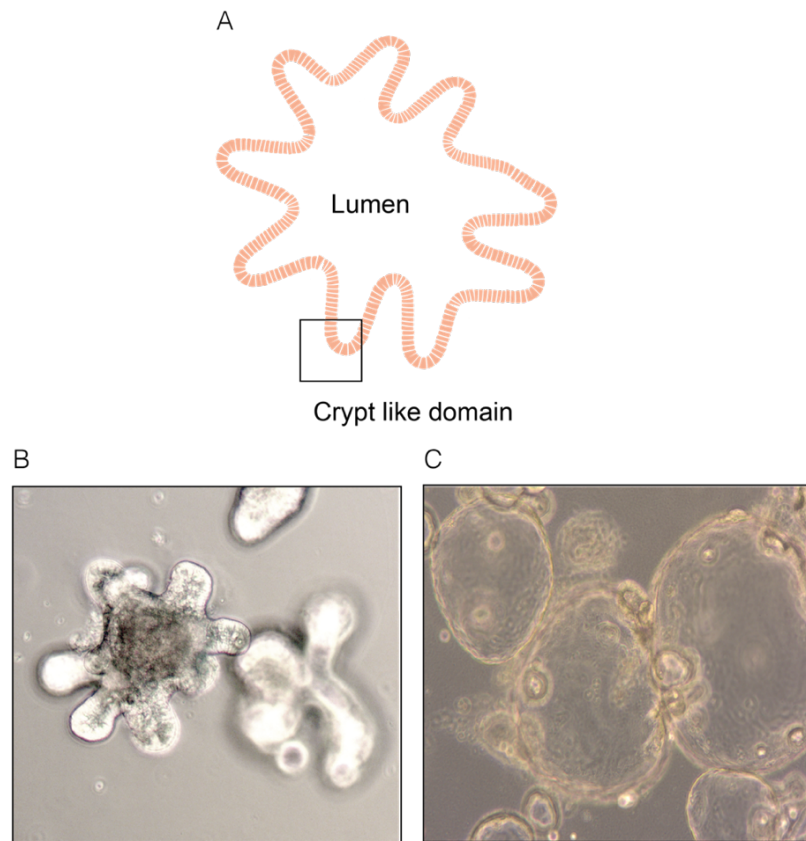
Figure 2: Scheme of an organoids. (A) Scheme of a small intestinal mature organoid depicting the lumen at the center of the epithelial monolayer with the budding of the crypt like domains. (B) A representative bright-field image of mouse small intestinal organoids after 4 days and of (C) human colon organoids after 7 days. Pictures originate from organoids culture generated for this thesis.

The Organoid technology creates a novel way of modeling and studying the molecular pathogenesis of diseases such as IBD. With this technology, stem cells and biopsies from human tissues can be used to study IECs. Upon embedment in Matrigel™, a soluble basement membrane matrix that resembles the laminin/collagen IV-rich basement membrane extracellular environment found in many tissues, these organoids will self-assemble with the luminal surface of epithelium being in the center of the organoid while the basolateral side is on the outside (**Figure 2B/C**)**.**

Though the organoid system is a massive breakthrough in research and is helpful in studying the complexities of the intestinal epithelium during homeostasis and disease states, this model has some limitations. The structure of the organoids creates a challenge in exposing the apical aspect to experimentation[113]. Additionally, it is harder to capture the interactions of other cell types to the luminal side of the epithelium as this is in the center of the organoid. Though techniques such as using a micromanipulator and microinjection are used to solve this problem, they are time-consuming[113, 114]. Another significant drawback is the absence of the immune element needed to understand the mechanisms driving intestinal inflammation during CD and UC *in vivo*. It is evident that there are some drawbacks to this technique; however, organoids are still advantageous models for studying diseases. Encouragingly, intestinal organoids can support the host's genetic profile *in vitro* stably and can be maintained in long-term culture. Therefore, organoids can be used for drug discovery and provide a unique perspective into the progress of personalized medicine.

1.4 The role of cytokines in homeostasis and inflammation

Cytokines are soluble extracellular proteins or glycoproteins and are one of the essential messenger molecules produced by the immune response to protect the host from injury, inflammatory agents, or microbial invasion. Cytokines are produced by both the innate and adaptive immune cells and regulate the biological functions of target cells through autocrine or paracrine mechanisms. Cytokines have indispensable functions in infection, inflammation, autoimmunity, cancer, and repair processes to restore homeostasis[7].

There are several types of cytokines, including chemokines, interferons, interleukins, lymphokines, and tumor necrosis factors. Cytokines can act synergistically or antagonistically and are redundant in their actions, implicating that similar functions can be stimulated by different cytokines[11, 12, 115]. They are often produced in a cascade and can be classified based on the essence of the immune response. In addition, individual cytokines perform specific roles based on cell type and location, stimulating their target cells to make additional cytokines[10].

Cytokines are classified into two categories, pro-inflammatory cytokines and anti-inflammatory cytokines. The pro-inflammatory cytokines are necessary mediators for an anti-infectious response. However, an exacerbated production of these pro-inflammatory cytokines may be lethal and linked with poor outcomes in human diseases such as inflammatory bowel disease (IBD)[11, 116]. On the contrary, anti-inflammatory cytokines are responsible for controlling the cascade of pro-inflammatory mediators[117, 118]. However, excessive production is associated with severe immune depression that also leads to poor outcomes in patients following trauma, making it clear that a given cytokine's amount influences its properties[12, 117, 118]. Moreover, pro-inflammatory cytokines are produced mainly by activated macrophages and participate in the upregulation of inflammatory reactions[12, 53].

Some of the vital pro-inflammatory cytokines are IL-1, IL-6, TNF, IFN-γ , IL-12, IL-18α, transforming growth factorβ (TGFβ) and granulocyte-macrophage colony-stimulating factor (GM-CSF)[10-12, 117] . On the other hand, anti-inflammatory cytokines are produced by various cells, including macrophages, T helper cells, and mast cells[11, 119]. Anti-inflammatory cytokines provide sufficient control over pro-inflammatory activities. Some anti-inflammatory cytokines are IL-4, IL-10, IL-13, interferon alpha (IFNα), and TGFβ[7, 10-12, 117, 120]. These cytokines have the ability to inhibit the release of pro-inflammatory cytokines by inducing the production of IL-1 receptor antagonist (IL-1ra) and the release of soluble TNF receptor (sTNFR), which in turn limit the pro-inflammatory activities of IL-1 and TNF[117].

Notably, a dynamic and capricious balance must exist between proinflammatory and anti-inflammatory cytokines to achieve control without inducing excessive damage to the host[10, 11, 121, 122]. Therefore, it is pivotal to identify and understand contextual drivers underlying the physiological cytokine responses in human diseases such as IBD to lessen the detrimental immunopathology in suffering patients.

1.5 The role of Oncostatin M

Oncostatin M (OSM) is a secreted glycoprotein that was first biochemically characterized from serum-free supernatant of U-937 histiocytic lymphoma cells in 1986[123, 124]. OSM is a multifunctional cytokine belonging to the IL-6 cytokine family that includes IL-6, leukemia inhibitory factor (LIF), IL-11, ciliary neurotrophic factor, cardiotrophin-1, and neutrophin-1/B-cell–stimulating factor-3[125, 126]. OSM is associated with multiple biological processes and cellular responses, including hematopoiesis, bone remodeling, differentiation, as well as chronic inflammatory conditions[125, 126].

1.5.1 Oncostatin M signaling and production

OSM displays the broadest signaling profile out of all the IL-6-type cytokines studied thus far. OSM activates the Janus kinase/signal transducer and activator of transcription (JAK/STAT), the mitogen-activated protein kinases ERK1/ERK2, the stress-activated protein kinases p38 and c-Jun N-terminal kinase (JNK), the phosphatidylinositol-3-kinase (PI3K)/Akt, and the protein kinase C delta pathways[126-128]. In addition, STATs 1, 3, and 5 are also phosphorylated and translocate to the nucleus, where they control transcription of diverse target genes. Consequently, STAT3 and ERK1/2 phosphorylation can drive the expression of suppressor cytokine signaling-3 (SOCS3), negatively regulates OSM (**Figure 3**)[126-128]. These biological activities of OSM are induced upon binding to receptor complexes that are dependent on glycoprotein-130 (gp130). Notably, OSM binds gp130 with low affinity ; thus, the recruitment of a second receptor chain is essential for its biological activities[126, 127]. OSM forms two distinct heterodimers of gp130 with either leukemia inhibiting factor receptor (LIFR) or OSM receptor-beta (OSMR β)[128, 129].
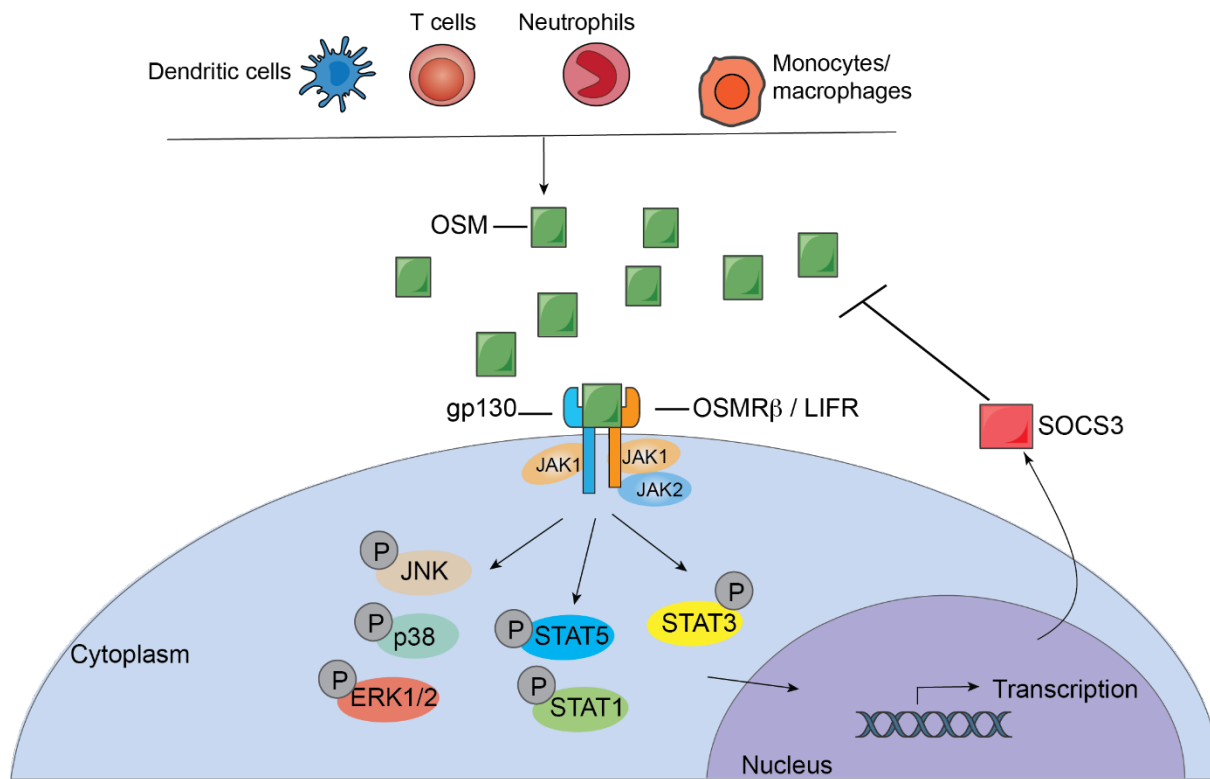
Figure 3: OSM production and signaling. OSM is largely produced by hematopoietic cells. OSM-Induced signal transduction through the OSMR-gp130 or the LIFR-gp130 Receptor Complex. Once connected, OSM triggers activation of Jak1 and Jak2, which leads to further phosphorylation of ERK1/2, JNK, p38, STAT1, STAT3, and STAT5. The STATs 1, 3, and 5 phosphorylate and translocate to the nucleus, controlling the transcription of diverse target genes. Notably, STAT3 and ERK1/2 are both drivers of SOCS3, which negatively regulates OSM-induced signaling. Figure adapted from West et al, 2018 [126].

The gp130/LIFR complex is known as the OSM receptor type I, while the gp130/OSMRβ complex as the OSM receptor type II in the human system[130, 131]. Studies have shown that the order of the complexes does not reflect a biological hierarchy, rather the date of discovery[130, 131]. The signaling of the type I and type II receptors are qualitatively distinctive and contribute to the specific effects of OSM in different tissues and cellular microenvironments. The OSM receptor is widely expressed in both tissue (heart, lung,

adipose tissue, skin, bladder, mammary tissue, adrenal gland, and prostate gland (GTExRNA-seqdataset: https://www.gtexportal.org/home/gene/OSMR) and cellular levels (epithelial, endothelial, smooth muscle cells, fibroblasts, and many tumor cell lines)[126]. In addition, OSM is produced largely from hematopoietic cells, including activated T cells, monocytes, dendritic cells, neutrophils, activated mast cells, and eosinophils (**Figure 3**)[132]. Notably, OSM expression is also regulated by PRRs. Exemplarily, the stimulation of human dendritic cells with lipopolysaccharide (LPS) or whole bacteria results in the secretion of a considerable amount of OSM [126].

Interestingly, unlike the human OSM, which activates both OSMRβ and LIFR, the mouse OSM ligand does not signal through the mouse LIFR but signals only through its specific murine OSMRβ. This indicates functional dissimilarities in the OSM biochemistry and functional differences in its biology between humans and mice[123, 125-127].

1.5.2 OSM a novel cytokine in inflammatory bowel disease pathogenesis

Dysregulations of both OSM and OSMR expression have been associated with different diseases. Many studies have explored OSM functions in cancer, bone metabolism, liver regeneration, chronic inflammation, and cardiovascular diseases. For example, a gain in the OSMR gene has been associated with worse clinical outcomes in cervical squamous cell carcinoma[127]. Furthermore, high OSM levels have been detected in various inflammatory diseases in humans, including rheumatoid arthritis, atherosclerosis, and inflammatory bowel disease[123, 125-127].

Although the exact etiology of IBD has not yet been unraveled, a complex interplay between multiple pathogenic factors contributes to IBD pathophysiology. A breakthrough study by West *et al*. identified OSM and OSMR expression in IBD patients as predictive biomarkers for anti-TNF responsiveness in IBD[132]. The authors identified that the manifestation/expression of OSM in the intestinal fibroblast, specifically, stroma cells was strongly correlated with the presence and severity of intestinal inflammation in IBD versus healthy controls. In addition, the authors demonstrated that compared to non-IBD controls, IL-6, IL-1α, IL-1β, and OSM were the four cytokines that were significantly

enriched in the inflamed tissue of the UC and CD patient cohorts. Since OSM was one of the cytokines that was the least described in the gut, the authors studied its role in IBD. They confirmed that, relative to the healthy colonic mucosa, in IBD patients, OSM was the most highly and consistently expressed cytokine. Moreover, West *et al*. observed that the increased levels of OSM and OSMR were associated with an upregulation of various gene clusters related to leukocyte recruitment, highlighting the importance of the OSM-OSMR axis in IBD pathogenesis[132]. Furthermore, they used the *H.h* model of colitis to confirm the findings from the human study. The data showed that inflamed mice had significantly increased OSM and OSMR expression compared to the wild-type control mice. Notably, OSM expression and numbers of OSMR-positive stromal cells expressing pro-inflammatory cytokines such as IL-1β and IL-6 were also increased in *H.h* treated mice compared to the steady state controls, which was consistent with the observations in the human samples. Moreover, human stroma cells increased the expression of pro-inflammatory chemokines in response to OSM, and the addition of TNF further increased this response. This finding suggested that the binding of OSM to its receptor on the stromal cells triggered pro-inflammatory synergism, contributing to increased intestinal pathology. Respectively, during late-phase inflammation, OSM-deficient mice demonstrated significantly less intestinal pathology in response to *H.h*–induced colitis compared to OSM-sufficient mice, highlighting the importance of OSM and OSMR for propagating inflammation and development of chronic disease[126, 132].

In contrast, a study by Biegel *et al.* has shown that OSM and OSMR are important in IBD since they promote STAT-3-dependent intestinal cell epithelial proliferation and wound healing[133]. The authors argued that OSM is essential in epithelial repair and modulating a barrier-protective host response in intestinal inflammation. However, these results were generated using transformed epithelial cell lines and not primary cells lines. This suggests that the actions of OSM are complex and depend on specific tissue and cell types. Moreover, the exact function and mechanism of action of OSM in IBD are undefined. Notably, there is little data on the regulation of OSMR receptor expression,

its signal transduction, and its specific biological functions in IECs. Taking together OSM's different signaling and distribution profiles, further investigations are required to analyze its clinical and therapeutic potential.

1.6 The role of IL-22

IL-22 is part of the IL-10 cytokine family, which comprises nine members and is divided into three subgroups based on their biological functions. The first group contains IL-10, whose main function primarily is to repress excessive inflammatory responses. The second group is the IL-20 subfamily cytokines, composed of IL-19, IL-20, IL-22, IL-24, and IL-26 [43, 134]. This group of cytokines is responsible for enhancing tissue remodeling and wound healing to aid in supporting and restoring homeostasis of epithelial layers during infection and inflammatory responses. Lastly, the third group is the type III IFN group which contains IL-28A, IL-28B, and IL-29 also referred to as IFN-λ2, IFN-λ3, and IFN-λ1[43, 134-138]. These cytokines are responsible for the induction of antiviral responses and act on epithelial cells[43, 134-138].

1.6.1 The production of IL-22

IL-22 is mainly produced by lymphocytes. Studies have shown that Th17 CD4⁺T cells can express both IL-17 and IL-22. Intriguingly, Th22 CD4⁺T cells can express IL-22 without producing IL-17. Other cells such as CD8⁺T cells, TCR γδ T cells, dendritic cells (DCs), neutrophils, NK cells, and group 3 innate lymphoid cell (ILC) populations, including ILC3 and lymphoid tissue inducer (LTi) cells are also producers of IL-22 (**Figure 4**)[43, 138-144]. IL-22 production by CD4⁺ cells is mediated mainly by proinflammatory cytokines such as IL-23, IL-6, TNFα, IL-1β, TGFβ, and IL-17[43, 134, 136, 139, 141, 145, 146]. Additionally, signal transducer and activator of transcription (STAT) 3, RAR-related orphan receptor (ROR)γt and aryl hydrocarbon receptor (AhR), and T regulatory cells (Tregs) are also known to regulate IL-22 expression[134, 138, 147, 148]. Notably, in Th17 cells, TGFβ, in the presence or absence of IL-6, plays an essential role in the production of both IL-17 as well as IL-22. While the presence of TNF-α and IL-6 leads naïve T cells to differentiate into Th22 cells to produce IL-22[43, 141, 149].
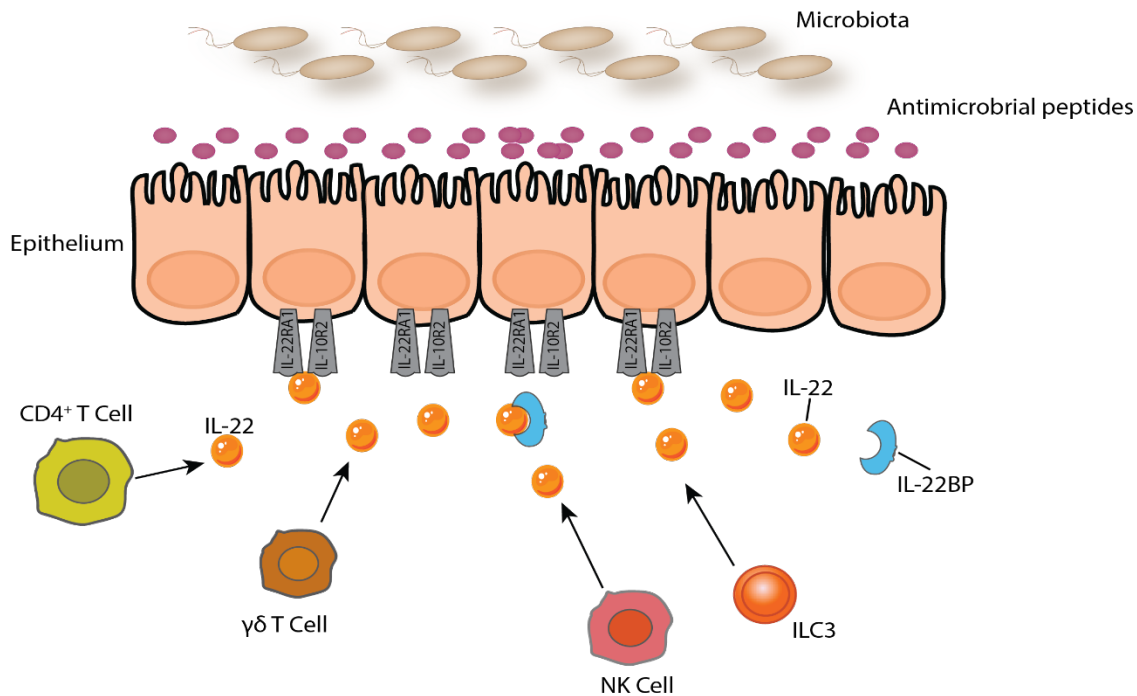
Figure 4: Scheme depicting IL-22 production and regulation. *An overview of the cells that produces IL-22 such as CD4+ and γδ T cells as well as NK cells and ILC3s. IL-22 acts on the intestinal epithelial cells and releases of antimicrobial peptides (AMPs), regulating the microbiota, and maintaining gut barrier homeostasis. Figure adapted from Parks et al, 2016 [150].*

1.6.2 IL-22 signaling

IL-22 signaling is through a heterodimeric receptor consisting of IL-22Rα1 and IL-10Rβ2 (**Figure 4-5**) The IL-22RA1 subunit is also used by IL-20 and -24, while the shared IL-10RB subunit is also used by IL-10 and -26, and IFNλ[43, 134, 135, 137, 138]. Interestingly, IL-22 must first bind the IL-22Rα1 subunit, which would lead to conformational changes that would allow the complex to bind to the IL-10Rβ2 subunit[151]. In addition, IL-22BP, also known as IL-22RA2, has been identified as the secreted IL-22R homolog that binds to IL-22 with high affinity to neutralize its activity (**Figure 4-5**)[135, 139, 144, 152]. Furthermore, upon binding, IL-22 induces the phosphorylation of the Jak1 and Tyk2 kinases as well as the STAT1, STAT3, and STAT5 transcription factors. Notably, IL-22 also activates the protein kinase B (AKT)/ mechanistic target of rapamycin(mTOR) and MAPK pathways[135,

[138, 141, 147, 148]. However, STAT3 signaling is the main signaling pathway involved in IL-22 activity on epithelial cells (**Figure 5**). Upon activating of the Jak-STAT signal transduction pathway, IL-22 can induce the production of antimicrobial peptides, as well as anti-apoptotic and proliferative pathways, to assist in the prevention of tissue destruction and aid in the repair and restoration of epithelial homeostasis. IL-22 is a potent inducer of antimicrobial peptides, including lipocalin-2, RegIIIβ (regenerating islet-derived protein 3), RegIIIγ , and mucins , as well as antimicrobial proteins (AMPs), such as the S100proteins, which are a vital part of host defense[135, 138, 139, 143, 144, 153-155].
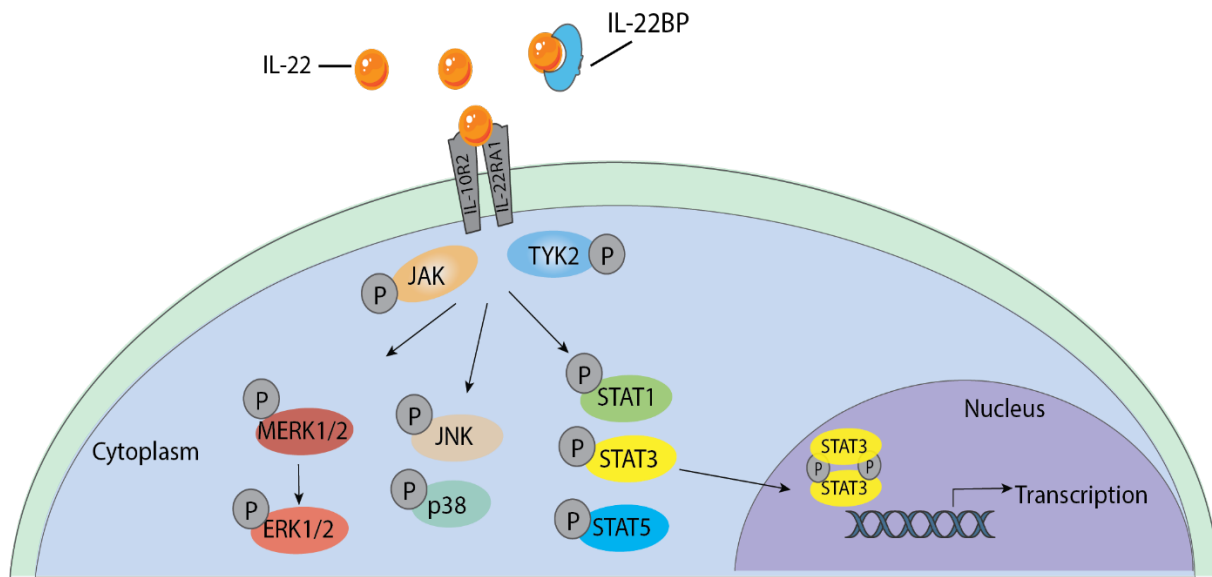
Figure 5: Scheme of the IL-22 downstream signaling pathways. IL-22 binds to its receptor complex, which leads to the activation of downstream signal transduction pathways. The binding of IL-22 activates JAK1 and TYK2 phosphorylation, which further phosphorylates, ERK1/2, MEK1/2, JNK, and p38 kinase (depending on the cell type), STAT1, STAT3, and STAT5. The phosphorylation of these downstream pathways leads to the dimerization and translocation of STATs to the nucleus. Typically, STAT3 is the primary transcription factor activated by IL-22 signaling, while STAT1 and STAT5 may also be activated to a lesser extent. Figure adapted from Xuan et al, 2021 [156].

IL22 is classified as an inflammatory cytokine as its level upon tissue injury is significantly enhanced. Importantly, IL-22 can be dual-natured depending on the inflammation. In liver inflammation, IL-22 has been reported to provide protection to the hepatocytes[157]. However, in dermal inflammation, IL-22 has been reported to be a potent driver and pathogenic[158]. In addition, IL-22 is highly expressed during chronic inflammatory diseases. IL-22 plays an essential role in the generation of the innate immune response against numerous infections. Notably, IL-22 also facilitates tissue repair by enhancing epithelial cell proliferation, such as goblet cells, to increase mucus production and epithelial cell survival[53, 135, 139-141, 153, 159, 160].

1.6.3 The role of IL-22 in inflammatory bowel disease

Surprisingly, IL-22 demonstrates a dual nature in IBD, as in some cases, IL-22 signaling fluctuates from having a reparative function to having pathological functions. Notably, IBD has long been defined as a Th1-mediated disease due to the increased level of IFN-γ[161]. It has now become apparent that though IFN-γ plays a role in the pathology, IL-22 is also a potent contributor. Andoh *et al*. demonstrated that in CD and UC patients, IL-22 is highly upregulated in their sera and their lesions[43]. A study carried out by Zenewicz *et al*. showed that mice double-deficient for *Il22*^{-/-} and *Rag*^{-/-} that received IL-22 deficient T cells had substantially higher disease compared to mice that received IL-22 wild-type T cells. This study highlighted that IL-22 is important and confers protections[162]. In a CD45RB^{high} CD4 T cell–mediated colitis model, the authors found that in the absence of innate IL-22, adaptive IL-22 was also capable of providing protection[162].

In contrast, A study by Eken *et al*. showed that in a colitis model where the mice were both *IL-23R*^{-/-} and *Rag*^{-/-} deficient, the neutralization of IL-22 ameliorated the colitis[163]. However, the colitis was restored when IL-22 was re-introduced in these mice. They also noted that IL-22 was able to induce even after the inhibition of IL12p40 (IL12/IL23). Their study highlighted the role of IL-22 in the pathogenicity of IBD. In general, in acute inflammatory settings, IL-22 displays protective roles by increasing mucin and antimicrobial peptide production to protect the host. However, in Chronic inflammation,

IL-22 is pathogenic, as it drives proliferation and inhibits apoptosis which can lead to hyperplasia and be detrimental to the host[138, 139, 141, 142, 153, 164]. Importantly, a study by Morrison *et al.* found that the neutralization of IL-22 in the *H.h* +α-IL10R colitis model prevented the development of inflammation in the colon but not in the cecum[165]. In addition, this study further showed that IL-17A had a disease-protective role in the cecum, while IL-22 was found to be pathogenic in the colon, highlighting that different Th17-type cytokines may have anti-inflammatory or proinflammatory effects in different locations of the intestine during *H.h.*–induced colitis[165]. Overall, further insight and understanding into IL-22 biology is advantageous for potential therapeutics of IBD.

2 Aim

OSM has both pro- and anti-inflammatory effects in IBD. However, the mechanism of action of OSM and OSMR in IBD are not well defined. Though some studies in transformed epithelial cell lines have shown that OSM may have protective effects on intestinal epithelial cells during inflammation, the regulation of the OSM receptor expression, signal transduction, and specific biological functions in intestinal epithelial cells are still unclear. Therefore, the aim of this PhD thesis was:

To explore the impact of OSM on tissue resident cells under steady-state and inflammatory conditions by investigating and identifying:

1. ***Which cells other than the stromal cells express the OSMR?***

2. ***Which signals promote OSMR expression on these non-stromal cells?***

3. ***Which impact or relevance does OSM and OSMR have on these cells' adaptation and function in intestinal inflammation?***

3 Material and Methods

3.1 Human studies

The local ethics officials in the application EA1/200/17 approved all human sample collections and usage in this thesis. In addition, the collection of the human samples complied with the recommendations of the World Medical Association *(Declaration of Helsinki, in the revised version decided upon by the World Medical Association in its 52nd General Assembly in October 2000 in Edinburgh/Scotland and supplemented by the "Clarification" Washington 2002 § 29).* This project does not contain any experiment done on human embryonic stem cells.

3.2 Mice

All Female C57BL/6 mice were purchased from the Jackson laboratories. In addition, The *Osmr*$^{fl/fl}$ was obtained from Jackson laboratories (B6;129-Osmrtm1.1Nat/J) and typed via real time PCR to confirm the deletion. The *Osmr*$^{fl/fl}$ mice or *Ai9*[166] referred to in this thesis as *DsRed* mice were crossed with the *Villin*^{creERT2}[167] *Col1a2*^{creERT}[168] or the *Cdh5*^{cre}[169] all purchased from Jackson laboratories, in order to generate the cell specific OSMR deficient mouse lines. *Rag2*$^{-/-}$[170] and *Rorc*$^{fl/f(l}$[171, 172] were crossed and used to gain insights on the innate immune cells. The *Villin*^{Cre}[173]x *Stat3*$^{fl/fl}$[174] mice were used from organoids isolation. Additionally, *Stat1*$^{fl/fl}$[175] and *Villin*^{creERT2} x *Stat3*$^{fl/fl}$ were used in the *in vivo* experiments to understand the downstream pathway of OSMR. Lastly, *Villin*^{CreERT} x *Il22ra1*$^{fl/fl}$[176] and *Il22*$^{-/-}$[177] mice were used to understand the role of IL-22 in the OSM-OSMR pathway. For *in vivo* experiments, mice were cohoused for at least 4 weeks before the initiation of the *H.hepaticus* and anti-IL-10R (clone:1B1.2, Hölzel Diagnostika) induced colitis. The respective mice received the appropriate amount of tamoxifen (Sigma aldrich) for 1 week after the cohousing of the mice and before the initiation of colitis. Tamoxifen was prepared following the Jackson laboratories protocol[166, 178] (material for tamoxifen preparation are listed in **Table 1**).

All mice used in this thesis were bred under specific pathogen-free conditions in the animal facility of the Federal Institute for Risk Assessment (Berlin, Germany) and the Research Institute for Experimental Medicine (FEM) of the Charité (Berlin, Germany). Animal experiments were conducted according to the German animal protection laws and were approved by the responsible governmental authority (Landesamt für Gesundheit und Soziales) in the application G 0291/18.

3.3 *In vivo* experiments

3.3.1 *Helicobacter hepaticus* culture and infection

Glycerol-stocked *Helicobacter hepaticus* (DSMZ, DSMZ no.: 22909) was grown on blood agar plates under microaerobic conditions at 37°C. Cultures were examined by microscopy for bacteria quality and purity and transferred into a tryptone soya broth (TSB) supplemented with 10% FCS, 10 µg/mL Vancomycin, 5 µg/mL Trimethoprim, and 2.5 IU/mL Polymyxin B (**Table 1**) in microaerophilic conditions at 37°C in a shaking incubator at 180 rpm.

The mice were gavaged with $1x10^8$ colony forming units (c.f.u.) of *H.h* on two consecutive days using a 22 G curved blunted needle. Additionally, the mice were treated with weekly intraperitoneal injection (i.p) of 1mg anti-IL10R antibody (clone 1B1.2).

Subsequently, the mice were sacrificed at the indicated time points and tissues (colon, SI, cecum, liver, spleen, and MLN) were harvested for analysis. Approximately, ~0.3 cm of samples from the SI and colon (proximal, middle, and distal) as well as the cecum were collected into 4 % (w/v) formaldehyde in saline solution for histological assessment as well as in RNA Later for gene expression analysis. Cecal contents and poop were collected and frozen for assessment of *H.hepaticus* colonization analysis.

3.3.2 *In vivo* blocking experiments

For the *in vivo* blocking of IL-22, mice were injected intraperitoneally with 450 µg of anti-IL-22 antibody (clone 8E11, provided by Genentech in collaboration with Nathaniel West)

on days 0 and 3 for 7 days of colitis, while for 14 days of colitis the mice were treated with anti-IL-22 on days 7 and 10. For the blocking of IL-12p40, mice were treated with 1 mg of anti-IL-12p40 (clone C17.8, produced by the Deutsches Rheuma-Forschungszentrum (DRFZ)) on day 0 for 7 days colitis. For the mentioned experiments, the control-inflamed mice received the respective concentration of rat IgG isotype (Jackson laboratories). For the blocking of OSM *in vivo*, the mice were injected with 0.5 mg of anti-OSM (clone 24A8) on day 14 for the duration of a 18 days colitis while the control mice received the respective amount of anti-gp120 (provided by Genentech in collaboration with Nathaniel West). Further details of the antibodies are on **Table 1**.

Table 1.

Reagent or Resource	Source	Identifier
Helicobacter hepaticus culture		
Vancomycin hydrochloride	Carlroth	1404-93-9
Trimethoprim, 98%, Acros Organics™	Fisher scientific	15345602
Polymyxin B sulfate salt	Sigma	P4932-1MU
Tryptone Soya Broth	Fisher Scientific	10525943
Oxoid# Blood Agar Base No. 2	Fisher Scientific	CM0271B or 10269522
Tryptone Soya Broth	Fisher Scientific	CM0129B or 10525943
Thermo Scientific Oxoid LAKED HORSE BLOOD	Fisher Scientific	SR0048C
Helicobacter hepaticus	DSMZ	DSMZ no.: 22909
Blocking antibodies		
Clone/Cat#	**Target**	**Source**
C17.8	anti-IL-12p40	DRFZ Lab Managers
8E11	anti-IL-22	DRFZ Lab Managers

Cat# 012-000-002	Rat Gamma globulin	Jackson laboratories
24A8	anti-OSM	Genentech
Unknown	anti-gp120	Genentech
1B1.2	anti-mouse IL-10R (CD210)	Hölzel Diagnostika Handels GmbH
Other material		
Tamoxifen	sigmaaldrich	T5648-1G
corn oil	sigma	C8267-500ML

3.3.3 Scoring of mouse colitis

The histological assessment of mouse colitis was performed as described previously by Izcue *et al*[179]. In brief, three pieces of mouse colon (proximal, middle, and distal colon) were collected and formalin-fixed, paraffin-embedded, and stained with hematoxylin and eosin. Then, these blocks were graded on a scale of 0 to 3 for four parameters: leukocyte infiltration, area affected, epithelial hyperplasia and goblet cell depletion, and features of severe disease activity. The features of disease activity were characterized by the formation of crypt abscesses, interstitial edema, and submucosal leukocyte infiltration (**Table 2A-D**). Each colon section receives an overall score for the added four parameters of 0 to 12. Finally, the data from the three colon sections are averaged and the mean of these values from each mouse was used for statistical analysis. The histological scoring was conducted in a blinded fashion and confirmed by an independent blinded observer.

Table 2.

A.	**EPITHELIUM**	**HYPERPLASIA and/or GOBLET CELL DEPLETION**
0	None	None
1	Mild (1.5x)	Mild (25%)
2	Moderate (2-3x)	Marked (25-50%)
3	Severe (>3x)	Substantial (>50%)

B. INFLAMMATION IN LAMINA PROPRIA

0	None - few leucocytes
1	Mild - some increase in leucocytes at tips of crypts OR many lymphoid follicles
2	Moderate - marked infiltrate (notable broadening of crypt)
3	Severe - dense infiltrate throughout

C. AREA AFFECTED (% of section)

0	None
1	up to 25%
2	25-50%
3	>50%

D. MARKERS OF SEVERE INFLAMMATION

0	None
1	Submucosal inflammation OR Few crypt abscesses (<5)
2	Submucosal inflammation AND Few Crypt Abscesses (<5)
2	Many crypt abscesses (<5) OR Extensive submucosal inflammation OR Crypt branching
3	Many crypt abscesses (<5) AND Extensive submucosal inflammation / Crypt branching
3	Ulceration OR Extensive fibrosis

3.4 Cell culture

3.4.1 Cell lines and reagents

3.4.1.1 Culturing of the Caco2 cell line

The human epithelial colorectal adenocarcinoma cell line (Caco-2) was cultured in DMEM (Invitrogen) supplemented with 10% fetal calf serum (FCS), 2 mM glutamine, 10,000 U/ml penicillin/streptomycin. The cell line was maintained at 37 °C and in a humidified atmosphere of 5% CO_2. The cells were starved for 24 hours prior to

stimulations with the above cytokines. The cells were stimulated for 15 min with the 100 µg/µl of recombinant human OSM, IFN−γ, or IL-22 (all from Peprotech) (**Table 3**). Protein cell lysates were prepared using RIPA buffer with 1x phosphatase and 1x protease inhibitors without EDTA (all from Thermofischer).

Table 3.

Reagent or Resource	Source	Identifier
Mouse Cytokines		
Recombinant mouse IL-1β	Peprotech	211-11B
Recombinant mouse IFN-α	Miltenyi Biotec	130-093-131
Recombinant mouse IFN-γ	BioLegend	575304
Recombinant mouse IL-12	Miltenyi Biotec	130-096-707
Recombinant mouse IL-13	Peprotech	210-13
Recombinant mouse IL-17A	Peprotech	210-17
Recombinant mouse IL-18	R&D Systems Inc.	9139-IL
Recombinant mouse IL-22	BioLegend	576202
Recombinant mouse IL-23	Peprotech	200-23
Recombinant mouse IL-33	BioLegend	580502
Recombinant mouse IL-4	Miltenyi Biotec	130-097-759
Recombinant mouse IL-6	BioLegend	575704
Recombinant mouse IL-7	Miltenyi Biotec	130-094-066
Recombinant mouse OSM	BioLegend	762804
Recombinant mouse TNF-α	BioLegend	575204
Recombinant mouse IL-2	Miltenyi Biotec	130-098-221
Bacterial lysate		
Bacteria lysate Escherichia coli Nissle	Prepared in house	
Bacterial lysate Helicobacter hepaticus	Prepared in house	
SCFA mix contains: Sodium propionate, Sodium butyrate, Sodium acetate, Sodium	Prepared in house	
TLR-ligands		
Flagellin	InvivoGen	tlrl-epstfla

LPS B5	InvivoGen	tlrl-b5lps
R848 ((Resiquimod)	InvivoGen	tlrl-r848
Human cytokines		
Recombinant human TNFα	Peprotech	041525 I2817
Recombinant human IFN-γ	Peprotech	300-02-20ug
recombinant human IL-22	peprotech	200-22-10

3.5 Organoid isolation

Small intestine and colon organoids were generated and cultured, as described previously, with some modifications[180]. The mice's bowels were opened vertically, cut horizontally into 2 – 5 mm pieces, and washed several times (10 – 20 times) with cold phosphate-buffered saline (PBS). Then, the tissue fragments were incubated in 10 mM of ethylenediaminetetraacetic acid (EDTA) with PBS. After the EDTA solution was removed, the crypts were liberated using mechanical disruption by vigorous pipetting and centrifugation steps. The crypts were screened through an 80 μm filter, centrifuged, suspended in ice-cold Matrigel Growth Factor Reduced (GFR) Basement Membrane Matrix, Phenol red-free, LDEV-free; Corning), and seeded in 24-well plates (500 crypts per 50 μL of Matrigel per well). Following the polymerization of the Matrigel (15 minutes at 37°C), 500 μl of crypt culture medium (advanced Dulbecco's modified Eagle medium/F12 supplemented with 10 mmol/L HEPES, Glutamax, 1× N2 (all from Thermo Fischer Scientific), 1× B27 (Invitrogen), penicillin/streptomycin (Gibco), EGF (Miltenyi), 1.25 mmol/L N-acetylcysteine (Sigma), was overlaid containing optimized growth factor combinations: The murine small intestinal crypts contained 20% R-spondin and 10% Noggin conditioned media. While the murine colonic crypts media contained Gastrin (Sigma), Nicotinamide (Sigma), TGFB receptor inhibitor A83-01, PGDE2 (both from Tocris), 20% R-spondin, 10% Noggin, and 50% of Wnt-3A conditioned medium. Rho-kinase inhibitor Y-27632 (Abmole) was included in both the small intestinal crypts and colonic crypts media for the first two days to avoid anoikis. The medium was changed every two days, and organoids were passaged by mechanical sheering through P1000 pipet tip connected to P200 pipet tip without a filter into single- crypts every 1-2 weeks

with a 1:2 split ratio. Please refer to **Table 4** for source and identifier of the above-mentioned reagents.

Table 4.

Reagent or Resource	Source	Identifier
Organoids		
Advanced DMEM/F-12-10 x 500 mL	ThermoFisher	Cat# 12634028
GlutaMAX Supplement-100 mL	ThermoFisher	Cat# 35050061
Rho kinase inhibitor Y-27632	Abmole	Cat# 1254
Trypsin-EDTA	Gibco	Cat# 25200072
TrypLE	Gibco	Cat# 12605010
B27	Invitrogen	Cat# 17504-044
Primocin	Invitrogen	Cat# ant-pm-1
Na2HPO4	Sigma	Cat# S5136-1KG
KH2PO4	Sigma	Cat# P5655-500G
NaCl	Sigma	Cat# S5886-1KG
KCl	Sigma	Cat# P5405-1KG
Sucrose	Sigma	Cat# S1888-1KG
D-sorbitol	Sigma	Cat# 240850-100G
N-acetylcysteine	Sigma	Cat# A9165-25g
Nicotinamide	Sigma	Cat# N0636-100g
Gastrin	Sigma	Cat# G9145-1mg
p38 inhibitor (SB 202190)	Tocris-über Biotechne	Cat# S7067
TGFB receptor inhibitor A83-01	Tocris-über Biotechne	Cat# 2939
PGDE2	Tocris-über Biotechne	Cat# 2296
Corning® Matrigel® Growth Factor Reduced (GFR) Basement Membrane Matrix, Phenol Red-free, *LDEV-free,	Corning	Cat# 356231
B27	Invitrogen	Cat# 17504-044

| N-2 Supplement | ThermoFischer Scientific | Cat# 17502048 |

3.6 Cell isolation

3.6.1 Mouse colon tissue preparation and cell isolation

Mice were euthanized by cervical dislocation and colons were removed and placed in ice-cold PBS. Colons were opened longitudinally, cleaned thoroughly with ice-cold PBS and cut into 2 mm pieces and washed in EDTA solution (RPMI ,10% FCS, and 5 mM EDTA) in a shaker at 37°C for 30 min to remove the epithelial cells. This step was performed in a shaking incubator at 37°C, and was repeated, with all supernatants being collected as epithelial washes. The remaining tissue was washed twice using RPMI containing 10% FCS, and 15 mM HEPES at room temperature. The tissue was then vortexed vigorously for 10 seconds and collected in C-tubes (Miltenyi) in complete RPMI, 10% FCS, 15 mM HEPES, and collagenase VIII (~500U/mL) for 35 min in a shaking incubator at 37°C to liberate the cell populations. Solutions were then passed through 100 µM cell strainers and washed with ice-cold PBS. Cells were suspended in 3 ml of the 30% fraction of a 30%/40%/70% Percoll (ThermoFisher, **Table 5**) gradient and carefully placed on top of 4 ml of the 40% fraction in 15 ml tubes. Percoll gradient separation was performed by 20 min centrifugation at 900 x g at 10° C. Cells at the 30%/40% interface were collected as the stroma-enriched fraction, while cells at the 40%/70% interface were collected as the lamina propria leukocyte enriched fraction. The different cell fractions were then washed with ice-cold PBS.

3.6.2 Epithelial cell isolation

The mice's bowels were opened vertically, cut horizontally into 2 – 5 mm pieces, and washed with cold phosphate-buffered saline (PBS). Then, the tissue fragments were incubated in 10 mM EDTA–PBS on ice for 60 min, shaking every 30 min. The tissue was shaken vigorously, and the supernatant was collected as fraction 1 in a new conical tube. The tissue was incubated in fresh EDTA–PBS, and a new fraction was collected. The

two fractions were pulled, washed twice in PBS, and centrifuged at 300g for 5 min. Samples were either lysed with Qiazol for RNA isolation or lysed with RIPA for protein isolation.

Table 5.

Reagent or Resource	Source	Identifier
Cell culture and isolation		
Bovine Serum Albumin,Fraction V, PAN Bio	PAN Biotech	Cat# P06-1391500
1,4-Dithiothreitol (DTT)	Roth	Cat# 6908.3
HEPES (1M)-100 mL	Pan Biotech	Cat# P05-01100
Trypsin-EDTA	Gibco	Cat# 25200072
HBSS(Hanks' Balanced Salt Solution), no calcium, no magnesium, no phenol red	Thermofischer/GIBCO	Cat# 14175129
RPMI 1640 Medium, GlutaMAX™ Supplement (1x)	Gibco	Cat# 61870-044
Penicillin-Streptomycin (10,000 U/mL)-10	Gibco	Cat# 15140122
D-Glucose	Sigma now Merck	Cat# G8270-100g
Ionomycin, calcium salt (From Streptomyces con	FISHER BIOREAGENTS	Cat# BP2527-5
Brefeldin A	Cayman	Cat# Cay11861-25
PMA	Sigma	Cat# P1585-1MG
Collagenase from Clostridium histolyticum (Collagenase VIII)	Sigma Aldrich	Cat# C2139-1G
EDTA	Sigma	E5134
FCS	Sigma	F7524
Penicillin-Streptomycin	ThermoFisher	Cat. No. # 15140148
Percoll	ThermoFisher	17-0891-01
DMEM, high glucose, GlutaMAX supplement-	Gibco	61965059

3.7 Gene expression analysis

3.7.1 RNA Isolation of intestinal epithelial cells and cDNA synthesis

RNA was isolated using the QIAzol Lysing Reagent (Qiagen Kit following the manufacturer's instructions. Samples were collected in RNA Later (Qiagen) or directly lysed with a phenol/guanidine-based reagent known as QIAzol. Upon lysis with QIAzol, the samples were homogenized, and chloroform was added to separate the homogenate into aqueous and organic phases by centrifugation. After centrifugation, the upper aqueous phase was collected, RNA was precipitated by the addition of isopropanol and GlycoBlue™ (ThermoFisher, RNase-free glycogen). The pellet was washed with 75 % ethanol and re-dissolved in RNase-free water. Then, the RNA concentration was measured using the NanoDrop. Lastly, the RNA samples were stored at -20 °C, for long-term at -80°C, or directly used for cDNA synthesis. Please refer to **Table 6** for additional product information.

3.6.2 cDNA Synthesis of large/high cell numbers

For all tested target-specific preamplification approaches, reverse transcription was conducted by High-Capacity cDNA Reverse Transcription Kit (Applied Biosystems). For this, 500 ng of RNA was combined with High-Capacity cDNA Reverse Transcription Kit reagents according to the manufacturers' instructions. The samples were diluted 1:60 and qPCR were run using PowerUp™ SYBR™ Green Master Mix (ThermoFisher Scientific) on an Applied Biosystems QuantStudio 5. The data were analyzed and gene expression was expressed relative to ACTB.

Table 6.

Reagent or Resource	Source	Identifier
RNA Isolation and cDNA synthesis		
2-Propanol min. 99,5 %, zur Synthese	Roth	9866.2

2-Propanol min. 99,5 %, zur Synthese	Roth	9866.1
Chloroform	Sigma	319988-1L
EthanolROTIPURAN®, min. 99,8 %, p.a., Glas	Roth	9065.1
GlycoBlue™ Coprecipitant	ThermoFisher	AM9516
High-Capacity cDNA Reverse Transcription Kit-200 reactions	Applied Biosystems	4368814
Monarch® RNA Cleanup Kit (10 µg)	New England Biolabs	T2030L
NUCLEASE FREE WATER 1 * 1 l Herst.ar	Omega	PD092
QIAzol Lysis Reagent (200ml)	qiagen	79306
RNAlater RNA Stabilization Reagent (50 ml)	Qiagen	76104
RNeasy Micro Kit (50)	Qiagen	74004
RNeasy Mini Kit	Qiagen	74106
Trizol	Life Technologies	15596026

3.7.3 RNA Isolation of mouse colon tissue and qPCR

Colon tissues were collected in RNA later and were placed at -80°C. The frozen tissues were homogenized and RNA was extracted using the Qiagen Mini RNA kit (Qiagen, listed in **Table 6**) according to the manufacturer's instructions. Then, 1 ug of RNA was reverse transcribed using the High-Capacity cDNA Reverse Transcription Kit (ThermoFisher Scientific). The samples were diluted 1:50 and qPCR was performed using PowerUp™ SYBR™ Green Master Mix (ThermoFisher Scientific) or TaqMan Universal Master Mix II, with UNG (Themo Fischer Scientific) using the Taqman Gene Expression Assays (Themo Fischer Scientific) on an Applied Biosystems QuantStudio 5. The data were analyzed and gene expression was expressed relative to ACTB. Please refer to **Table 7** for primer information.

Table 7.

Reagent or Resource	Source	Identifier
Oligonucleotides		
quantitative PCR Murine forward primer_Actb: GATGTATGAAGGCTTTGGTC	KiCqStart® SYBR® Green Primers	ST03816663
quantitative PCR Murine reverse primer _Actb: TGTGCACTTTTATTGGTCTC	KiCqStart® SYBR® Green Primers	ST03816664
quantitative PCR Murine forward primer_Socs3: CCAAAGAAATAACCACTCCC	KiCqStart® SYBR® Green Primers	ST03816673
quantitative PCR Murine reverse primer _Socs3: GATCTGCGAGGTTTCATTAG	KiCqStart® SYBR® Green Primers	ST03816674
quantitative PCR Murine forward primer _Ifng: CTAGCTCTGAGACAATGAAC	KiCqStart® SYBR® Green Primers	ST03947811
quantitative PCR Murine reverse primer _Ifng: CTCTTTTCTTCCACATCTATGC	KiCqStart® SYBR® Green Primers	ST03947812
quantitative PCR Murine forward primer_Il10rb:ATAGAATCCCTTGCTGAGTC	KiCqStart® SYBR® Green Primers	ST03947819
quantitative PCR Murine reverse primer _Il10rb:CTTGAAACTTCTCATTAGTCCC	KiCqStart® SYBR® Green Primers	ST03947820
quantitative PCR Murine forward primer_Il22:ATCAGTGCTACCTGATGAAG	KiCqStart® SYBR® Green Primers	ST03947831
quantitative PCR Murine reverse primer _Il22:CATTCTTCTGGATGTTCTGG	KiCqStart® SYBR® Green Primers	ST03947832
quantitative PCR Murine forward primer_Il22ra1:CTGTTATCTGGGCTACAAATAC	KiCqStart® SYBR® Green Primers	ST03947835
quantitative PCR Murine reverse primer _Il22ra1:GTACGTGTTCTTGGATGAAG	KiCqStart® SYBR® Green Primers	ST03947836

quantitative PCR Murine forward primer _Lifr:GATTTGTCTGCTGACTTCTTC	KiCqStart® SYBR® Green Primers	ST03947851
quantitative PCR Murine reverse primer_Lifr:GTGCTGAACGGTATCTTTAC	KiCqStart® SYBR® Green Primers	ST03947852
quantitative PCR Murine forward primer_Osm:GAACACAGAATCACTCTTGG	KiCqStart® SYBR® Green Primers	ST03947871
quantitative PCR Murine reverse primer _Osm:TGTCTTAAAGCATCCAGTTG	KiCqStart® SYBR® Green Primers	ST03947872
quantitative PCR Murine forward primer_Osmr:CCATAGAGTTCATCCAAAGG	KiCqStart® SYBR® Green Primers	ST03947877
quantitative PCR Murine reverse primer _Osmr:GATCACTGAAGAGGTAGTTTG	KiCqStart® SYBR® Green Primers	ST03947878
quantitative PCR Murine forward primer _Reg3b:TATCTCAGGTTCAAGGTGAAG	KiCqStart® SYBR® Green Primers	ST04183442
quantitative PCR Murine reverse primer _Reg3b:GTATCTGAAACAAGGCATAGC	KiCqStart® SYBR® Green Primers	ST04183443
quantitative PCR Murine forward primer_Reg3g:AACAGTGGCCAATATGTATG	KiCqStart® SYBR® Green Primers	ST04183444
quantitative PCR Murine reverse primer _Reg3g:TCTCTCTCCACTTCAGAAATC	KiCqStart® SYBR® Green Primers	ST04183445
quantitative PCR Murine forward primer_Il22ra2:CACTAGAGAAGGAGCAAAAAG	KiCqStart® SYBR® Green Primers	ST05070559
quantitative PCR Murine reverse primer _Il22ra2:TAGCTGGAATGAGGTATCAG	KiCqStart® SYBR® Green Primers	ST05070560
Taqman Oncostatin M receptor	Thermofischer/Taqman	4453320 / Mm01307326_m1

Taqman Actin, beta	Thermofischer/Taqman	4453320 / Mm01205647_g1
Taqman Oncostatin M	Thermofischer/Taqman	4453320/Mm01193966_m1
TaqMan Universal Master Mix II, with UNG	Thermofischer/Taqman	4440038

3.7.5 Reverse transcription of low RNA quantity

Small intestinal and colonic organoids were stimulated with the mentioned cytokines listed in **Table 3**. After stimulation the organoids were washed and lysed using QIAzol Lysis Reagent (Qiagen), and RNA was isolated according to the manufacturer's instructions. cDNA synthesis and pre-amplification were performed using the SMART-PCR approach, as described previously[181, 182]. In brief, 100ng of total RNA was mixed with 1 mM dNTPs (ThermoFisher Scientific) and 10µM of oligo-dT primer (5′-AAGCAGTGGTATCAACGCAGAGTACT30VN-3′, where "N" is any base and "V" is either "A," "C" or "G"; Biomers), denatured and placed on ice. Then, the First-strand synthesis for each sample was achieved using 5 U/µl Maxima H minus reverse transcriptase (200 U/µl, Invitrogen), 1 U/µl Recombinant RNasin Ribonuclease Inhibitor (PROMEGA), 1x SuperScript VI Reverse Transcriptase (5×, ThermoFisher Scientific), 1 M betaine (5 M, Sigma), 10 mM MgCl2 (1 mM, ThermoFisher Scientific), 1 µM ISPCR-TSO (Template Switching Oligos): 5′-AAGCAGTGGTATCAACGCAGAGTACATrGrG+G-3′; two riboguanosines (rG) and one LNA-modified guanosine (+G), and nuclease-free water (Invitrogen). Subsequently, the reverse transcriptase was inactivated, and an adapter – based PCR pre-amplification was carried out using 1x KAPA HiFi HotStart ReadyMix (2×, KAPA ROCHE), 200 nM ISPCR primers (10 µM, 5′AAGCAGTGGTATCAACGCAGAGT-3′, Biomers) and nuclease-free water (Invitrogen). Finally, cDNA was treated with Exonuclease I (NEB) following the manufacturer's instructions. All items are listed in **Table 8**.

Table 8.

Reagent or Resource	Source	Identifier
SMART-PCR		
13243159 - EP0753 - Maxima H Minus RT 4x10000u	ThermoFisher	EP0753
Exonuclease I (E. coli)	NEB	M0293L
384-well PCR plate for index sorting/ direct lysis	Sarstedt	72.1984.202
2x KAPA HiFi HotStart Ready Mix	ROCHE	7958935001(KK2602)
SuperScript VI Reverse Transcriptase (with 5X RT buffer, 1 mL 0.1 M DTT, 500 µL)	ThermoFisher	18090050
100µM TSO: 5′- AAGCAGTGGTATCAACGCAGAGTACATrGrG+G- 3′; two riboguanosines (rG) and one LNA-modified guanosine (+G)	Biomers	
5M betaine	Sigma-Aldrich	B0300-1VL
Recombinant RNasin Ribonuclease Inhibitor, 10000 u	PROMEGA	N2515
adapter-oligo-dT (5′– AAGCAGTGGTATCAACGCAGAGTAC(T30)VN-3′)	Biomers	
1M Magnesium chlorides (in RNase-free water)	ThermoFisher	AM9530G
dNTP Mix (10 mM each) (for RNA)	ThermoFisher	R0191
Maxima H Minus Reverse Transcriptase (200 U/µL)	Thermofischer	EP0753
PowerUp™ SYBR™ Green Master Mix	ThermoFisher	A25742
KAPA SYBR FAST	Sigma	KK4605

3.7.5 Single cell RNA-library preparation and sequencing

The lamina propria mononuclear cells (LPMC), stromal, and epithelial cells were FACS-sorted and were individually hash-tagged per mouse group and per cell type. Then, the single cell suspensions were obtained and applied to the 10x Genomics workflow for cell capturing and scRNA gene expression (GEX) and CITE-Seq library preparation using the Chromium Single Cell 5' Library & Gel Bead Kit version 2 and the Single Cell 5' Feature Barcode Library Kit (10x Genomics). After cDNA amplification, the Cite-Seq libraries were prepared separately using the Dual Index Kit TN Set A while, the final GEX libraries were obtained after fragmentation, adapter ligation, and final Index PCR using the Dual Index Kit TT Set A. Qubit HS DNA assay kit (Life Technologies) was used for library quantification and fragment sizes were determined using the Fragment Analyzer with the HS NGS Fragment Kit (1-6000bp) (Agilent). Furthermore, the sequencing was performed on a NextSeq2000 device (Illumina) applying the sequencing conditions recommended by 10x Genomics for libraries prepared with Next Gem Reagent Kits v2. Finally, NEXTSeq 1000/2000 P3 reagent kits (100 Cycles, Illumina) were used for 5' GEX and Cite-Seq libraries with the following sequencing settings: read1: 26nt, read2: 90nt, index1: 10nt, index2: 10nt.

3.7.6 Bulk RNA sequencing sample preparation

For the sequencing analysis of the $Villin^{CreERT2}$ x $Osmr^{fl/fl}$ and $Villin^{creERT2}$ x $Osmr^{fl/+}$, the EpCAM$^+$ epithelial cells were FACS-sorted and lysed in the RLT lysis buffer and RNA was extracted using the RNeasy Micro Kit (Qiagen, Table 6) according to the manufacturer's protocol. The quality of the RNA was tested and analyzed according to the manufacturer's protocol. The continuation of the protocol was done together with the Novogene Experimental Department. In brief, the mRNA was purified from total RNA using poly-T oligo-attached magnetic beads. After fragmentation, the first strand cDNA was synthesized using random hexamer primers, followed by the second strand cDNA synthesis using either dUTP for directional library or dTTP for non-directional library. For the non-directional library, it was ready after end repair, A-tailing, adapter ligation, size selection, amplification, and purification. For the directional library, it was ready after end

repair, A-tailing, adapter ligation, size selection, USER (Uracil-Specific Excision Reagent) enzyme digestion, amplification, and purification. The library was checked with Qubit and real-time PCR for quantification and bio-analyzer for size distribution detection. Quantified libraries will be pooled and sequenced on Illumina platforms, according to effective library concentration and data amount. Clustering and sequencing (Novogene Experimental Department) of the index-coded samples was performed according to the manufacturer's instructions. After cluster generation, the library preparations were sequenced on an Illumina platform and paired-end reads were generated.

3.7.7 Bulk RNA sequencing data analysis

Data analysis for the bulk RNA sequencing was done in collaboration with Novogene. First, the sequenced reads/raw reads were filtered by removing the reads containing adapters, N > 10%, where N represents base that were undetermined, and low-quality reads where the quality value was over 50% bases of the read is <= 5. The mapping of the clean reads was carried out using the HISAT2 software for the alignment of the sequencing data analysis. The analysis of differentially expressed genes were done by the normalization of the read counts, model dependent P-value estimation, and the FDR value estimation based on multiple hypothesis testing.

3.7.8 *Osmr* and *Il22* detection by *in situ* hybridization

The RNAScope Reagent Kit was used in order to detect both the mouse and human *Osmr* mRNA. In brief, paraffin sections were cut, dried for 1 hour at 60°C, and dewaxed prior to unmasking with Target Retrieval buffer and protease. Pretreated sections were hybridized with specific probes to *Omsr* or *Il22* and *Ppib* (positive control) and the irrelevant probe to *dapb* as a negative control. The punctae were analyzed and quantified using Ilastik, a software for image classification and segmentation and ImageJ. The RNAScope *in situ* hybridization protocol was performed in collaboration with the iPATH department at the Charité.

3.8 Analysis of protein expression

3.8.1 Bicinchoninic Acid Assay

The bicinchoninic acid assay (BCA) Kit (Serva) was used to determine the total protein concentration in the respective cell lysates. The cells were initially lysed with RIPA mixed with phosphatase and protease inhibitor cocktail (ThermoFisher). Then, the samples were diluted at a 1:20 ratio with the protein lysis buffer mentioned in a 96-well microplate with a V-shaped bottom. After diluting the samples, bovine serum albumin (BSA)(Serva) was used to create a standard curve (in a serial dilution). Then, 25 µl of the samples and the standards were transferred to a flat-bottom 96-well microplate. The BCA solution was then prepared according to manufacturers' instructions. 200 mL of this solution was added to the flat-bottom 96-well plate. The plate was incubated at 37 °C for 30 min. The protein concentration was detected using the Molecular Devices ThermoMax Microplate Reader at 550 nm wavelength. The data was then used to calculate the protein concentration of the samples via linear regression using the dilution series of the standard's concentrations linear curve. Please refer to **Table 9** for further product details.

Table 9.

Reagent or Resource	Source	Identifier
Western blot and protein isolation		
RIPA Lysis and Extraction Buffer	ThermoFisher	Cat# 89900
Methanol	carlroth	Cat# 0082.3
BCA Protein Assay Macro Kit	Serva	Cat# 39228.01
Tris Buffered Saline with Tween	Cell Signaling	Cat# 9997S
Halt™ Phosphatase Inhibitor Cocktail	ThermoFisher	Cat# 78420
Halt™ Protease Inhibitor Cocktail (100X)	ThermoFisher	Cat# 87786
SuperSignal™ West Pico PLUS Chemiluminescent Substrate	ThermoFisher	Cat# 34577
Nonfat Dry Milk	Cell Signaling	Cat# 9999S
Immobilon Blotting Filter Paper	Sigma	Cat# IBFP0813C
Immobilon-NC Transfer Membrane	Sigma Aldrich	Cat# IPVH00010

2-Mercaptoethanol (electrophoresis grade)	Serva	Cat# 28626.01
Laemmli Buffer 10x, for SDS PAGE	Serva	Cat# 42556.04
SERVAGel™ Neutral HSEprecast gel, 12 sample wells	Serva	Cat# 43245.01
SERVA Pink Color Protein Standard II	Serva	Cat# 39259.01
MagicMark™ XP Western Protein Standard	ThermoFisher	Cat# LC5602

3.8.2 Western-Blots

For immunoblotting of STAT1, STAT3, pSTAT1, pSTAT3, and β-actin, cells were lysed in RIPA buffer including protease inhibitors (ThermoFisher) and phosphatase inhibitor cocktail (ThermoFisher). Sodium dodecyl sulfate–polyacrylamide gel electrophoresis (SDS–PAGE) was performed with gels containing 10% polyacrylamide. Proteins were transferred to polyvinylidene fluoride (PVDF) (Carl Roth) membranes for 1- 2 h at 200 mA. Membranes were blocked with 5% dry milk (Cell Signaling) in a Tris-buffered saline with Tween20 (TBST) solution for 1 h at room temperature. Then, the membranes were incubated overnight with primary antibodies at 4°C on a rotator. All primary antibodies (anti-phospho-Stat3 Tyr705) (polyclonal) or anti-Stat3 Ab (polyclonal) (both from Cell Signaling Technology) were diluted 1:1000 in 5% BSA-TBST solution. After, the membranes were washed with 1X TBST solution and incubated in a 1:2000 diluted HRP-linked secondary antibodies (Cell Signaling) in 5% dry milk-TBST solution for 1 h at room temperature. Protein detection was visualized using chemiluminescent substrate (ThermoFisher) and the luminescent image analyzer LAS-4000 mini). Lastly, the densitometric analysis was performed using the ImageJ (1.48V) software (National Institutes of Health, USA). Please refer to **Table 9** product information and **Table 10** antibody information.

Table 10.

Reagent or Resource	Source	Identifier
Western-blot antibodies		
β-Actin (13E5) Rabbit mAb	Cell Signaling Technology	Cat# 4970, RRID:AB_2223172

Anti-rabbit IgG, HRP-linked Antibody	Cell Signaling Technology	Cat# 7074, RRID:AB_2099233
STAT3 (D3Z2G) Rabbit mAb	Cell Signaling Technology	Cat# 12640, RRID:AB_2629499
STAT1 (D1K9Y) Rabbit mAb	Cell Signaling Technology	Cat# 14994, RRID:AB_2737027
Phospho-Stat3 (Tyr705) (D3A7) XP Rabbit mAb	Cell Signaling Technology	Cat# 9145, RRID:AB_2491009
Phospho-Stat1 (Tyr701) (D4A7) Rabbit mAb	Cell Signaling Technology	Cat# 7649, RRID:AB_10950970

3.8.3 Calprotectin and Lipocalin ELISA

Stool samples were collected and stored at –20°C until analysis. Briefly, approximately 100 mg of feces were homogenized in 1 mL of extraction buffer consisting of PBS and 1x protease inhibitor cocktail (Serva). In short, 96-well flat bottom ELISA plates (eBioscience) were coated for 12 hours at 4 °C with 100 µl/well with the appropriate antibody. For example, for the detection of lipocalin, the plates were coated with a capture purified anti-mouse NGAL antibody highly specific to lipocalin (see **Table 11**). Next, the plate was brought to room temperature and washed with PBS/Tween. Next, 200 µl/well blocking buffer containing 1% BSA was used to block non-specific binding. The plate was sealed and incubated at room temperature for 1 hour. After, the plate was washed and the standards and samples were added and incubated at room temperature for 2-4 hours at room temperature or at 4 °C overnight. Then the detection biotin anti-mouse NGAL was used for detection, followed by HRP Avidin (all from Biolegend). Finally, the TMB substrate reagents were used together with the TMB stop solution to stop the reaction. The plate was immediately taken to the microplate reader set to 450 nm to read the optical density. The samples were prepared following the same procedures as indicated above in order to detect fecal calprotectin protein expression. However, the detection of the fecal calprotectin level was analyzed with the Mouse

S100A8/S100A9 Heterodimer ELISA Kit (RD) following the manufacturer's instructions. All product information is listed in **Table 11.**

Table 11.

Reagent or Resource	Source	Identifier
ELISA		
Mouse S100A8/S100A9 Heterodimer DuoSet ELISA, 5 Plate; 1 Kit (for 5 Plates)	RD	DY8596-05
Biotin anti-mouse NGAL (Lipocalin-2) 532304	BIOLEGEND	532304
Purified anti-mouse NGAL (Lipocalin-2) 532202	BIOLEGEND	532202
Recombinant Mouse NGAL (Lipocalin-2) (ELISA Std.)	BIOLEGEND	563601
Stop Solution for TMB Substrate	Biolegend	423001
TMB Substrate Set, Biolegend	Biolegend	421101

3.9 FACS staining and cell sorting

Fresh LPMCs, spleenocytes, mLN, stroma, and epithelial cells were prepared accordingly and distributed for surface, transcription factor (TF), and intracellular cytokine staining (ICS). For staining of the surface markers, the cells were centrifuged at 300 x g for 5 min at 4°C, resuspended in 50µl surface antibody mix (**Table 12**) and incubated for 30 min at 4°C. Next, for the myeloid panel the cells were fixed with BD lysis buffer (BD) for 30 min. Then, the cells were washed and centrifuged for 5 min at 4°C. Subsequently, the cells were then mixed with Precision Count Beads (Biolegend) and taken to the BD FACSymphony for acquisition.

Table 12.

Reagent or Resource	Source	Identifier
Myeloid surface antibodies and material		
Mouse anti-CD19 Antibody	Biolegend	Cat# 115543, RRID:AB_11218994
Mouse anti-CD8a Antibody	Biolegend	Cat# 100748, RRID:AB_2562100
Mouse anti-NK-1.1 Antibody	Biolegend	Cat# 108736, RRID:AB_2563159
Zombie Aqua™ Fixable Viability Kit	Biolegend	423102
Mouse anti-CD3	Biolegend	Cat# 100214, RRID:AB_493645
Mouse anti-Ly-6G/Ly-6C (Gr-1)	Biolegend	Cat# 108424, RRID:AB_2137485
Mouse anti-CD45 Antibody	Biolegend	Cat# 103128, RRID:AB_493715
Mouse/human anti - CD11b	Biolegend	Cat# 101218, RRID:AB_389327
Mouse anti-Ly-6C	Biolegend	Cat# 128018, RRID:AB_1732082
Mouse anti-CD44	Biolegend	Cat# 103010, RRID:AB_312961
Mouse anti-CD11c	Biolegend	Cat# 117348, RRID:AB_2563655
Mouse anti-CD170 (Siglec-F)	Biolegend	Cat# 155506, RRID:AB_2750235
Mouse anti-CD4	Biolegend	Cat# 100538, RRID:AB_893325
Mouse anti-I-A/I-E	Biolegend	Cat# 107616, RRID:AB_493523
Precision Count Beads(TM) 100 tests	Biolegend	424902
BD FACS Lysing Solution	BD	349202

For the stromal panel, protein expressions were analyzed using the FoxP3 staining buffer set (eBioscience) according to the manufacturer's instructions. The cells were first stained with the surface antibodies (**Table 13**), followed by fixation with 1x Fixation/Permeabilization buffer. Then, intracellular staining with fluorochrome-labeled antibodies (**Table 13**) against the listed transcription factors above in 1x permeabilization buffer for 30-45 min at 4°C. Cells were washed with 1x permeabilization buffer and immediately analyzed at the BD FACSymphony.

Table 13.

Reagent or Resource	Source	Identifier
Stromal and epithelial surface and intracellular antibodies		
Mouse anti-CD326 (EpCAM)	Biolegend	Cat# 118208, RRID:AB_1134107
eBioscience™ Fixable Viability Dye eFluor™ 780	eBioscience	Cat# 65-0865-18
Mouse anti-CD45 Antibody	Biolegend	Cat# 103128, RRID:AB_493715
Mouse anti-Podoplanin	Biolegend	Cat# 127410, RRID:AB_10613649
Mouse anti-CD31	Biolegend	Cat# 102408, RRID:AB_312903
Mouse anti-CD54 Antibody	Biolegend	Cat# 116121, RRID:AB_2715949
Mouse anti-Ki67	BD Bioscience	Cat# 563462, RRID:AB_2738221
Calcein AM Viability Dye	Ebioscience	Cat# 65-0853-78
Other material		
eBioscience Foxp3 / Transcription Factor Staining Buffer Set-1 kit	Invitrogen	Cat# 00-5523-00

For the acquisition and analysis of the ILC panel, cells were stimulated for 30 min at 37°C with PMA (Sigma, 5ng/ml) and Ionomycin (Sigma, 500ng/ml). Subsequently, brefeldin A (Cayman, Cay11861-25, 5µg/ml), IL-23 (20 ng/ml; Prepotech), and IL1b (10 ng/ml; Prepotech) (**Table 3**) was added to the cells for an additional 4 h. After, the cells were stained with the appropriate surface marker antibodies (**Table 14**) for 20 min at 37°C. After washing, biotin was stained with fluorochrome labelled streptavidin for 10 min at 4°C. Next, the cells were fixed for 45 min at room temperature, permeabilized and TF markers (Table 13) were stained intracellularly at room temperature for 30 min using the Foxp3 / Transcription Factor Staining Buffer Set (eBioscience). Cells were

resuspended in 200 µl of PBS/BSA and taken directly to the BD FACSymphony or BD LSR Fortessa for acquisition. Lastly, flow cytometry analyses were performed using the FlowJo v.10.6.01 software.

Table 14.

Reagent or Resource	Source	Identifier
ILC surface antibodies		
Mouse anti CD127 (IL-7Rα) Antibody	Biolegend	Cat# 135037, RRID:AB_2565269
Mouse anti CD90.2 Antibody	Biolegend	Cat# 105349, RRID:AB_2800564)
Mouse anti CD45 Antibody	Biolegend	Cat# 103151, RRID:AB_2565884
eBioscience™ Fixable Viability Dye eFluor™ 780	eBioscience	Cat# 65-0865-18
Mouse anti-CD19 Antibody	Biolegend	Cat# 115543, RRID:AB_11218994
Mouse anti-Ly-6G/Ly-6C (Gr-1)	Biolegend	Cat# 108424, RRID:AB_2137485
Mouse anti-CD11c	Biolegend	Cat# 117348, RRID:AB_2563655
Mouse anti-F4/80	Biolegend	Cat# 123105, RRID:AB_893499
Mouse anti-FcERIa	Biolegend	Cat# 612803, RRID:AB_2870130
Mouse anti-TCR gamma/delta (eBioGL3 (GL-3, GL3)	eBioscience	Cat# 15-5711-82, RRID:AB_468804
Mouse anti-CD4	Biolegend	Cat# 100456, RRID:AB_2565845

Mouse anti-CD3	BD Bioscience	Cat# 134303, RRID:AB_1626100
ILC surface antibodies		
Mouse anti-Mouse RORγt	BD Bioscience	Cat# 562894, RRID:AB_2687545
Mouse anti-Ki67	BD Bioscience	Cat# 563462, RRID:AB_2738221
Mouse anti-IL-17A	Biolegend	Cat#506927, RRID:AB_11126144
Mouse anti-IFN-γ	Biolegend	Cat# 505823, RRID:AB_2561299
Mouse/human anti-Gata-3 (TWAJ)	eBioscience	Cat# 12-9966-42, RRID:AB_1963600
Mouse/human anti-T-bet	Biolegend	Cat# 644824, RRID:AB_2561761
Mouse anti-IL-22 (1H8PWSR)	eBioscience	Cat# 12-7221-82, RRID: AB_10597428
Mouse anti-EOMES (Dan11mag)	ebioscience	Cat# 53-4875-80, RRID:AB_2802207

3.10 Cell sorting

As mentioned in the previous sections, fresh LPMCs, stromal, and epithelial cells were isolated. The cells were stained accordingly for 20 min at 4°C in the dark with the appropriate antibody mixes. The cells were also hash-tagged for the single-cell RNA sequencing experiments according to their assigned group, following the 10x Genomics protocol. Subsequently, the cells were washed twice with PBS + 1% BSA for 10 min at a speed of 300 x g at 4°C. The cells were resuspended in MEM + 5 mM EDTA medium and filtered prior to the sorting. Next, 4',6-diamidino-2-phenylindole (DAPI) or propidium iodide (PI) was added to the cells for the viability assessment. Finally, the cells were sorted into MEM + 50% FCS medium, washed, and counted accordingly for single-cell RNA sequencing experiments.

For the Bulk RNA sequencing experiments, the sorted cells were placed directly into RLT buffer. Subsequently, the RNA was extracted using the RNeasy Micro Kit according to the manufacturer's protocol as indicated in section 3.7.6. The LPMCs were sorted on the FACS Aria I (BD Bioscience) with a 70-um nozzle. In contrast, the stromal and epithelial cells were sorted on the SH800S cell sorter (Sony Biotechnology) with a 100-um nozzle.

3.11 Statistical analysis

The sample sizes for the respective experiments are included in the figure legends. Statistical tests used are stated in each figure legend. If two or more groups are compared, then an Anova followed by a Tukey's test was run for paired samples. When comparing unpaired samples from two or more groups, the Kruskal-Wallis analysis of variance with a Dunn's post-hoc test were performed. The Mann Whitney U test was used to compare two unpaired samples, respectively. The Spearman analysis was used to look at the correlations of several gene expression in some samples. Results were considered statistically significant where $P \leq 0.05$ and non-significance was stated as "ns". Statistical analyses were performed using Prism v.8 software.

4 Results

4.1 Epithelial cells upregulate the Oncostatin M receptor in intestinal inflammation.

As the overexpression of Oncostatin M (OSM) is seen in numerous human inflammatory diseases[123, 125, 126, 132, 133] and OSM is known to have both pro- and anti-inflammatory effects, the exact function and mechanism of action of OSM have proven to be perplexing and its role in IBD remains ill-defined. Furthermore, there is insufficient data on the regulation of the OSM-receptor (OSMR) expression, its specific biological functions, and its signal transduction in cells other than stromal cells.

To explore the broad expression of OSMR in both immune and non-immune cells in the intestinal tissue, we performed single cell RNA sequencing of steady-state mice and mice treated with oral *Helicobacter hepaticus* (*H.h*) and systemic anti-IL-10 receptor blockade (*H.h* + αIL-10R model) for 18 days. We wanted to identify differences in the OSMR expression between stromal cells, IECs, and immune cells at steady-state and during inflammation. Colitis was induced for 18 days in six C57BL6/J mice while the other six mice were used as steady-state controls. The mice were sacrificed and pooled in groups of twos for cell isolations. Subsequently, the different cell populations were isolated, stained, and hashtagged (**Figure 6A**). Then, the stromal cells were FACS sorted and defined through negative expression of the classical hematopoietic cell marker CD45, the epithelial marker EpCAM, and positive for Calcein AM, a cell-permeant dye (CD45$^-$ EpCAM$^-$ Calcein$^+$), the intestinal epithelial cells (IECs) were sorted as CD45$^-$ and EpCAM$^+$, and the lamina propria mononuclear cells (LPMCs) were sorted as CD45$^+$ and EpCAM$^-$. Single-cell RNA sequencing was then performed on the isolated cell subsets, as previously described in section 3.7.5. The single-cell information was then visualized using uniform manifold approximation and projection (UMAP), a dimensionality reduction which clusters cell types based on the similarity of genetic transcripts. Three clusters emerged, depicting the distribution of the three different cell types (**Figure 6B**).
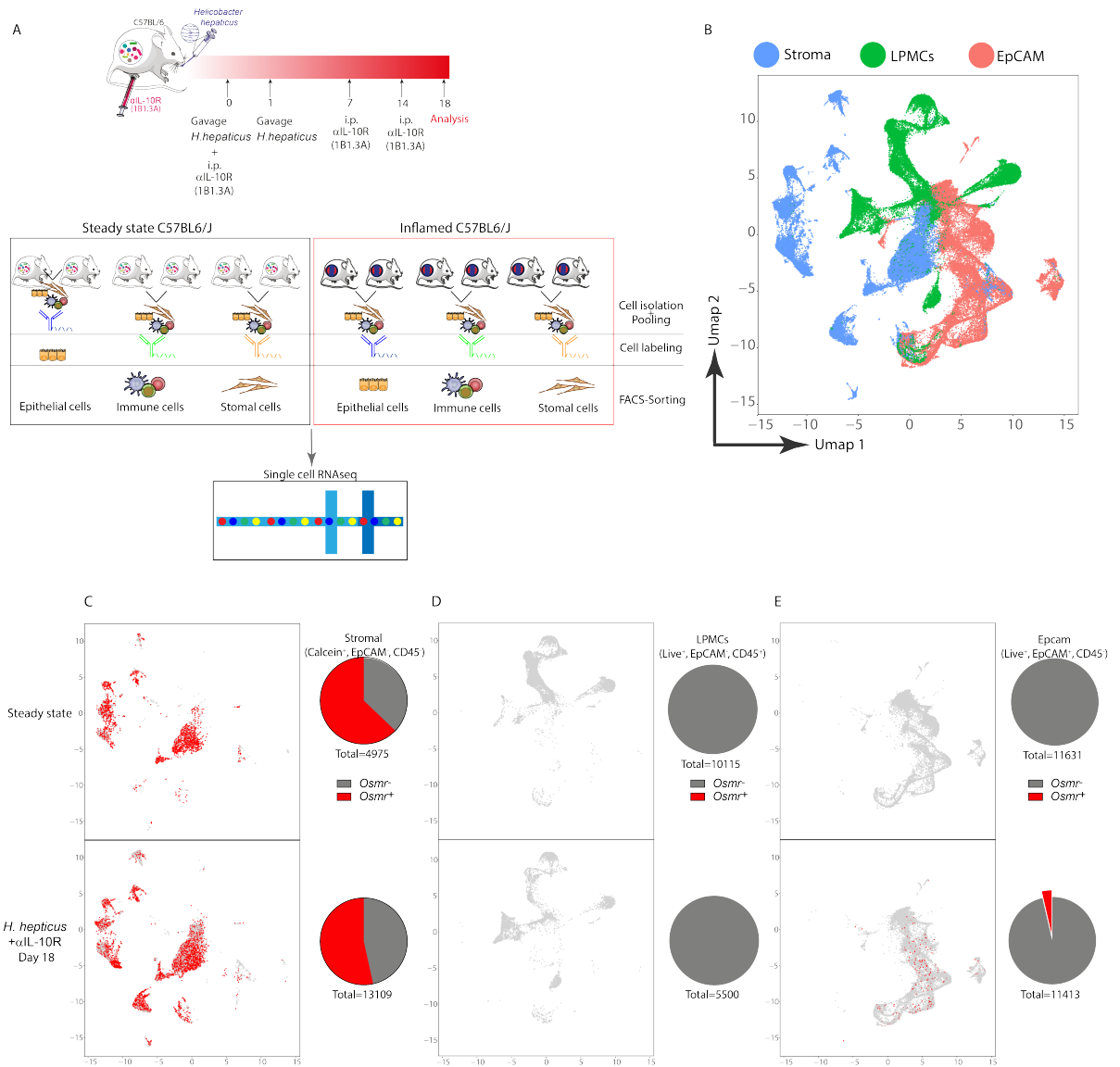
Figure 6: Intestinal epithelial cells express Osmr during inflammation*. (**A**) Schematic representation of the experimental set-up for single-cell data retrieval for stromal cells, immune cells, and IECs from Inflamed and steady-state controlled mice. A total of 12 mice were used in this experiment, the mice were further divided into six mice per treatment group, with mice being pulled in twos. (**B**) A summary of the cell identified within the uniform manifold approximation and projection (UMAP) plot depicting the different cell clusters identified in the colon of the mice. Depicted are the three cell clusters that were sequenced (stroma cells depicted in blue, LPMCs in green, and epithelial cells in pink). (**C**) UMAP (left) and pie graphs (right) show the stromal cell cluster positive for Osmr in red and the Osmr negative cells in gray. (**D**) The LPMC cell cluster, and (**E**) the epithelial cell cluster depicting Osmr positive (red) and Osmr negative (grey) cells.*

The data confirmed that *Osmr* transcripts are expressed on stromal cells at steady-state and during inflammation (**Figure 6C**). The LPMC fraction showed no expression of *Osmr*, neither at steady-state nor during inflammation (**Figure 6D**). Interestingly, the IECs did not express the *Osmr* at steady-state; however, during inflammation, IECs showed *Osmr* expression (**Figure 6E**).

Next, we assessed the spatial and temporal expression of *Osmr* in mouse colon at steady-state and on days 3, 7, 14, 21, and 31 after colitis induction using RNA-Scope *in situ* hybridization and qPCRs of the IECs. The expression of *Osmr* increased during colitis and was strongly expressed in inflamed tissue and restricted predominantly to epithelial cells and stromal cells (**Figure 7A-D**). Moreover, the upregulation of *Osmr* in the different colon segments and the IECs strongly correlated with intestinal inflammation and was maintained for 31 days after colitis initiation (**Figure 7B/D**). Interestingly, the peak in the histopathology score in the *H.h.* induced colitis time kinetic was seen at days 14 and 21 post colitis induction (**Figure 7C**). Additionally, as previously mentioned in section 1.5.1, the mouse OSM ligand does not signal through the murine LIFR but signals only through its specific murine OSMRβ, unlike the human OSM, which activates both OSMRβ and LIFR[125-127]. We further confirmed this phenomenon by looking at the *Lifr* expression in the inflamed mice. Notably, no significant differences were observed in the heterodimer partner *Lifr* as well as *Il31* which uses the OSMR as one of its heterodimeric receptors[183] (**Figure 7E**). Thus, we concluded that in the murine model of colitis, there is a long-term induction of the OSM-receptor in the epithelial cells.
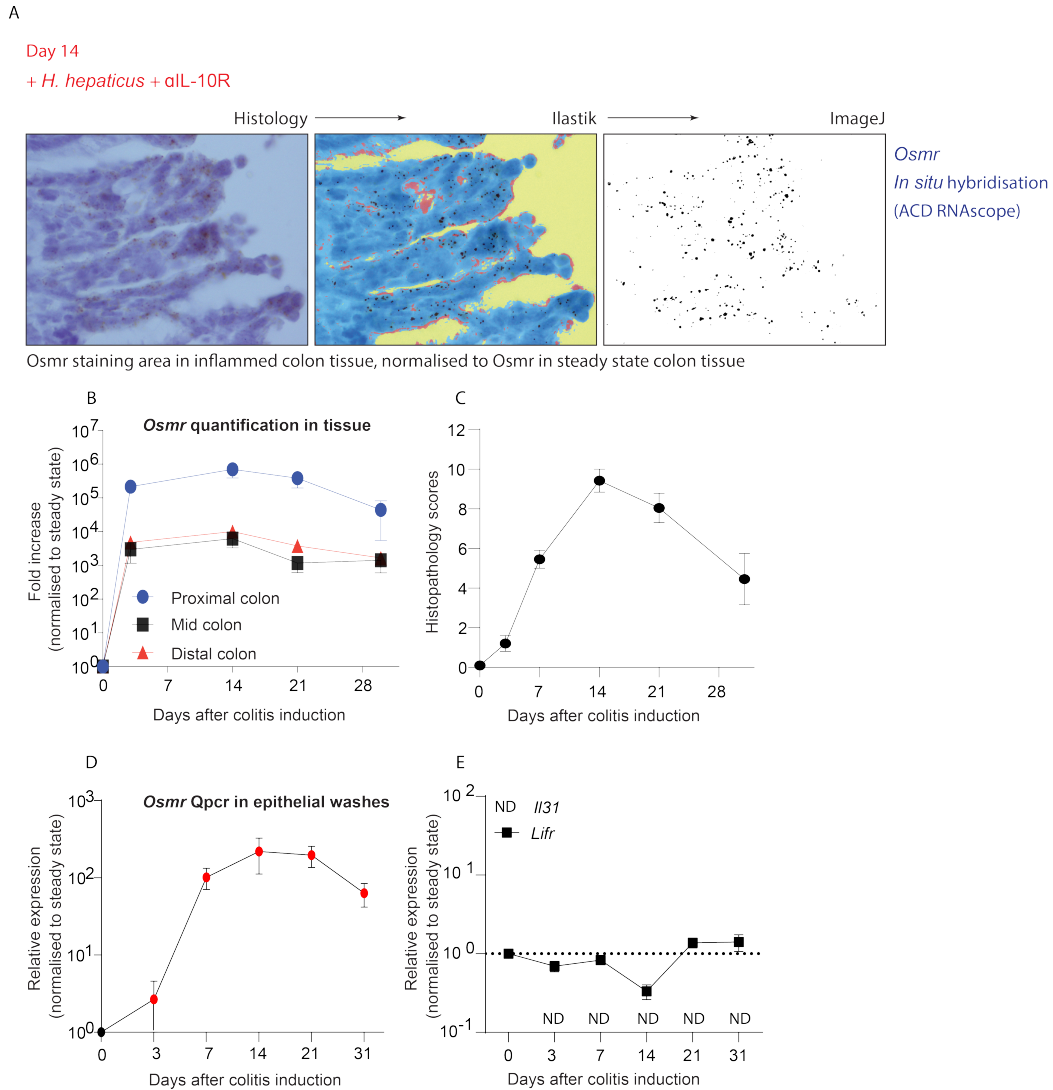
Figure 7: The Osmr is induced in epithelial cells early during colitis. (**A**) The workflow for detecting and quantifying the Osmr expression in the mouse colon by ISH. Detection of Osmr expression in steady state and H.h +αIL-10R colitic mouse colon tissue using in situ hybridization (ISH, punctate brown signal). Tissues were counterstained with hematoxylin. The images were processed with Ilastik, and the expression of Osmr wasquantified with ImageJ. (**B**) ImageJ quantification of the Osmr expression in colitic mice compared to the expression in steady-state mice. The expression was normalized to the steady-state tissue area, error bars represent SEM, n=4 mice per time-point, from one experiment. (**C**) Histopathology scores of the colitic mice during the different time points, the data was normalized to the steady-state mice, error bars represent SEM, n=8 mice per time-point, from two independent experiments. (**D**) Q-PCR of the Osmr, (**E**) Il31, and Lifr expression in the epithelial washes in inflamed mice normalized to the steady-state mice, error bars represent SEM, n≥8 mice per time-point, from 2-4 independent experiments, ND = Not detectable.

Subsequently, the relevance of the murine findings was assessed in human IBD samples. Using the RNAscope *in situ* hybridization (*ISH*) assay based on the Advanced Cell Diagnostics (ACD) technology, which is an improved method that localizes mRNA molecules with greater sensitivity and specificity in a faster time-frame than the conventional *ISH* methods[184]. We demonstrated that *OSMR* transcripts are expressed in the epithelium of IBD patients during inflammation (**Figure 8A**). Additionally, qPCR analysis of the epithelial cell fractions from the IBD patients showed a significant increase in the expression of the *OSMR* compared to the non-inflamed controls (**Figure 8B**).
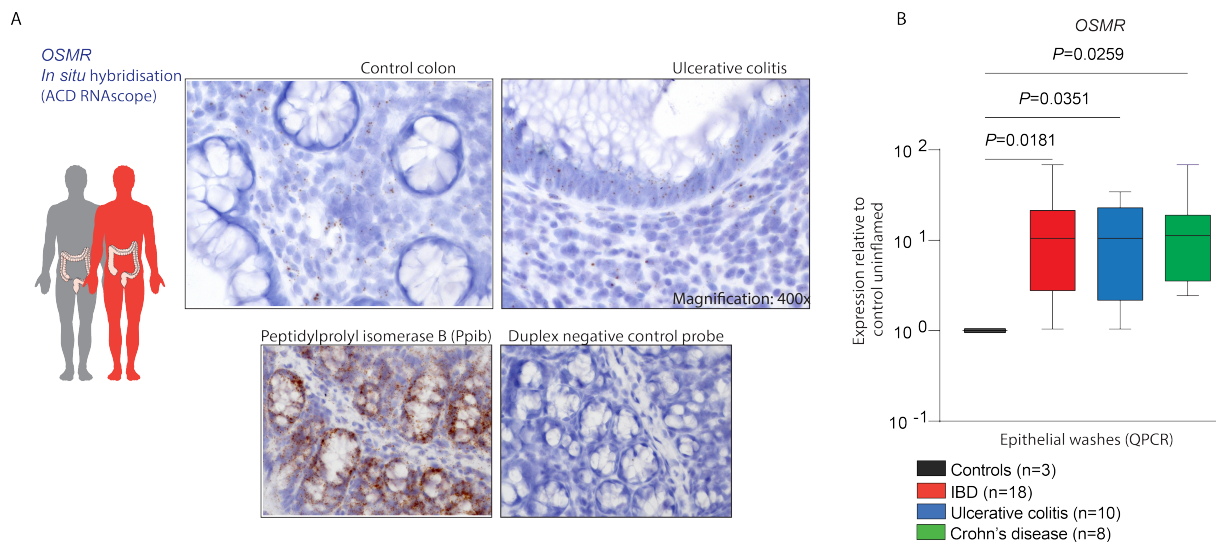

Figure 8:The OSMR is expressed in human epithelial cells during inflammation.*(A) Detection of the OSMR expression in healthy and Ulcerative colitis mucosal samples using RNAscope in situ hybridization based on ACD (Advanced Cell Diagnostics) patented technology (punctate brown signal, upper panel; positive and negative control probes, lower panel). Data represents n=2. (B) Q-PCR gene expression analysis of OSMR in epithelial washes from healthy controls, IBD patients, or samples segregated according to underlying condition (UC and CD). The data represents n=3-10 per condition. P values derived from a Kruskal-Wallis, followed by Dunn's multiple comparison test.*

Together, these results indicate that under homeostatic conditions, the intestinal epithelial cells do not express the *OSMR*; however, during inflammatory conditions, there is a significant expression of the *OSMR* in the epithelial cells. Nevertheless, it remains to be conclusively ascertained whether the expression of *OSMR* on the epithelial cells is pathogenic or protective during inflammation. Therefore, we hypothesized that we would only fully unveil the role of OSMR on epithelial cells through the use of conditional knockout mice.

4.2 OSMR expression in IECs drives intestinal inflammation.

In order to investigate the role of OSMR on different cell populations *in vivo*, we used transgenic mice with the *Discosoma* red Express 2 fluorescent protein (DsRed) to identify specific cell populations. We generated transgenic mice, such as the *Col1a2^{creERT2} x Ai9* henceforth referred to as *DsRed,* targeting stroma cell type*, Villin^{creERT2} x DsRed,* targeting epithelial cell type*,* and *Cdh5^{cre} x DsRed*, targeting endothelial cell type (**Figure 9 A-C**). The appropriate mice were given tamoxifen via intraperitoneal injection (i.p.) once every 24 hours for five consecutive days following the Jackson Laboratory protocol to induce the mentioned cell type-specific reporter expression[166,178].
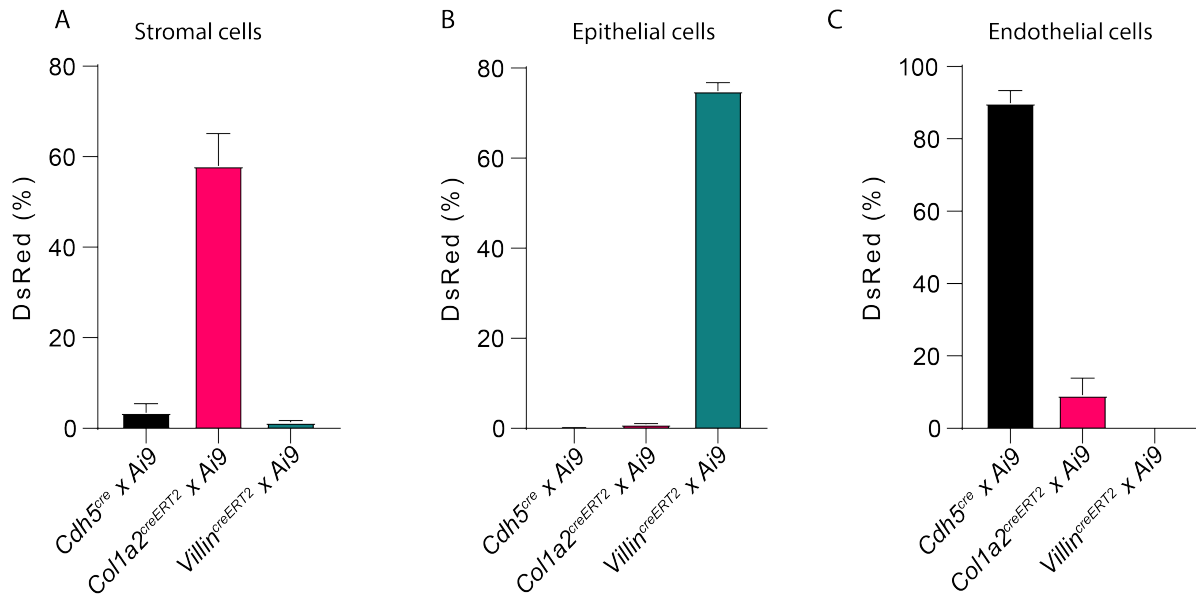
Figure 9: Confirmation of the conditional knockout mice. *(**A-C**) The mice were treated with tamoxifen for 5 days and were analyzed on day 14 after the treatment. The different cell fractions, stromal cells, epithelial cells, and endothelial cells were collected, stained, and analyzed by flow cytometry. The stromal cell fractions were gated as CD45-, CD31-, EpCAM-, and Calcein+, while the epithelial cell fractions were gated as EpCAM+, CD45-, and Calcein+. Lastly, the endothelial cell fractions were gated as EpCAM-, CD45-, CD31+, and Calcein+. (**A**) FACS analysis showing the stromal cell fraction, (**B**) epithelial cell fraction, and (**C**) endothelial cell fraction in the Col1a2^{CreERT} x Ai9, Villin^{CreERT2} x Ai9, and Cdh5^{Cre} x Ai9 mouse lines. The data represents one experiment, n≥ 4 per mouse line.*

The appropriate cell fractions were isolated and analyzed by flow cytometry to track the DsRed labeled cells. FACS analysis of the stromal cell fraction showed that the *Col1a2^{CreERT} x DsRed* mice had the highest frequency of DsRed positive cells compared to the other genotypes (**Figure 9A**). In addition, the *Villin^{CreERT2} x DsRed* mouse line showed the highest frequency of DsRed positive cells in the EpCAM+ epithelial cell fraction compared to the other genotypes (**Figure 9B**). Lastly, the *Cdh5^{Cre} x DsRed* mouse line had the highest frequency of DsRed positive cells in the endothelial CD31+ cell fraction (**Figure 9C**). Overall, this demonstrated the efficiency of the targeted cell types in each mouse line.
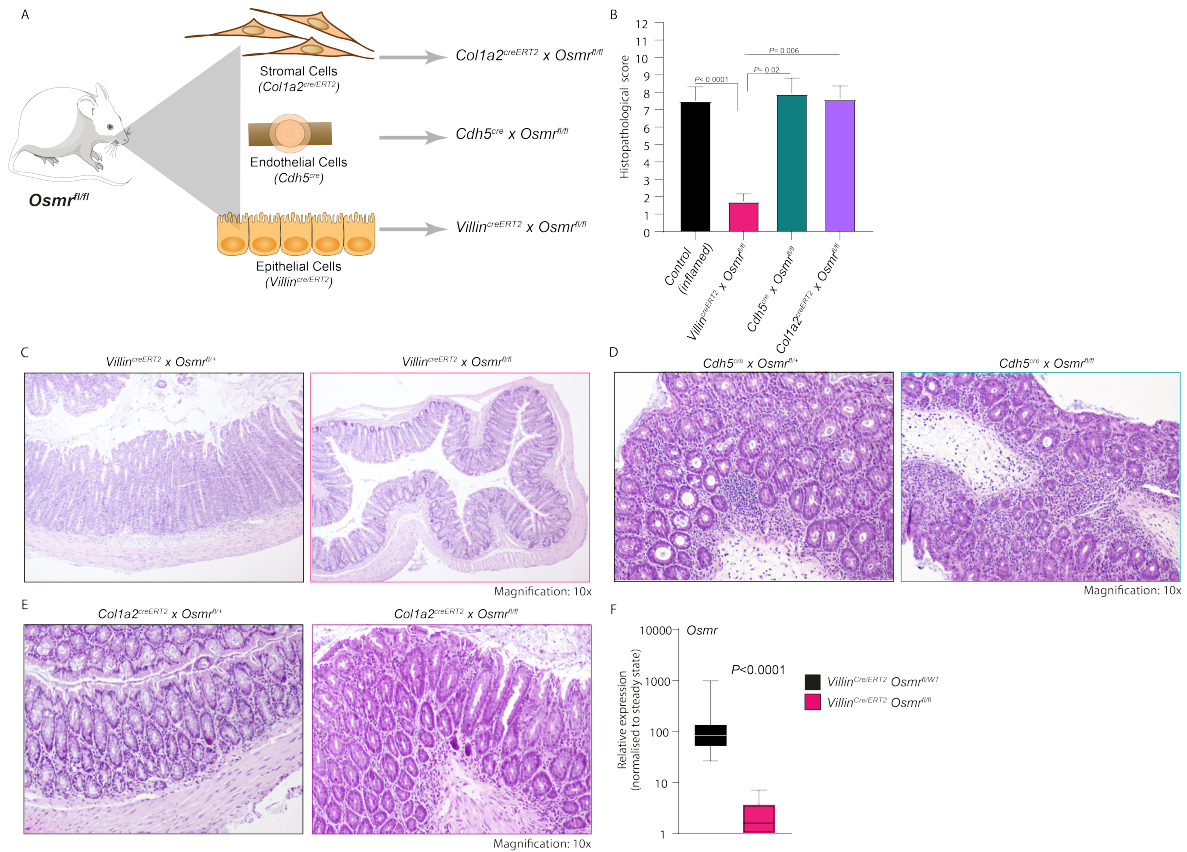
Figure 10: OSMR expression in epithelial cells promotes intestinal inflammation. (**A**) Scheme depicting the crossing of the different cell-specific reporter mouse lines (Villin^{CreERT2}, Cdh5^{Cre}, and Col1a2^{CreERT2}) with Osmr$^{fl/fl}$. (**B**) Histopathology scores for day 21 after colitis induction. The data is representative of two independent experiments, n=8-14 mice per group. P values reflect differences between inflamed Osmr deficient mice, and their respective wild-type mice derived from Kruskal-Wallis test, followed by Dunn's multiple comparison test, error bars represent SEM. (**C**) Representative H&E-stained colon of inflamed Villin^{CreERT2} x Osmr$^{fl/fl}$ mice and Villin^{CreERT2} x Osmr$^{fl/+}$ animals on day 21. (**D**) Representative H&E-stained colon of inflamed Cdh5^{Cre} x Osmr$^{fl/fl}$ mice and Cdh5^{Cre} x Osmr$^{fl/+}$ animals on day 21. (**E**) Representative H&E-stained colon of inflamed Col1a2^{CreERT2} x Osmr$^{fl/fl}$ mice and inflamed Col1a2^{CreERT2} x Osmr$^{fl/+}$ animals on day 21. (**F**) The efficiency of the knockout in the epithelial washes of the Villin^{CreERT2} x Osmr$^{fl/fl}$ mice and Villin^{CreERT2} x Osmr$^{fl/+}$ mice was analyzed by qPCR of the Osmr expression. The data is representative of two independent experiments, n=8-14 mice per group. P values derived from the Mann Whitney U-test.

In line with the validation of the cell-specific reporter mouse lines, we studied the relevance of the OSMR-expressing cell types in intestinal inflammation; we evaluated the *Villin*[CreERT2] *x Osmr*^{fl/fl}, *Cdh5*[Cre] x *Osmr*^{fl/fl}, and *Col1a2*[CreERT2] x *Osmr*^{fl/fl} mouse lines (**Figure 10A**). The appropriate mice were treated with tamoxifen for five days, and colitis was induced for 21 days. Interestingly, we observed a significant decrease in the overall histopathology score in the *Villin*[CreERT2] *x Osmr*^{fl/fl} mice (**Figure 10B/C**). Furthermore, the removal of the *Osmr* from the stromal and endothelial cells showed no significant reduction in the histopathology score (**Figure 10B/D/E**). Lastly, we confirmed the efficiency of the OSMR knockout in the *Villin*[CreERT2] *x Osmr*^{fl/fl} and *Villin*[CreERT2] *x Osmr*^{fl/+} by qPCR after tamoxifen injection and colitis induction for 21 days. Notably, the *Villin*[CreERT2] *x Osmr*^{fl/fl} had significantly lower *Osmr* expression compared to the *Villin*[CreERT2] *x Osmr*^{fl/+} (**Figure 10F**).

It has been well-described that during inflammation, there is a substantial increase in the infiltration of inflammatory cells, including monocytes, macrophages, neutrophils, eosinophils, and T cells[45, 52, 143, 185-188]. We therefore used different gating strategies (**Figures 11&12**) to identify the infiltrating leukocytes in *H.h* + αIL-10R induced colitis[132].
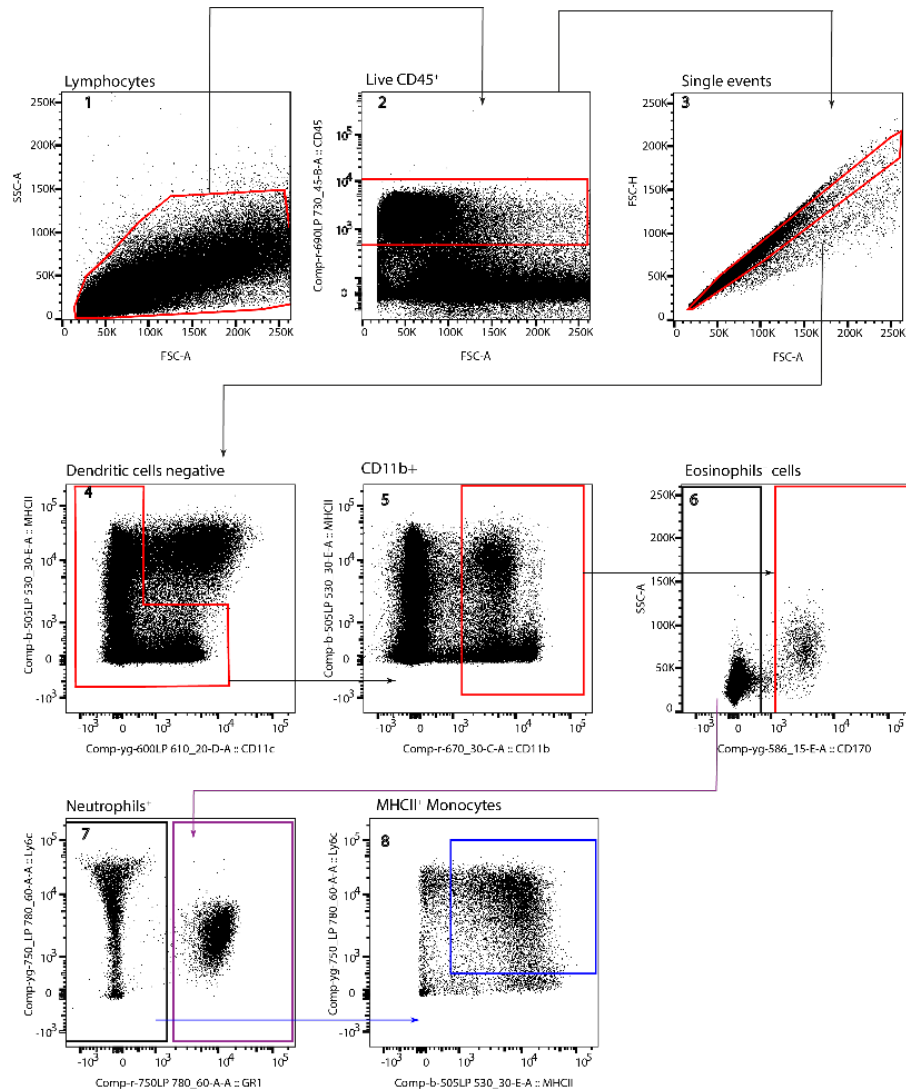
Figure 11: Flow-cytometry gating strategy scheme. *(A) Gating strategy for identifying the myeloid cells in the LP of the mice. Representative data from the LP of colitis mice on day 21 after H.h colitis induction.1) Lymphocytes were first gated based on FSC-A and SSC-A, followed by 2) live-gated CD45+ colonic cells and the exclusion of 3) doublets. Then, 4) negative dendritic cells were further analyzed based on MHCII and CD11c expression. 5) CD11b+ and MHCII+ cells were gated on, followed by 6) eosinophil-positive cells based on Siglec-F expression. Siglec-F negative cells were further analyzed based on Ly6C+/GR1+ labeled as 7) neutrophil positive cells (purple). The negative neutrophil fraction was further gated on, and Ly6C+/MHCII+ monocytes were identified.*
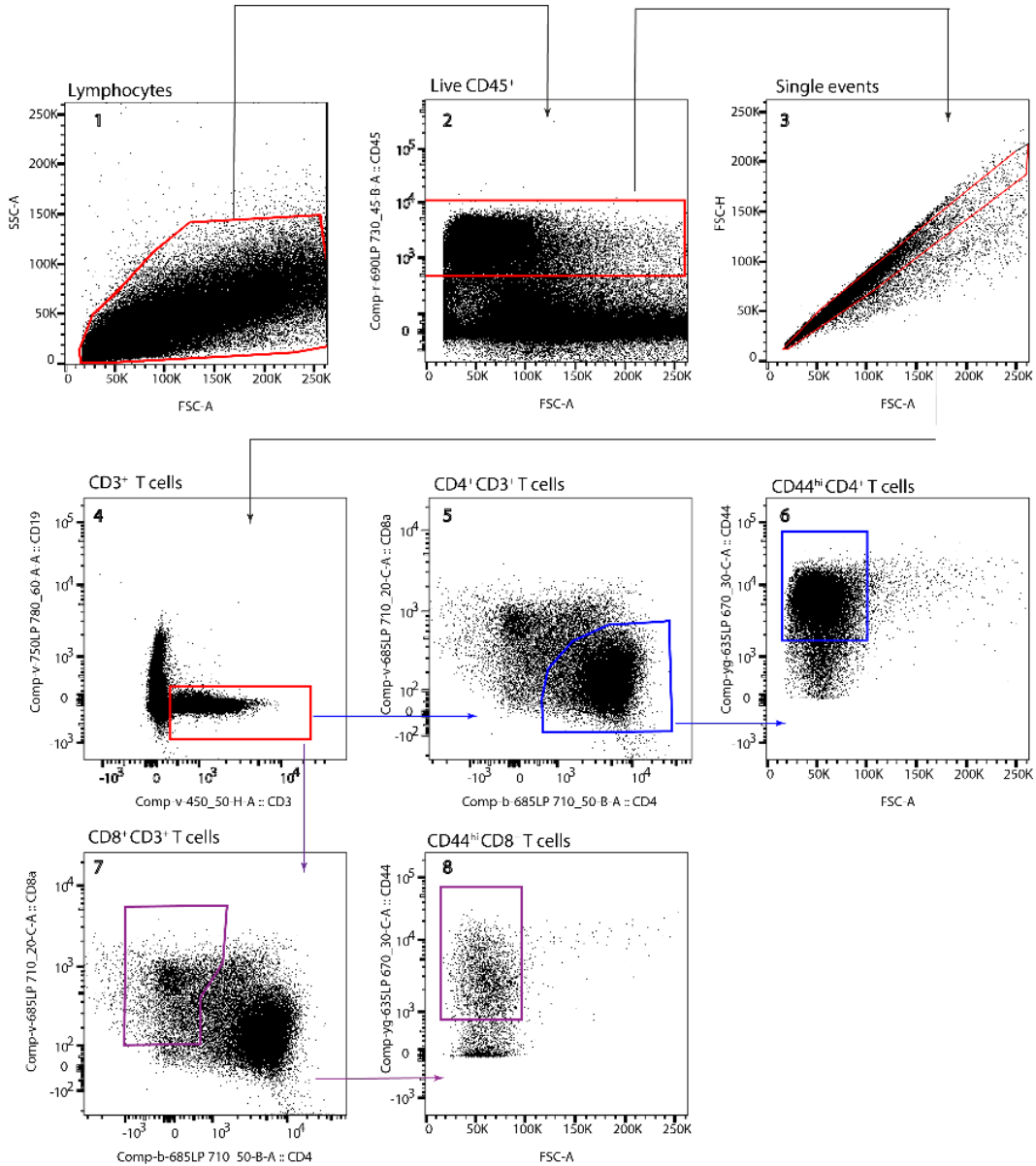
Figure 12: Flow cytometry gating strategy of LP of different T-cell populations. *(A) Representative data from the LP of colitis mice on day 21 after H.h colitis induction.1) Lymphocytes were first gated based on FSC-A and SSC-A, followed by 2) live-gated CD45⁺ colonic cells and the exclusion of 3) doublets. Then, 4) CD3⁺/CD19- cells were identified. 5) CD4⁺ and CD3⁺ (blue) cells were gated on, followed by identifying 6) CD4 high/CD4⁺ T-cells. 7) CD8⁺/CD3⁺ cells were also gated to identify CD44high/CD8⁺ T cells (Purple).*

Moreover, we investigated the accumulation of immune cells in the *Villin^CreERT2* x *Osmr*-deficient mice mentioned. Interestingly, the *Villin^CreERT2* x *Osmr^fl/fl* mice had significantly less immune cell accumulation compared to the *Villin^CreERT2* x *Osmr^fl/+* mice (**Figure 13A**).
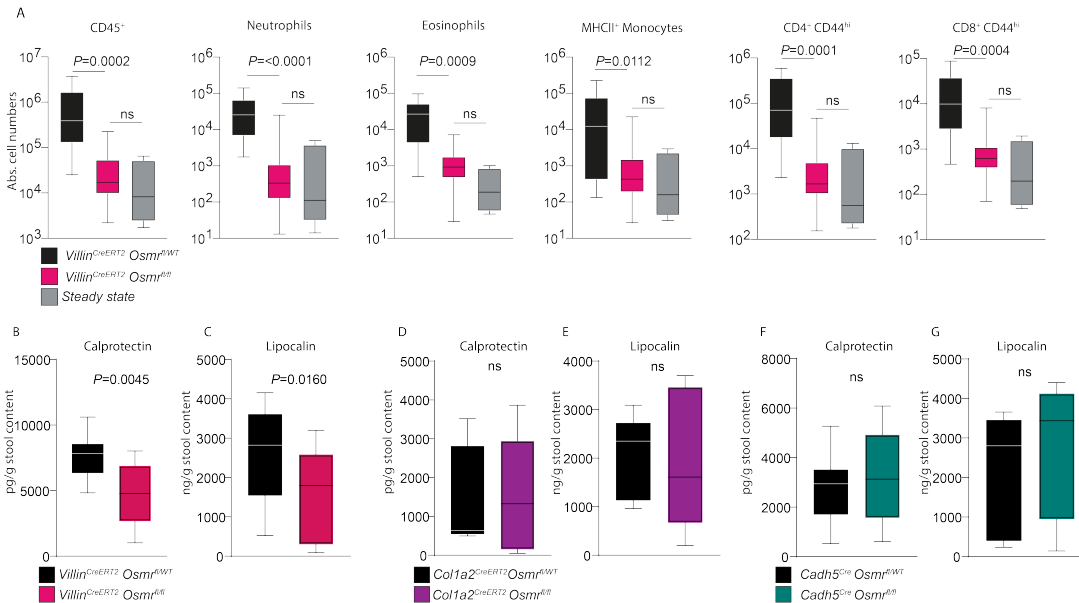

***Figure 13: OSMR expression in epithelial cells promotes the accumulation of immune cells and pro-inflammatory markers**. (**A**) Flow cytometry was used to analyze the frequency and absolute numbers in the different mouse genotypes. Cells were identified as live-gated CD45+ colonic cells, eosinophil positive cells based on Siglec-F expression. Neutrophil-positive cells were characterized based on Ly6C+/GR1+, and MHCII positive monocytes were characterized as Ly6C+/MHCII+. CD44^high/CD4+ T-cells and CD44^high/CD8+ T-cells were also analyzed. The data is representative of two independent experiments, n≥ 5 mice per group. P values were derived from a Kruskal-Wallis, followed by Dunn's multiple comparison test. (**B**) Calprotectin and (**C**) lipocalin ELISA from mouse fecal samples from the Villin^CreERT2 x Osmr^fl/fl vs Villin^CreERT2 x Osmr^fl/+ mice. (**D**) Calprotectin and (**E**) lipocalin ELISA from mouse fecal samples from the Col1a2^CreERT2 x Osmr^fl/fl vs Col1a2^CreERT2 x Osmr^fl/+ mice. (**F**) Calprotectin and (**G**) lipocalin ELISA from mouse fecal samples from the Cdh5^Cre x Osmr^fl/fl vs Cdh5^Cre x Osmr^fl/+ mice. The data is representative of two independent experiments, n≥ 7 mice per group. P value derived from the Mann Whitney U-test, ns= not significant.*

Additionally, the putative fecal inflammatory biomarkers, neutrophil gelatinase-associated lipocalin (NGAL), known as lipocalin 2 (LCN2) and calprotectin, were assessed in the *Villin^CreERT2* x *Osmr* deficient and sufficient mice. Our data showed significant decrease in the lipocalin and calprotectin levels in the fecal samples of the *Villin^CreERT2* x *Osmr^fl/fl* mice (**Figure 13B/C**). In addition, no significant changes were

observed in the lipocalin and calprotectin levels of the *Col1a2^CreERT2 x Osmr^fl/fl* mice or the *Cdh5^Cre x Osmr^fl/fl* compared to their respective controls (**Figure 13D-G**).

Next, we investigated the changes in the gene expression of the IECs in inflamed *Villin^CreERT2 x Osmr^fl/fl* and the *Villin^CreERT2 x Osmr^fl/+* using conventional bulk RNA sequencing. In brief, IECs were isolated from the mentioned mouse strains and RNA was isolated using the RNeasy Micro kit from Qiagen, following the manufacturer's protocol. In line with our previous data, the bulk-RNA analysis of the *Villin^CreERT2 x Osmr^fl/fl* mice showed a decrease in the expression of chemokines and antimicrobial peptides (**Figure 14A**). In addition, the presence of OSM promoted robust defense and inflammatory responses (**Figure 14B**). Collectively, the results revealed the pathogenic characteristics of OSM and OSMR in IECs during inflammation.
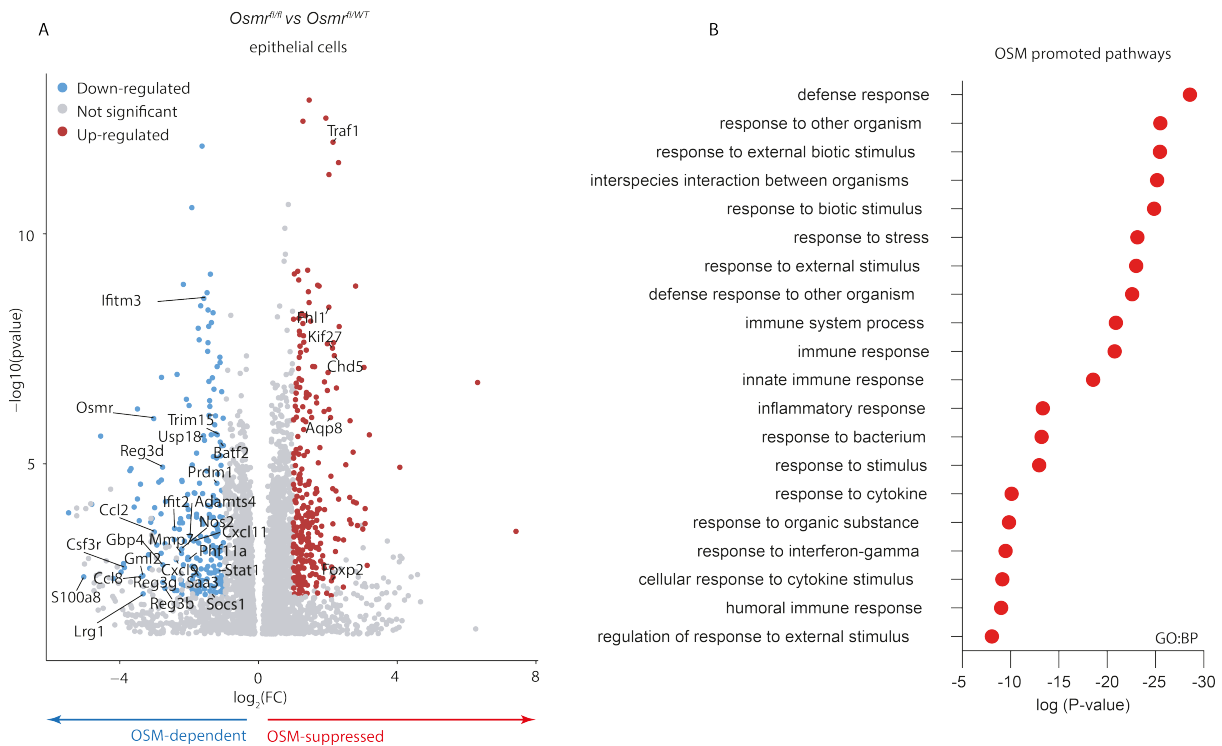
Figure 14: OSMR expression in epithelial cells drives the expression of chemokines and antimicrobial peptides (**A**) Volcano plot showing the proportion of differentially expressed genes on *Villin^CreERT2 x Osmr^fl/fl* mice colonic epithelial cells. (**B**) Top 20 biological processes associated with common differentially expressed genes on *Villin^CreERT2 x Osmr^fl/fl* mice colonic epithelial cells. Data collected from two independent experiments, n≥4.

4.3 IL-22 induces the OSMR expression in IECs during intestinal inflammation.

Based on our findings, we sought to determine which signals were required to modulate the upregulation of OSMR in intestinal epithelial cells. Using the Fluidigm Biomark HD platform and qPCR, we established a high-throughput screening system with mouse intestinal organoids treated with various cytokines, TLR stimuli, and bacterial lysates. Our initial qPCR analysis of the stimulated colonic intestinal epithelial organoids showed IL-22 was the main cytokine that robustly induced the OSMR in epithelial cells *in vitro* (**Figure 15A-B**).

IL-22 has been implicated in facilitating the restitution of epithelial cells in acute colonic infections and injury in the *Citrobacter rodentium* murine model and the dextran sulfate sodium (DSS)-induced murine colitis[134, 135, 141, 153, 189-192]. To address the question of whether IL-22 was expressed in our *H.h* + αIL-10R model, we looked at *Il22* expression in the colon at steady-state and days 3, 7, 14, 21, and 31 after colitis induction. Our analysis showed that *Il22* expression increased significantly in the *H.h* + αIL-10R colitis model on days 7 and 14 (**Figure 15C**). Moreover, IL-22bp is known for its ability to bind to IL-22 and interfere with its ability to bind to its receptor[138, 141, 142, 144, 152, 153, 155]. Therefore, the expression of *Il22bp* was measured to ensure that IL-22 in this *H.h* + αIL-10R colitis mouse model was able to bind and modulate cell signaling. There were no significant differences in the *Il22bp* expression in the *H.h* + αIL-10R colitis model compared to the steady-state mice (day 0) (**Figure 15C**).
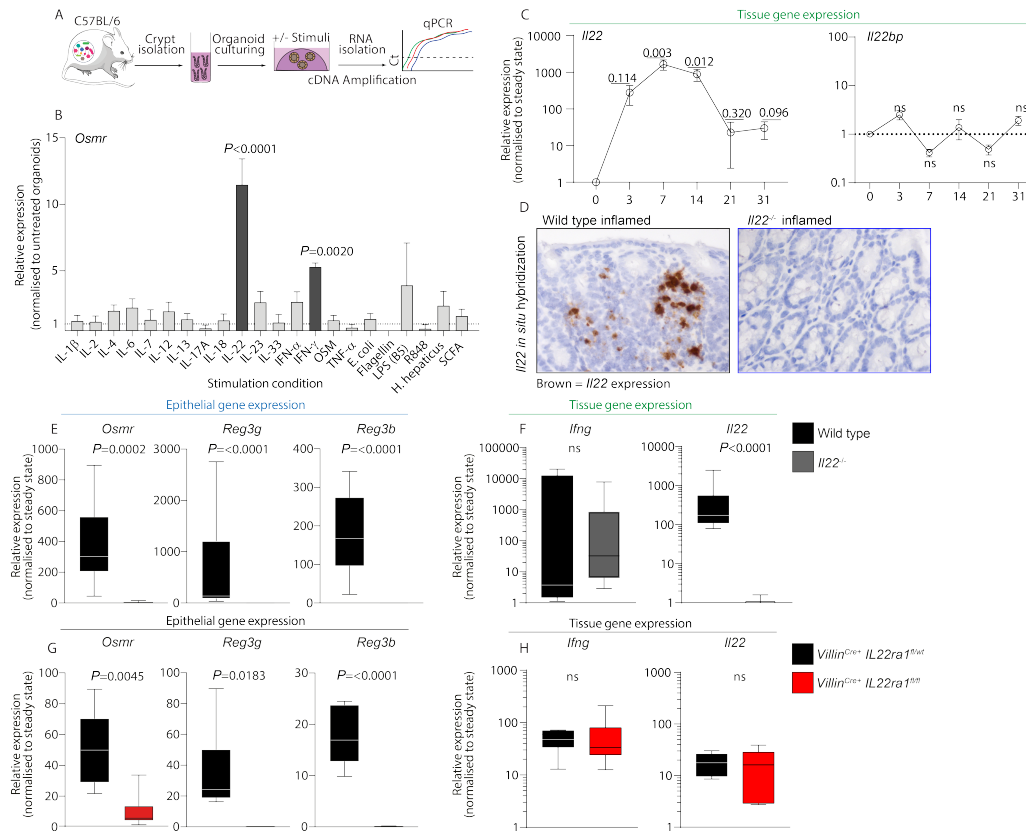
***Figure 15: IL-22 induces the Osmr expression in colonic epithelial cells.** (**A, B**) Mouse colon organoids were generated from female C57BL6/J mice and were stimulated with various stimuli as depicted. Organoids were stimulated with the depicted conditions for 24h (**B**) Detection of Osmr expression by q-PCR. The data is derived from one independent experiment with three independent biological replicates. (**C**) The expression of Il22 and Il22bp in colons of colitic mice (n=7-14 mice per time point and is representative of 2-5 independent experiments). Statistics: one sample t and Wilcoxon test were performed on the data; error bars represent SEM. (**D**) Detection of Il22 expression in inflamed Il22-/+ and Il22-/- mice mucosal samples using in situ hybridization (punctate brown signal). (**E, F**) Il22-/- or littermate WT inflamed mice from 7 days after the induction of colitis. **E**) Q-PCR gene expression analysis of Osmr, Re3g, and Reg3b in epithelial cells from inflamed mice normalized to epithelial cells isolated from steady-state mice. **F**) Q-PCR gene expression analysis of Il22 and Ifng in the colon tissue from inflamed mice normalized to steady-state mice. n≥ 5 mice per genotype, the data is representative of two independent experiments. Statistics: Mann-Whitney U test. (**G, H**) Inflamed Villin^CreERT x Il22ra1^fl/fl or Villin^CreERT x Il22ra1^fl/+ from 7 days after colitis induction. **G**) Q-PCR gene expression analysis of Osmr, Re3g, and Reg3b in epithelial cells from inflamed mice normalized to epithelial cells isolated from steady-state mice. (**H**) Q-PCR gene expression analysis of Il22 and Ifng in the colon tissue from inflamed mice normalized to steady-state mice. The data is representative of one independent experiment (n= 6 mice per genotype). Statistics: Mann-Whitney U test, ns= not significant.*

66

To further understand the importance of IL-22 in orchestrating intestinal inflammation, we induced colitis for 7 days in IL-22–deficient animals (**Figure 15D-F**). We first confirmed the expression of IL-22 in the *H.h* + αIL-10R colitis mouse model using *ISH* of the colon tissue of the *Il22$^{-/-}$* and *Il22$^{+/+}$* mice (**Figure 15D**). Markedly, *Il22* expression was undetectable during inflammation in the colonic tissue of the *Il22$^{-/-}$* mice, while the *Il22$^{+/+}$* inflamed mice showed *Il22* expression in their colonic tissue (**Figure 15D**). Next, we showed that the *Il22* deficient mice had significantly less expression of the *Osmr* as well as *Reg3g* and *Reg3b*, antimicrobial proteins upregulated downstream of IL-22 signaling (**Figure 15E**).

To further comprehend the significance of IL-22 in inducing the expression of OSMR in IECs, we used mice with the IL22RA1 deletion in epithelial cells (*Villin^{CreERT}xIl22ra1$^{fl/fl}$*) and induced colitis for 7 days. The *Villin^{CreERT}* x *Il22ra1* deficient mice showed reduced *Osmr* upregulation on epithelial cells in colitis as well as *Reg3g* and *Reg3b* (**Figure 15G**). Though we saw a decrease in the histopathology score of the *Villin^{CreERT}* x *Il22ra1* deficient mice, the level of *Ifng* and *Il22* in the colonic tissue of the mice were not significantly different, highlighting that the inflammation was not entirely ameliorated (**Figure 15H**).
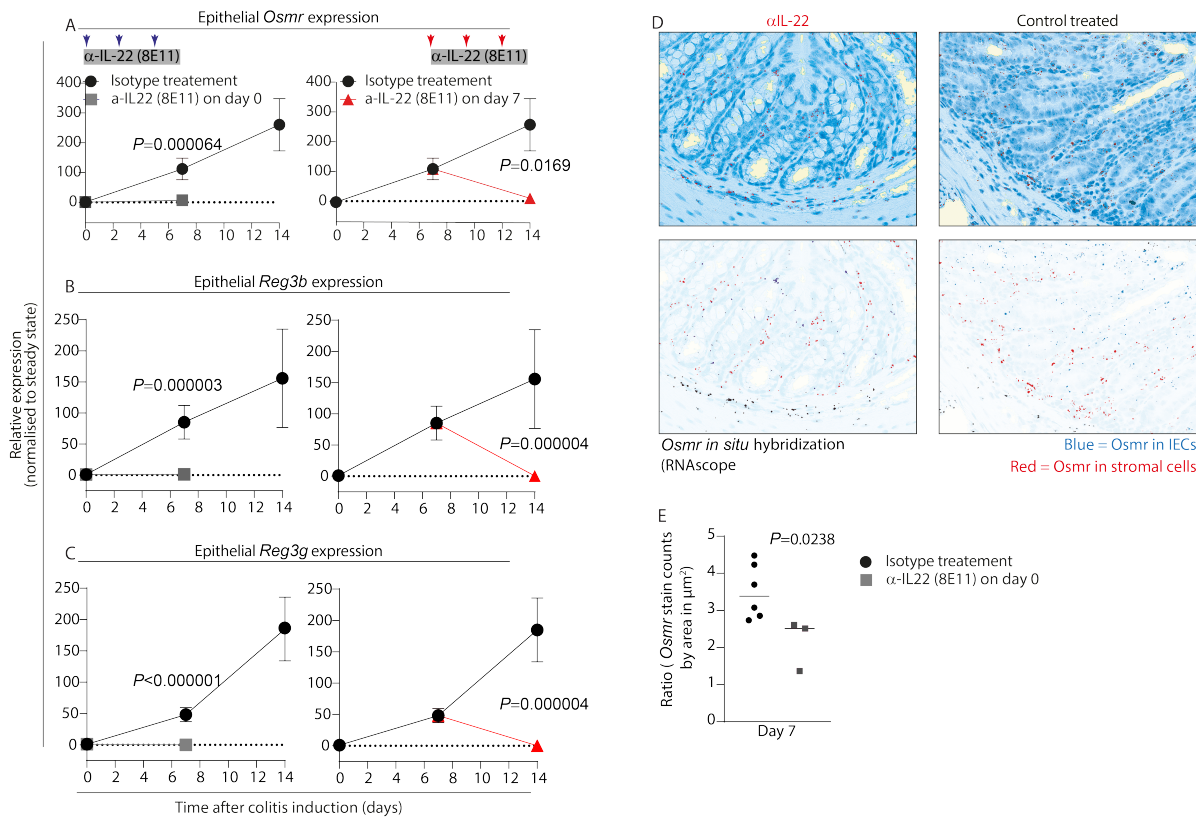
Figure 16: IL-22 blockade led to a decrease in the Osmr expression in colonic epithelial cells
*(**A-C**) Induction of colitis using the H.h +αIL-10R protocol. Mice were treated with anti-IL-22, and control mice were treated with isotype controls. Mice were analyzed on day 7 or day 14, which corresponds to peak disease severity. (**A**) Osmr (**B**) Reg3b (**C**) Reg3g expressions were quantified in epithelial washes by q-PCR. The data is representative of at least two independent experiments with n=≥8 per time point, P values derived from Mann-Whitney U test comparing the respective time points. (**D**) Detection of Osmr expression in anti-IL-22 or isotype treated mouse colon using in situ hybridization (punctate red depicting Osmr in stromal cells and blue depicting Osmr in epithelial cells, upper panel; Ilastik processed picture, lower panel). Data represents n=2. (**E**) Quantification showing the ratio of detected Osmr from anti-IL-22 (gray square) treated or isotype (black circles) treated mice. Statistics: Mann-Whitney U test.*

To evaluate further the relevance of IL-22 in driving OSMR expression in intestinal inflammation, we used an anti-IL-22 antibody to block IL-22 *in vivo*. IL-22 was blocked at two different time points. We blocked IL-22 at the beginning of the colitis induction (day 0) and analyzed the mice at day 7, while at the second time point, IL-22 was blocked after 7 days of colitis induction (day 7), and these mice were analyzed at day 14. Both blocking strategies strongly reduced *Osmr* as well as *Reg3g* and *Reg3b* expression on

epithelial cells during colitis induction (**Figure 16 A-C).** Further confirmation using *ISH* depicted a decrease of *Osmr* in the anti-IL-22 treated mice at day 7 after colitis induction (**Figure 16D/E**).
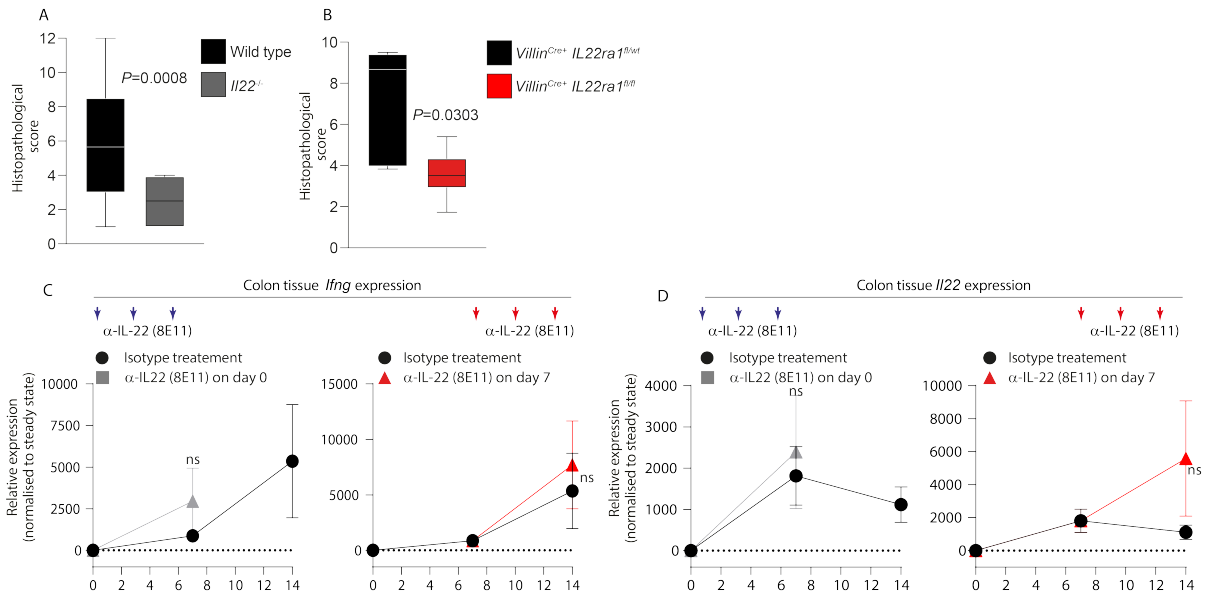

Figure 17: IL-22 is important for decreasing the histopathology scores in H.h induced colitis but does not impact the expression of Ifng in the colonic tissue*. (A) Histopathology scoring of Il22^{-/-} or littermate WT inflamed mice from 7 days after the induction of colitis, the data is representative of two independent experiments, n≥5 mice per genotype, P value derived from Mann-Whitney U test. (B) Histopathology scoring of Inflamed Villin^{CreERT} x Il22ra1^{fl/fl} or Villin^{CreERT} x Il22ra1^{fl/+} from 7 days after colitis induction, the data is representative of one experiment, n=6 mice per genotype, P value derived from Mann-Whitney U test. (C, D) Q-PCR gene expression analysis of (C) Ifng and (D) Il22 from mice treated with anti-IL-22 or isotype control. Mice were analyzed on days 7 or 14. The data is representative of at least two independent experiments with n=≥8, P values derived from Mann-Whitney U test comparing the respective time points, ns= not significant.*

Furthermore, we assessed the histology of the *Il22* deficient and *Il22* sufficient mice. The *Il22^{-/-}* had a significantly lower histopathology score compared to their respective littermate inflamed controls (**Figure 17A**). In addition, the *Villin^{CreERT}* x *Il22ra1* deficient mice also had a significantly lower histopathology score compared to their respective control inflamed mice (**Figure 17B**). Interestingly, though the expression of *Osmr* was reduced, we did not see a significant reduction of *Il22* and *Ifng* expression in the colonic tissue (**Figure 17C/D**).

Using the Fluidigm Biomark HD platform, we further confirmed IL-22 as a cytokine that induces the OSMR expression in intestinal epithelial organoids (**Figure 18A**). Moreover, the platform allowed the authentication/validation of the efficiency of the various stimulants used in the experiment. We could check the response genes of the different stimuli to determine their potency. In turn, this fostered the indisputable insight that IL-22 is responsible for the OSMR expression in IECs. Notably, IL-22 stimulation led to the upregulation of antimicrobial peptides, such as the IL22-responsive transcripts, *Reg3b*, and *Socs3* in the intestinal organoids (**Figure 18B**). Furthermore, the stability of the OSMR after IL-22 removal was assessed using colonic organoids. Intriguingly, IL-22 is needed to maintain the OSMR expression on the intestinal organoids (**Figure 18C**).
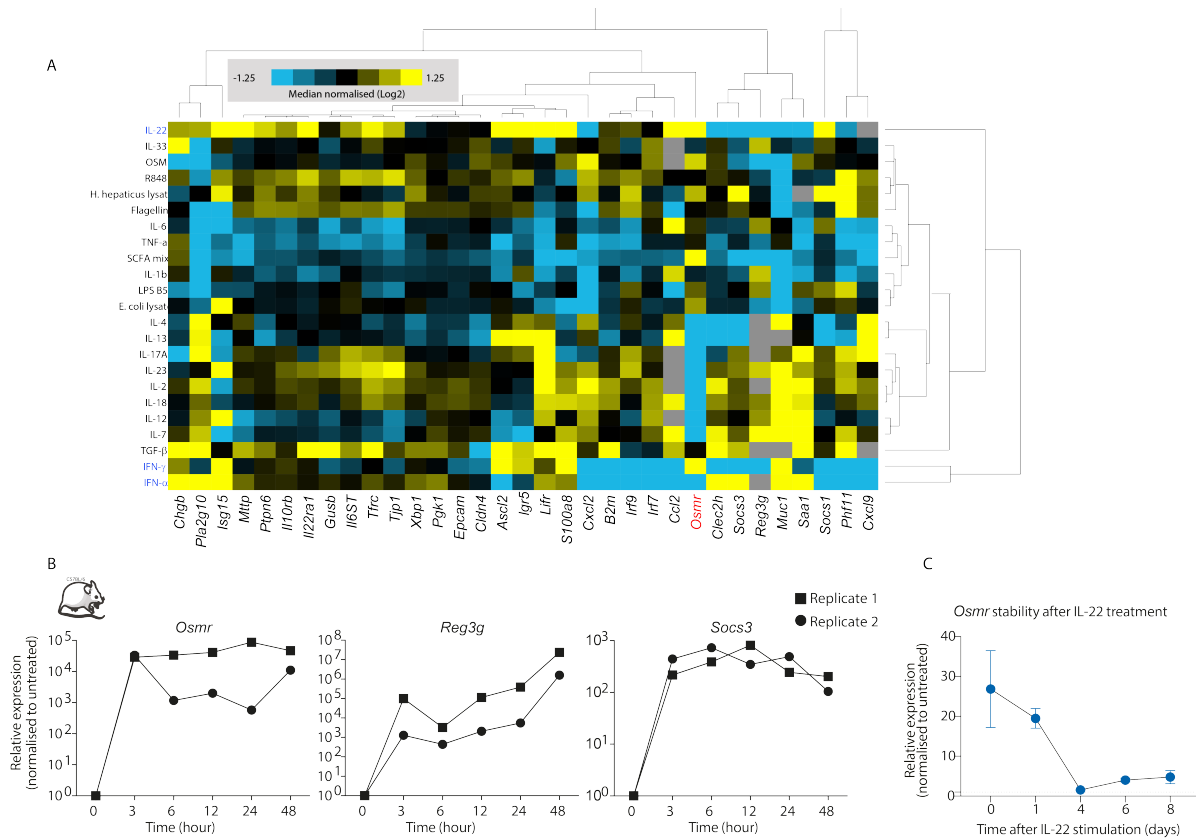
***Figure 18: IL-22 induces as well as maintains the Osmr expression in colonic epithelial cells** (A) Q-PCRs were performed on the Fluidigm Biomark platform using indicated primers. The data is derived from one independent experiment with three independent biological replicates. The expression was normalized to the median expression and log$_2$ transformed. **(B)** Epithelial organoids generated from the colon of C57BL/6J WT mice were stimulated with 10 ng/µl IL-22 for 3 to 48h. The respective organoids were collected at 3h, 6h, 12h, 24h, and 48h after stimulation with IL-22 and analyzed by qPCR. The gene expression analysis of Osmr, Reg3g, and Socs3 from the different time points were normalized to the unstimulated control. **(C)** Intestinal epithelial organoids isolated from the colon of C57BL/6 mice were stimulated with 10 ng/mL of IL-22 for 48h. Then the organoids were cultured in a medium without IL-22 for 24h and subsequently passaged by the mechanical splitting technique. Samples were taken on days 0, 1, 4, 6, and 8. Q-PCR gene expression analysis of Osmr from the stimulated organoids was normalized to the unstimulated controls. Data is shown for n=1 biological replicate with n=2 technical replicates, error bars represent SEM.*

To determine whether IL-22 induces OSMR in human epithelial cells, we stimulated human intestinal organoids with IL-22, IFN-γ, TNF, and LPS. Our data revealed only the stimulation with IL-22 induced OSMR in human epithelial organoids (**Figure 19A/B**). In addition, *ISG15*, an IFN-γ response gene, and *REG3g* were analyzed to confirm the viability/efficacy of the cytokine stimulations (**Figure 19B**). Moreover, IL-22 stimulation

led to the expression of OSMR and SOCS3 in human organoids (**Figure 19C**). To further investigate the relevance of these signals in human IBD, we confirmed the association between *IL22, IFNG, IL23A, IL12A, IL12B*, and *OSMR* expression in mucosal tissue samples from publicly available datasets of the RISK IBD cohort. The cohort is from the Gene Expression Omnibus (GEO) dataset GSE57945, composed of ileal biopsies from pediatric healthy control patients and patients newly diagnosed with ileal CD, colonic CD, and UC (**Figure 19D/E**). Together, these data identify IL-22 as a critical regulator and maintainer of the OSMR, at the transcript level in the intestinal epithelial cells.
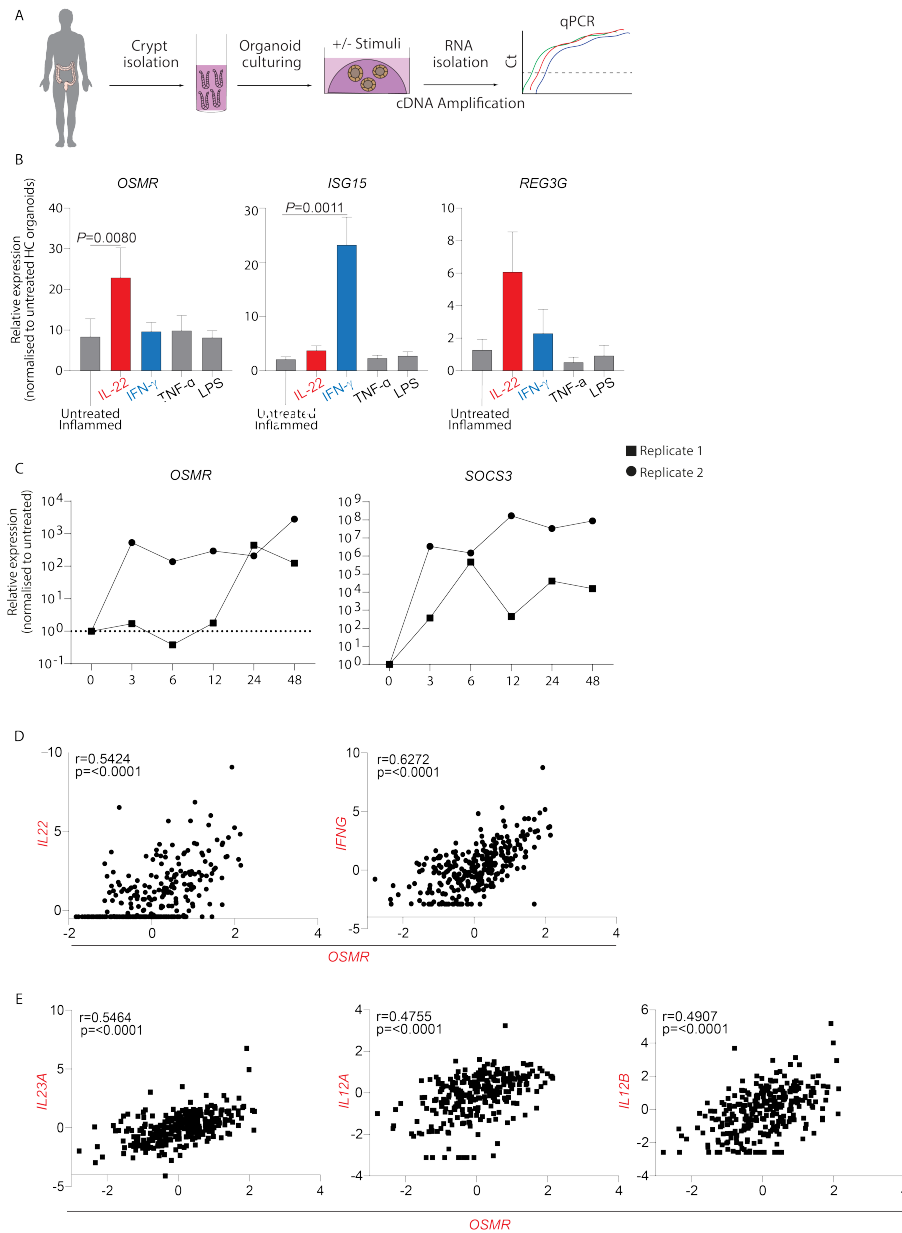
Figure 19: IL-22 induces the OSMR expression in human colonic epithelial organoid. (**A**)Scheme depicting the workflow for human organoid culturing. (**B**) Human epithelial organoids were generated from human specimens (healthy, IBD samples; IBDome Cohort). Organoids were stimulated with the depicted conditions for 24h. Statistics: one-way ANOVA with Dunn's multiple comparisons tests, error bars represent SEM, n=4. (**C**) Human epithelial organoids were stimulated with 10 ng/µl of IL-22 for 3 to 48h. The respective organoids were collected at 3h, 6h, 12h, 24h, and 48h after stimulation with IL-22 and analyzed by qPCR. The qPCR gene expression analysis of OSMR and SOCS3 from the different time points were normalized to the unstimulated control. (**D**) Spearman correlation of OSMR expression with IL22 and IFNG, as well as (**E**) IL23A, IL12A, and IL12B in pooled healthy control and IBD biopsies assessed by RNAseq (RISK IBD cohort, n = 280).

4.4 IL-22 induction of OSMR is STAT3- dependent.

The downstream signaling of IL-22 occurs through a plethora of signal transducers and transcription factors such as the Jak1, tyrosine kinase 2 (Tyk2), and transcription factor-3 (STAT3), STAT1, STAT5, protein kinase B (AKT)/ mechanistic target of rapamycin (mTOR), and MAPK[134, 138, 142, 147, 148, 164]. Particularly, IL-22 predominantly signals through STAT3 to promote epithelial cell survival; however, several of the pro-inflammatory effects are caused by STAT1[43, 189, 193]. As our data demonstrated that IL-22 is needed for OSMR upregulation on IECs, we questioned which downstream signaling factors were essential for OSMR on epithelial cells during inflammation.

To address the downstream signaling factors driving OSMR induction in epithelial cells, we analyzed the promoter regions of mouse *Osmr* and detected STAT1 and STAT3 binding sites upstream of the transcription start site (data not shown). The STAT3 pathway was examined using the *Villin*^{CreERT2} x *Stat3*$^{fl/fl}$ and *Villin*^{CreERT2} x *Stat3*$^{fl/+}$ and for the assessment of the STAT1 pathway, *Stat1*$^{-/-}$ and *Stat1*$^{+/+}$ mice were used. Colitis was induced for 7 days in these mice, and the epithelial cells and tissues were analyzed. Our data revealed that the deletion of STAT3 from the IECs led to a significant reduction of OSMR as well as the IL-22 response genes *Reg3g* and *Reg3b* (**Figure 20A**). A significant reduction in the histopathology of these mice was also observed (**Figure 20B**). Though we detected a decrease in the histopathology of the *Stat1* deficient mice (**Figure 20D**), we can construe that the deficiency of *Stat1* did not influence the OSMR expression in the IECs (**Figure 20C**). Furthermore, the phosphorylation of STAT3 was evaluated in the inflamed mice that received the anti-IL-22 blocking antibody and the inflamed mice that received the isotype control. Indeed, blocking IL-22 significantly decreased STAT3 phosphorylation and *Osmr* expression in the IECs (**Figure 20 E-G**).
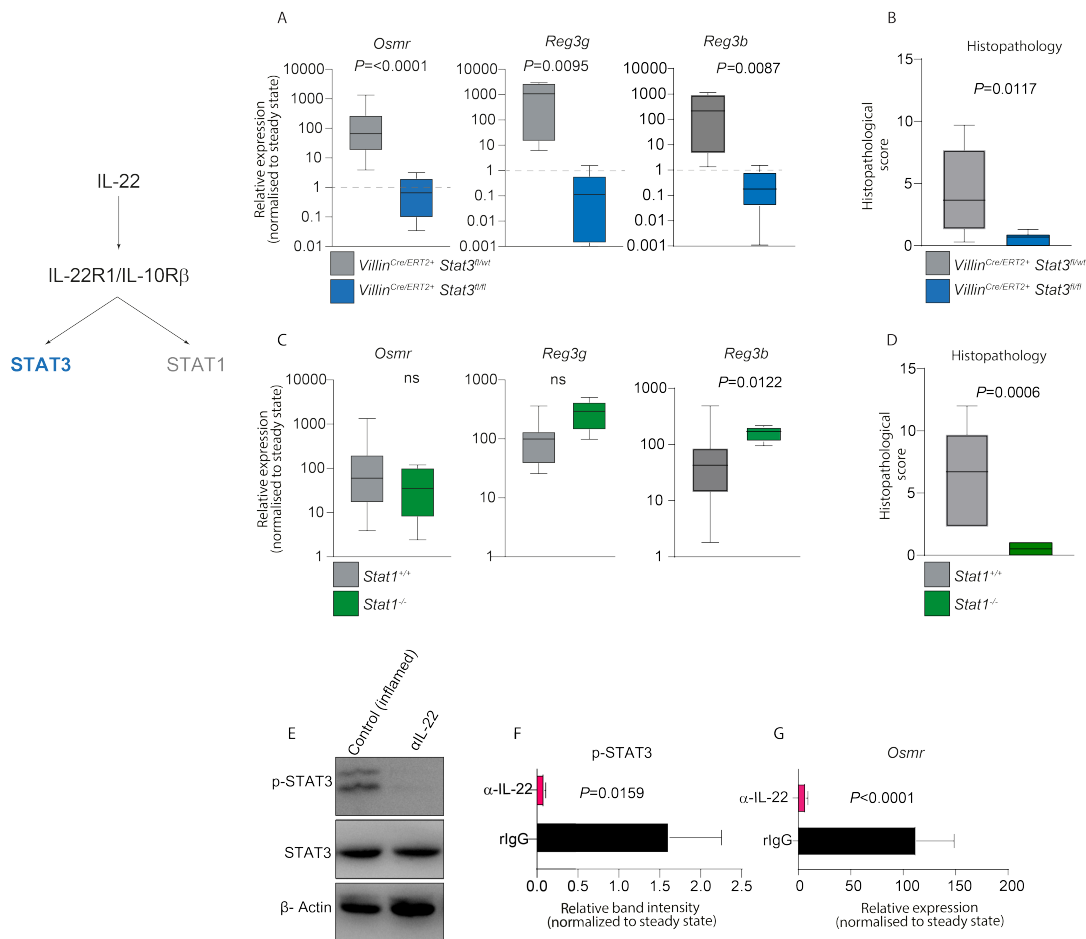
Figure 20: OSMR induction in epithelial cells is STAT3-dependent. (A, B) *Colitis was induced in the Villin^CreERT2 x Stat3^fl/fl or Villin^CreERT2 x Stat3^fl/+ using the H.h +αIL-10R protocol for 7 days. (**A**) Q-PCR gene expression analysis of Osmr, Reg3g, and Reg3b in epithelial cells from inflamed mice normalized to epithelial cells isolated from steady-state mice. (**B**) Histopathology scoring of the inflamed Villin^CreERT2 x Stat3^fl/fl or Villin^CreERT2 x Stat3^fl/+. The data is representative of one experiment (n≥ 5 mice per genotype). Statistics: Mann-Whitney U test. (**C, D**) Colitis was induced in the Stat1^-/- or Stat1^+/+ for 7 days. **C**) Q-PCR gene expression analysis of Osmr, Reg3g, and Reg3b in epithelial cells from inflamed mice normalized to epithelial cells isolated from steady-state mice. (**D**) Histopathology scoring of the respective mice. The data is representative of one experiment (n≥ 5 mice per genotype). Statistics: Mann-Whitney U test. (**E-G**) Protein and gene analysis of the intestinal epithelial cells from the anti-IL-22 or isotype-treated inflamed mice. (**E**) Western-blot membrane depicting STAT3 phosphorylation. (**F**) Quantification of STAT3 phosphorylation using ImageJ. The relative band intensity of the inflamed mice was normalized to steady-state untreated mice. (**G**) Q-PCR gene expression analysis of Osmr in the epithelial washes. The data is representative of at least two independent experiments with n=≥8. Statistics: Mann-Whitney U test.*

75

Next, we generated organoids from the *villinCre* x *Stat3*-deficient mice treated with and without IL-22. Our data showed that IL-22-mediated OSMR induction was impaired in the STAT3-deficient organoids as well as the IL-22 response genes (**Figure 21A/B**).
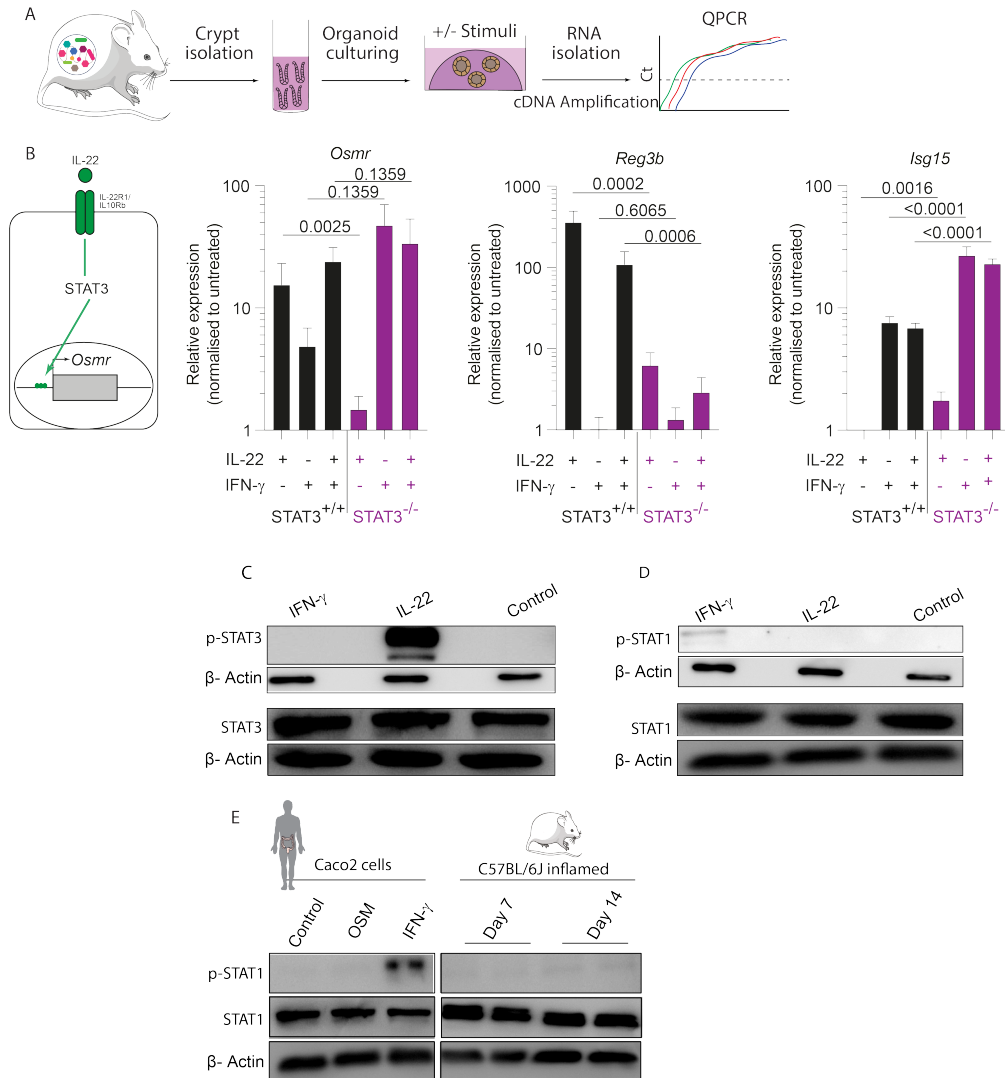
Figure 21: In vitro experiments confirmation of Osmr dependency on STAT3. (**A, B**) *Mouse colon organoids were generated from VillinCre x Stat3-/- or VillinCre x Stat3+/+ mice and were stimulated with the indicated conditions. (**B**) Quantification of Osmr by qPCR is depicted. The data is representative of three independent experiments done from three independent biological replicates. Statistics: Multiple Mann-Whitney test using the Holm-Sidak method, error bars represent SEM. (**C, D**) Western-blot membrane depicting STAT3 (**C**) and STAT1 (**D**) phosphorylation in mouse colon organoids stimulated with the indicated cytokines. (**E**) Western blot of STAT1 phosphorylation in the Caco2 cell line (left) and C57BL/6J inflamed mice at days 7 and 14 (right).*

Additionally, western-blot analysis of IL-22 stimulated organoids showed STAT3 phosphorylation, while STAT1 phosphorylation was detected only with IFN-γ stimulation (**Figure 21C/D**). Interestingly, STAT1 phosphorylation was detected in the colorectal carcinoma derived Caco2 human cell line, while the epithelial cells from the *H.h.* and anti-IL-10R treated mice showed no detection (**Figure 21E**).

Together, the data highlights the importance of STAT3 for OSMR induction on IECs.

4.5 Type 3 innate lymphoid cells (ILC3s) drive early OSMR induction on IECs.

The expression of OSMR on IECs at day 3, an early stage of colitis induction (**Figure 7C**), hinted that the innate immune cells might be implicated in disease development. Therefore, we presumed that the innate immune cells might be responsible for promoting OSMR expression through the early production of IL-22. Markedly, the innate immune pathways, including the ILCs, are crucial regulators of homeostasis and inflammation and are critical drivers of intestinal inflammatory responses in *H.h*-driven colitis[3, 194, 195]. In addition, these cells are major sources of IL-22, at both steady-state and inflammation[3, 194, 195].

To determine whether the innate cells can directly induce OSMR expression on epithelial cells, we analyzed the expression of OSMR in the *H.h* + αIL-10R treated Rag-deficient (*Rag2-/-)* mice. Though IL-22 expression was modulated in the Rag deficient mice, *Osmr* was expressed in epithelial cells on days 7 and 14 post-infection (**Figure 22A**). Furthermore, the expression of *Osmr* was significantly lower in the *Rag2-/-* mice compared to the *Rag2+/+* mice only at day 7 post-infection. Intriguingly, our data showed that a slight increase of *Il22* expression at days 7-14 was sufficient to increase the *Osmr* expression in the IECs (**Figure 22A**). Interestingly, the *Rag2-/-* mice did not show *Osm* expression in the tissue during inflammation, highlighting the vital role of IL-22 in driving the OSM-receptor expression in IECs during inflammation (**Figure 22A**). In addition, the *Rag2-/-* mice showed less intestinal pathology to that observed in the wild-type inflamed *Rag2+/+* mice (**Figure 22B**).
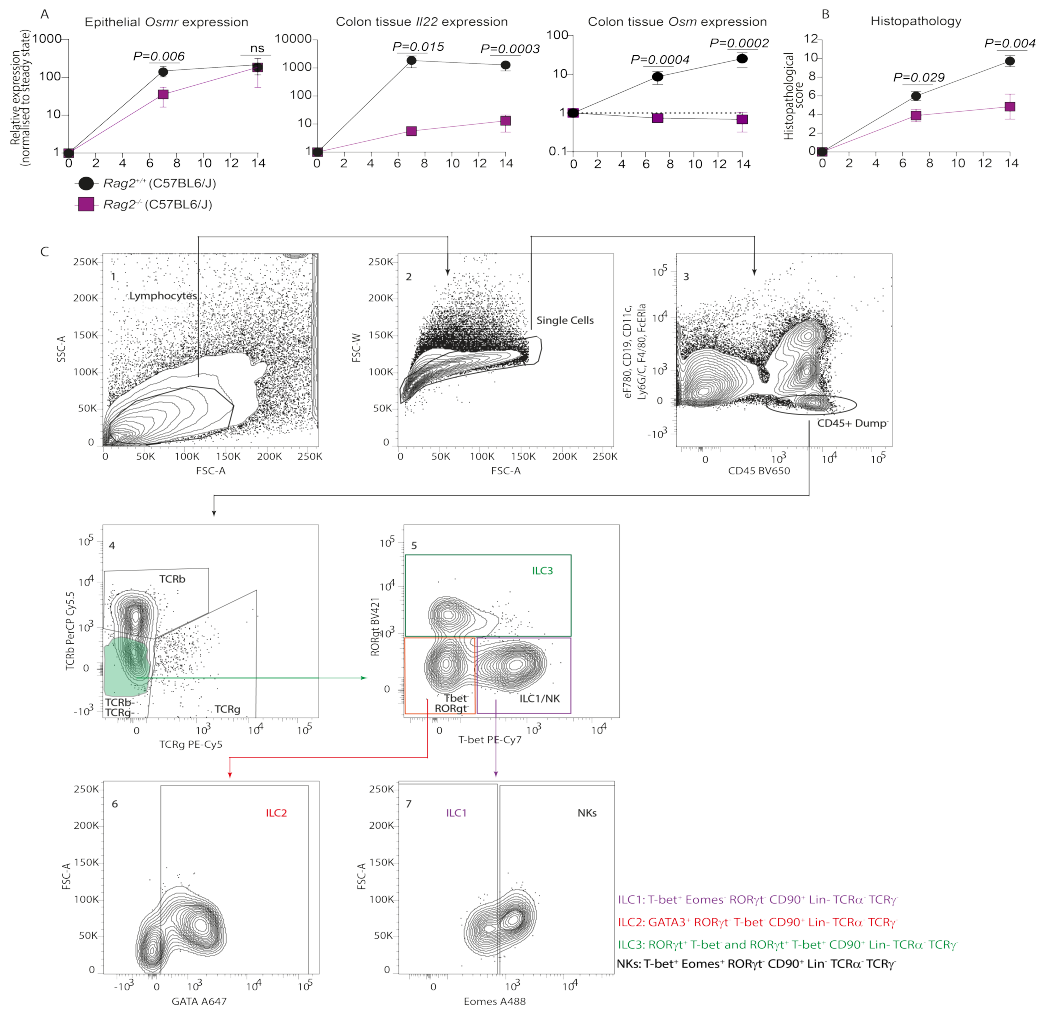
Figure 22: Colitis induction in RAG-2-deficient mice led to a decrease in inflammation but did not modulate OSMR expression. (*A, B*) *Colitis was induced in the Rag2$^{-/-}$ or Rag2$^{+/+}$ using the H.h +α-IL-10R protocol for 7 and 14 days. (**A**) Q-PCR gene expression analysis of Osmr in the intestinal epithelial washes (left), Il22 expression (middle), and Osm expression (right) in the colon tissue from inflamed mice normalized to the steady-state mice. (**B**) Histopathology scoring of the Rag2$^{-/-}$ or Rag2$^{+/+}$. The data is representative of two independent experiments, n=≥8, error bars represent SEM, P values derived from Mann–Whitney U tests comparing the groups to their respective experimental day. (**C**) Representative gating strategy of the different ILC populations. ILC subsets were identified by flow cytometry on mouse LPMCs (n = 6 per group). 1) Lymphocytes we first gated, followed by the removal of 2) doublets. Then, the ILC population was characterized as 3) CD45$^+$, Lin$^-$ (i.e. CD19$^-$, CD11c$^-$, Ly6G/C-, F4/80$^-$, FcERIa$^-$) and live cells. Subsets were further defined based on specific transcription factor markers. 5) ILC3 were further gated as RORγt$^+$ T-bet$^-$ and RORγt$^+$ T-bet$^+$ CD90$^+$ Lin$^-$ TCRα$^-$ TCRγ$^-$. While, 6) ILC2 were categorized as GATA3$^+$, RORγt$^-$, T-bet$^-$, CD90$^+$ Eomes$^-$, Lin$^-$, TCRα$^-$, TCRγ$^-$. 7) ILC1 were identified as T-bet$^+$ Eomes$^-$ RORγt$^-$ CD90$^+$ Lin$^-$ TCRα$^-$ TCRγ$^-$. 7) NKs were characterized as T-bet$^+$ Eomes$^+$ RORγt$^-$ CD90$^+$ Lin$^-$ TCRα$^-$ TCRγ$^-$.*

Therefore, we sought to determine whether the innate lymphoid cells could candidly induce OSMR expression in epithelial cells by evaluating the early source of IL-22 in the colonic lamina propria through FACS analysis. All ILC subsets, ILC1, ILC2, ILC3 and NK cells, were identified from the colonic LP of steady-state and inflamed mice according to the transcription-factor-based gating strategy defined in **Figure 22C**.
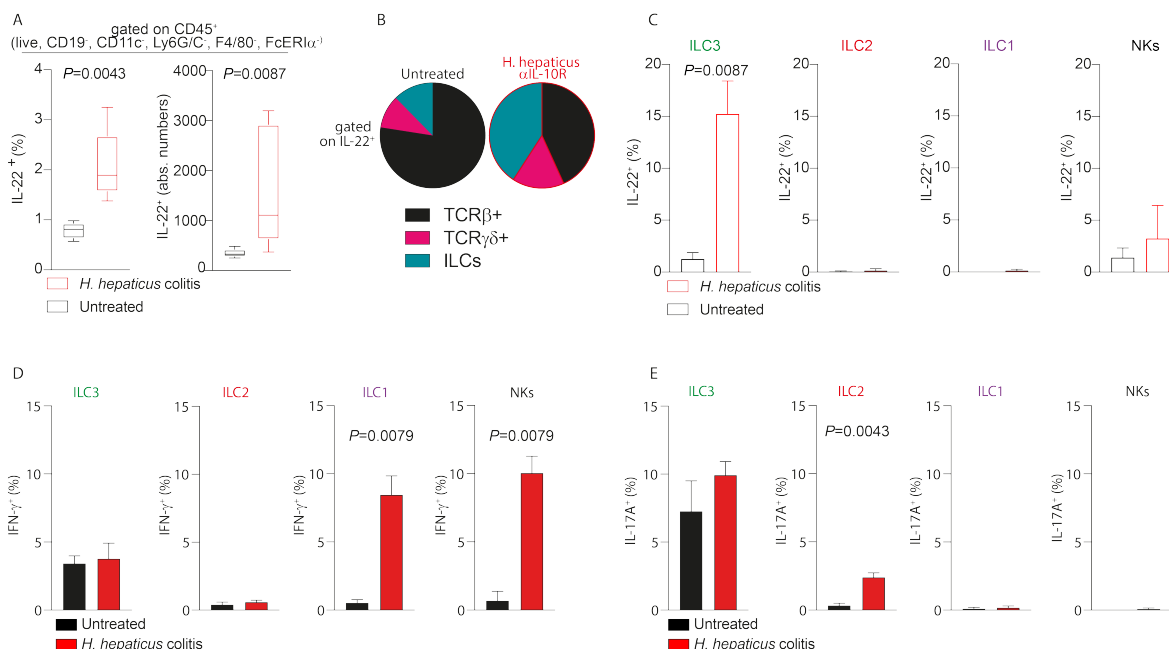
Figure 23: Type three innate lymphoid cells are the primary source of IL-22 in H.h-induced colitis. *(**A**) Absolute cell numbers of IL-22 expressing CD45+cells in naïve mice and after colitis induction using the H.h +αIL-10R protocol on day 7. Flow cytometry assessed cytokine expression after stimulation with PMA/Ionomycin, IL-23, and IL-1b. (**B**) Pie graph showing the cellular source of IL-22 on day 7 of colitis. (**C**) IL-22 production by ILC3 (RORγt+, Lin-, TCRα-, TCRγ-), ILC1 (T-bet+, Eomes-, RORγt-, Lin-, TCRα-, TCRγ-), ILC2 (GATA3+, RORγt-, T-bet-, CD90+ Eomes-, Lin-, TCRα-, TCRγ-) and NK cells (T-bet+, Eomes+, RORγt-, Lin-, TCRα-, TCRγ-). (**D**) IFN-g and (**E**) IL-17A production by ILC3, ILC1, ILC2, and NK cells. The data is representative of 1 independent experiment, n=6 per condition. Statistics: Mann–Whitney U tests.*

Our data showed that in the *H.h* + αIL-10R colitic mice, there was an increase in the IL-22 positive cells on day 7 post-colitis induction (**Figure 23A**). Evidently, there was an increase in IL-22 production by the ILC cell population in the inflamed mice compared to the steady-state mice (**Figure 23B**). Importantly, the ILC3 cell population was

responsible for producing IL-22 in the *H.h* + αIL-10R colitis model (**Figure 23C**). As expected, the ILC1 and NK cells were responsible for IFN-γ production, while the ILC2s produced IL-17A during inflammation (**Figure 23D/E**). To further understand the role of the ILC3s in the *H.h* + αIL-10R colitis model, double deficient mice (*Rag2$^{-/-}$ x Rorc$^{-/-}$*), which lack the critical ILC3-lineage-defining transcription factor and are hence ILC3 deficient, were studied. The *Rag2$^{-/-}$ x Rorc$^{-/-}$* mice showed a significant reduction in OSMR expression in the epithelial cells compared to the inflamed control mice (**Figure 23A**). In addition, a decrease in *Il22* expression as well as a decrease in the histopathological score was observed in the *Rag2$^{-/-}$ x Rorc$^{-/-}$* inflamed mice (**Figure 23B/C**). These results indicate that the group 3 ILCs are important drivers of IL-22 production in the *H.h* + αIL-10R colitis model, which consequently drives OSMR expression on the IECs.

IL-12 and IL-23 are essential drivers of early innate cell activation in intestinal inflammation and exemplify promising therapeutic targets in IBD. In addition, IL-23-responsive innate lymphoid populations have been associated with mediating intestinal immune pathology[87, 177, 196]. Notably, ILC3s are essential in promoting epithelial barrier integrity and disease-driving responses by producing IL-22. The pathogenic role of ILC3s is highlighted by Geremia *et al.* to be IL-23 dependent[186, 196]. Furthermore, IL-23-responsive ILC3s were found to be increased in the intestines of CD patients[186, 196].

To highlight the role of IL-12 and IL-23 in OSMR induction in IECs, we blocked IL-12p40 and assessed whether OSMR was induced in IECs. Indeed, IL-12p40 blockade significantly reduced tissue expression of *Il22* and consequently, *Osmr* expression in IECs (**Figure 24D-E**). We also observed a significant reduction in the histopathology score of the anti-IL-12p40 treated mice compared to the isotype treated controls (**Figure 24F**).

Together, our data support that the ILC3s are the primary producers of IL-22 in the *H.h* + αIL-10R colitis model. In addition, IL-12/23 promotes innate immune cell expression of IL-22 during early colitis, which enhances OSMR induction in IECs.
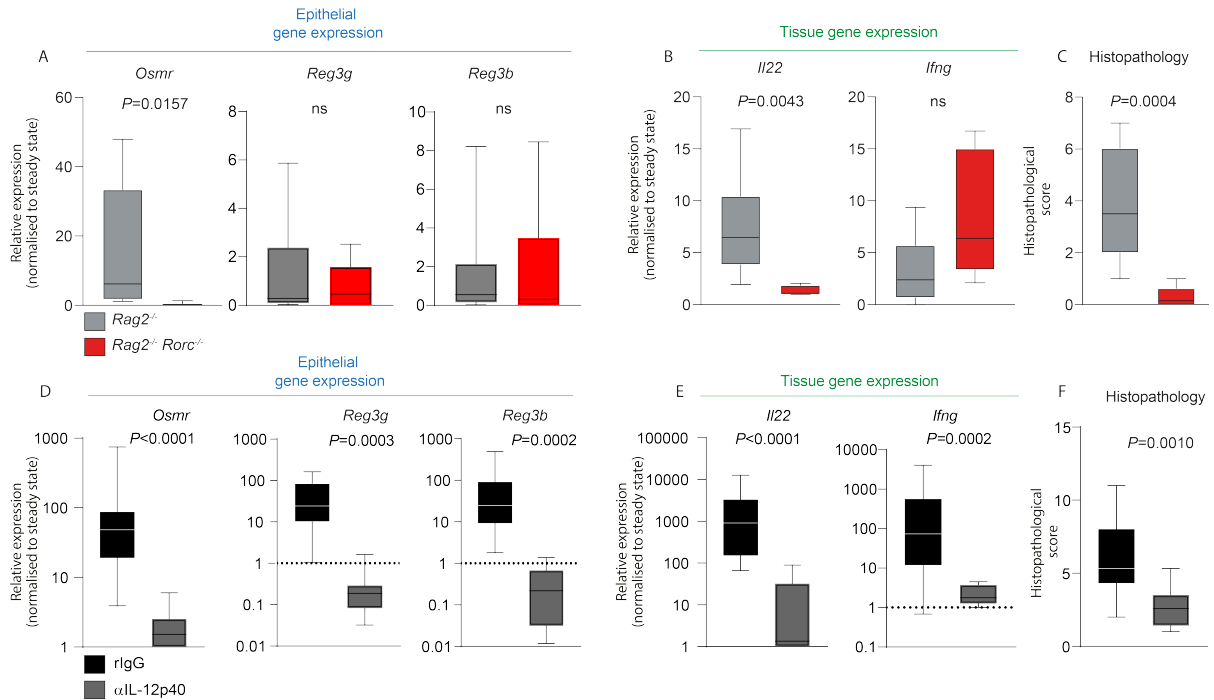
Figure 24: The absence of type 3 innate lymphoid cells and the blockade of IL-12p40 ameliorated inflammation through the suppression of OSMR. (A-C) *Induction of colitis using the H.h +α-IL-10R protocol in the Rag2⁻/⁻ x Rorc⁻/⁻ and Rag2⁻/⁻ for 7 days. (**A**) Epithelial Osmr, Reg3g, and Reg3b expression were quantified by qPCR, as well as (**B**) Q-PCR analysis of Il22 and Ifng expression in the colon tissue. (**C**) Histopathology score of the respective mice. The data is from 1-2 independent experiments, n≥ 6, statistics: Mann–Whitney U tests. (**D-F**) Induction of colitis using the H.h +α-IL-10R protocol. Mice were treated with anti-IL-12p40 on day 0 or the isotype control (rIgG). (**D**) Osmr, Reg3g, and Reg3b expression were quantified in epithelial washes on day seven by qPCR as well as (**E**) Il22 and Ifng expression was quantified in the colon tissue. (**F**) Histopathology score of the anti-IL-12p40 or isotype-treated mice. The data is from two independent experiments, n=6-14, Statistics: Mann–Whitney U tests.*

4.6 OSMR enhances STAT3 activation in epithelial cells and inflammatory gene signature.

To gain insight into whether the pathogenic effects of OSMR on the IECs were time-dependent, we used the *Villin^CreERT2 x Osmr^fl/fl* mice and induced colitis for 7, 14, and 21 days (**Figure 25A**). The *Villin^CreERT2 x Osmr^fl/+* mice had a significant increase in *Osm* expression on day 7 of colitis compared to the knockout (**Figure 25B**). Additionally, the *Villin^CreERT2 x Osmr^fl/fl* mice showed significant reduction in the expression of *Il22* at day 14 and *Ifng* at day 21 (**Figure 25B**). Intriguingly, only at day 21 did we notice a significant

difference in the expression of IL-22 regulated and STAT3 activated genes, *Reg3g* and *Reg3b*[43, 147, 189, 197, 198]. The *Villin*^{CreERT2} x *Osmr*$^{fl/fl}$ had lower *Reg3g* and *Reg3b* than the *Villin*^{CreERT2} x *Osmr*$^{fl/+}$ mice (**Figure 25C**).

Additionally, we investigated the proliferation of the IECs during inflammation at days 0, 7, 14, and 21 using Ki67 as a proliferation marker. Interestingly, the data showed a significant decreased in Ki67 positive cells in the *Villin*^{CreERT2} x *Osmr*$^{fl/fl}$ compared to the *Villin*^{CreERT2} x *Osmr*$^{fl/+}$ mice at day 21 (**Figure 25D**). Subsequently, the phosphorylation of STAT3 was significantly lower in the *Villin*^{CreERT2} x *Osmr*$^{fl/fl}$ mice at day 21 post colitis when compared to the *Villin*^{CreERT2} x *Osmr*$^{fl/+}$ mice (**Figure 25E**). This outcome highlighted the late-phase effect of the OSMR on the downstream signaling pathway of STAT3.

As the intestinal barrier function is essential for keeping homeostasis, we questioned whether OSMR on the IECs modulated the barrier integrity. Studies have shown that a compromised intestinal barrier, such as increased intestinal permeability, is strongly associated with IBD patients[26, 53, 72, 199-201]. A recent study by Turpin *et al.* found that intestinal permeability was 50% greater in IBD patients compared to their healthy relatives[202]. As tight junction proteins are known to play a central role in barrier regulation[79, 99, 103, 105, 203], we screened for tight junction protein expression unbiasedly using immunoblotting at day 21 of colitis in the epithelial washes of the *Villin*^{CreERT2} x *Osmr*$^{fl/fl}$ and *Villin*^{CreERT2} x *Osmr*$^{fl/+}$ mice. We found that the tight junction scaffolding ZO-1 was significantly lower in the OSMR-sufficient inflamed mice compared to the inflamed knockout mice (**Figure 25F**).

Additionally, our bulk RNA sequencing data showed that chemokines such as *Ccl2*, *Ccl8*, *Cxcl9*, and *Cxcl11* were significant downregulated in the absence of OSMR in IECs (**Figure 14A**). IL-22 has been implicated to be functionally important in regulating the recruitment of neutrophils to the colon especially during inflammation where *Il22* expression is augmented[204].
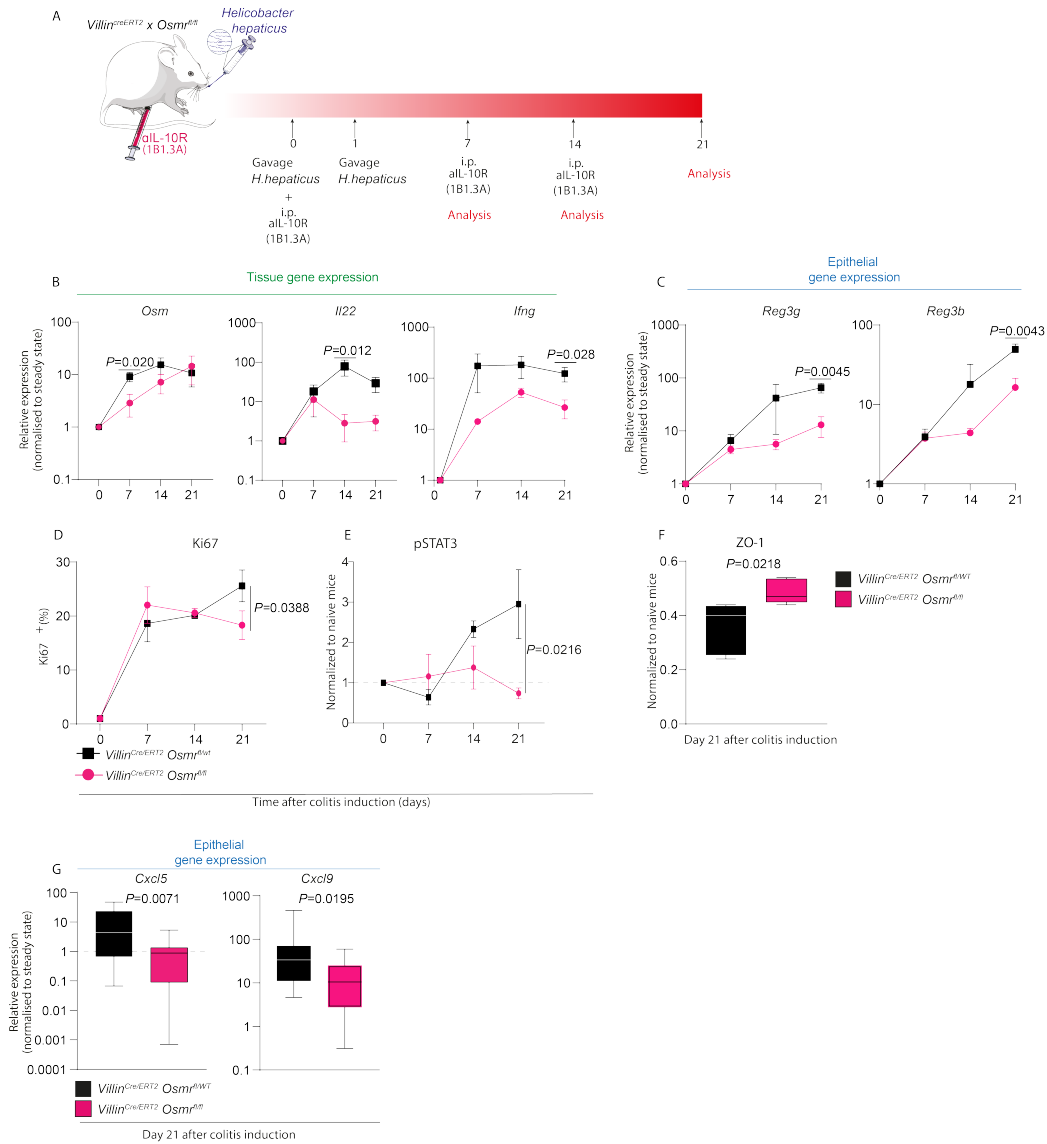
Figure 25: The Osmr is important during late-phase colitis. (***A***) *Scheme depicting the colitis-induced timeline in which the Villin^{CreERT2}x Osmr^{fl/fl} or Villin^{CreERT2}x Osmr^{fl/+} were analyzed.* (***B***) *Osm, Il22, and Ifng expression were quantified in the mice's colonic tissue at day 0, 7, 14, and 21.* (***C***) *The expression of Reg3g and Reg3b in epithelial washes were also analyzed by qPCR on the days mentioned. The data represent 1-2 independent experiments, n≥ 7 mice per time-point. P values reflect differences between inflamed Villin^{CreERT2}x Osmr^{fl/fl} mice and their respective wild-type mice and are derived from Multiple Mann–Whitney U tests, error bars represent SEM.* (***D***) *STAT3 phosphorylation and* (***F***) *ZO-1 in epithelial cells were assessed by immunoblotting. Statistic: Mann–Whitney U tests, the data represents two independent experiments, n≥ 7 mice.* (***G***) *The expression of the Cxcl5 and Cxcl9 were analyzed by qPCR in the Villin^{CreERT2}x Osmr^{fl/fl} or Villin^{CreERT2}x Osmr^{fl/+} at day 21, as well as* (***G***) *tissue gene expression of Il22bp. The data is representative of two independent experiments, n≥ 7 mice. Statistic: Mann–Whitney U tests.*

As mentioned previously, our data showed that in the absence of the OSMR on the IECs, *Il22* expression was significantly reduced (**Figure 25B**); therefore, we investigated whether this effect modulated neutrophil attracting chemokines, such as CXCL5 and CXCL9. QPCR analysis showed a significant reduction of *Cxcl5* and *Cxcl9* in the IECs of the *Villin^{CreERT2} x Osmr^{fl/fl}* compared to the *Villin^{CreERT2} x Osmr^{fl/+}* mice (**Figure 25G**). In keeping with the hypothesis that the OSMR is pathogenic during inflammation, this observation confirms that the OSMR is imperative for the expression of neutrophil-active chemokines during late phase colitis.

Collectively, these data revealed that during inflammation, OSMR is expressed on the IECs and enhances STAT3 activation and inflammatory gene signatures. The effect of the OSMR on the IECs is pathogenic, and this pathogenesis is time-dependent as it is only seen in late-phase colitis.

5 Discussion

It has become indisputable that cytokines are essential in the pathogenesis of IBD. Cytokines are critical regulators for cell signaling processes, and their therapeutic manipulation has shown promising results in reducing disease severity. IBD has been characterized as a chronic relapsing disorder in the GI tract with severe complications, including epithelial injury[47, 53, 72, 205]. Numerous pro-inflammatory cytokines have been reported to affect the IECs and cause apoptosis, decreasing the integrity of the epithelial barrier[53, 199]. In contrast, other studies have shown that some cytokines induce IEC activation and survival via downstream signaling and lead to mucosal healing[189, 197]. To date, several recombinant anti-inflammatory cytokines or antibodies specific for pro-inflammatory cytokines have been used in the attempt to treat IBD. Several cytokine treatments, such as IL-10, IFNβ, and IL-11, had disappointing outcomes[206-208]. However, neutralizing antibodies specific for TNF (infliximab) showed discernable clinical improvement in IBD patients[65, 78]. Still, some IBD patients are nonresponsive to anti-TNF therapy, highlighting the need to identify new cytokine pathways involved in IBD.

A significant discovery by West *et al*. found OSM, a proinflammatory cytokine as a novel biomarker in IBD that is correlated with disease severity and poor anti-TNF response[132]. The breakthrough study showed that out of 64 candidate cytokines, OSM was the most significantly expressed cytokine in IBD patients. They revealed that the expression of OSM was associated with an overexpression of OSMR on intestinal stromal cells[132]. They highlighted that this overexpression of OSMR on the stromal cells is the predominant cause of increased severity of intestinal inflammation in IBD patients.

Though the implications of cytokines in inflammatory diseases have been studied extensively, there are still gaps in our knowledge about their involvement in IBD. West *et al*. were the first to show that the OSM-OSMR axis is involved in the pathogenesis of IBD. Their data uses OSM as a biomarker to help clinicians in determining whether to prescribe anti-TNF antibodies. Although the study used OSM deficient mice to show a decrease in mouse colitis, the OSM-OSMR pathway was not dissected fully. Therefore, the work done in this thesis further investigated the OSM-OSMR pathway on other cell

types and the effect that axis has on intestinal inflammation. This work ultimately shows that the OSM-OSMR pathway is crucial in epithelial cells and drives disease severity.

5.1 The intestinal epithelial cells express the OSMR as a consequence of inflammation

While stroma cells express the OSMR at steady-state and during intestinal inflammation, the data in this research showed that the intestinal epithelial cells only express the OSMR during intestinal inflammation (**Figure 6E**). One of the most critical functions of the IECs is maintaining homeostasis by forming a barrier that mediates the balance between gut microbes and the host's immunity and tolerance[26, 54, 55, 57, 80, 199]. Therefore, we investigated whether the expression of the OSM receptor on the epithelial cells was pathogenic or protective.

West *et al*. had clearly shown that OSMR is overexpressed on stromal cells during intestinal inflammation[132]. However, Biegel *et al*. showed that OSM was essential for repair after injury in a colon carcinoma cell line[133.]. Therefore, we combined scRNAseq and conditional deletion to remove the OSMR on the IECs (*Villin^CreERT2 x Osmr^fl/fl*) to explore the relevance of the OSM-OSMR axis on IECs during intestinal inflammation. One of the key findings was that the histopathology score was significantly lower in the *Villin^CreERT2 x Osmr^fl/fl* mice compared to the *Villin^CreERT2 x Osmr^fl/+* during *H.hepaticus*-induced colitis (**Figure 10B**). Additionally, the *Villin^CreERT2 x Osmr^fl/+* mice showed severe goblet cell depletion, a common pathologic finding in IBD[98, 209]. Importantly, goblet cells are essential for the production and secretion of mucin, which protects the mucosa from invading pathogens[98, 209]. Van der Sluis *et al.* showed that MUC2 deficient mice developed spontaneous chronic colitis, emphasizing that the loss of appropriate mucin secretion and production is associated with chronic inflammation[101]. Moreover, the loss of goblet cells observed in the *Villin^CreERT2 x Osmr^fl/+* during colitis confirms the assumption that the expression of the OSMR on the epithelium is detrimental during inflammation.

In addition, the epithelial washes from the IBD patients had significantly higher OSMR expression compared to the controls from healthy patients. Furthermore, visual analysis of *in situ* hybridization depicted in **Figure 8** showed that during colitis, the OSMR can be seen on the epithelium of the IBD patients, an observation that is not seen in healthy patients. This finding revealed that the expression of the OSMR on the membranes of the IECs is relevant in intestinal inflammation in mice and humans.

Our initial findings highlighted a pathogenic effect of the OSM-OSMR pathway on IECs during inflammation.

5.2 IL-22 drives the OSMR expression IECs during inflammation

The hypothesis brought forth by this study is that the expression of the OSMR on epithelial cells during inflammation had a pathogenic effect. This result led to further exploration of the underlining signals driving the OSMR expression on the IECs.

West *et al*. had previously described that OSM drove the expression of OSMR on mouse colon stroma cell cultures ex vivo[132]. Therefore, through the exploitation of the organoids technology and stimulation using various stimulants aided in identifying the potential signal inducers of the OSMR in IECs. Surprisingly, in both human and mouse organoids, IL-22 was the key cytokine driving OSMR expression in IECs (**Figure 15B**). Previous studies have shown that while IL-22 is constitutively expressed in human and mouse small intestines under healthy conditions [134, 135, 138, 141, 144, 153, 160]. In addition, the expression of IL-22 is detected in the colon during inflammatory conditions such as IBD[134, 135, 138, 141, 144, 153, 160]. Verifiably, in the *H.hepaticus* colitic C57B/6J mice, IL-22 was significantly expressed compared to the steady-state C57B/6J mice (**Figure 15C**). Intriguingly, IL-22 deficient mice (*Il22$^{-/-}$*) (**Figure 15E**) and mice receiving the anti-IL-22 blocking antibody (**Figure 16**) had significantly lower epithelial OSMR expression than their respective controls. This data coherently depicted that IL-22 was an essential inducer of the OSMR on epithelial cells during intestinal inflammation, and that this interaction is pernicious in IBD.

Various studies have shown that IL-22 has both protective and pathogenic roles in intestinal inflammation. For example, in acute intestinal infections such as the *Citrobacter rodentium* infectious model, IL-22 plays a beneficial role by potentiating host defense via the expression of anti-microbial peptides[210, 211]. Additionally, in the DSS colitis model, IL-22 is protective as it facilitates the restitution of the epithelium[190]. Based on these findings, it is equitable to assume that IL-22 is advantageous where fast colonic epithelial repair is necessary. However, human IBD is characterized by chronic immune-mediated inflammatory responses and not as an acute injury that can be resolved rapidly. In contrast to its beneficial roles, studies have shown that while IL-22 can be protective, it can promote colitis context-dependently. For example, a study by Kamanaka *et al*. showed that in an adaptive transfer colitis model where Treg-depleted memory/effector CD4+CD45RB^{lo} T cells are transferred into Rag deficient mice, IL-22 was pathogenic; however, in CD4+CD45RB^{hi} naïve T cells were transfer experiments, IL-22 was protective[212].

Our data revealed that during *H.h.* induced colitis, IL-22 is pathogenic. This finding coincides with the observations made by Morrison *et al*. which showed that IL-22 was pathogenic in the *H.h.*-induced colitis model, as it promoted the development of inflammation in the colon[165]. During *H.h.* colitis, IL-22 deficient mice and the mice that received the IL-22 blocking antibody showed not only lower expression of OSMR but significantly lower histopathology scores compared with the respective IL-22 sufficient inflamed controls and isotype controls. Conclusively, IL-22 promotes the expression of the OSMR on IECs and this contributes to intestinal inflammation.

5.3 ILC3s produce IL-22 in the *H. hepaticus* colitis model

The main source of IL-22 in the *H.h* colitis model was the group 3 innate lymphoid cells (ILC3s). Human ILC3s are described by their expression of the RAR-related orphan receptor-γt (RORγt)[213] and surface expression of CD117 (c-kit)[214]. ILC3s respond to IL-23 and IL-1β stimulations and produce Th17/Th22 cytokines IL-17A, IL-17F, and IL-22[145,]

[149, 210, 213, 214]. Our data revealed that compared to the Rag deficient mice (*Rag⁻/⁻*), mice that were *Rag⁻/⁻* x *Rorc^{fl/fl}* deficient produced significantly lower IL-22 expression. This decrease in IL-22 was linked to the lower expression of the OSMR in the epithelium. The data highlighted the pathogenic role of the ILC3s production of IL-22 in *H.hepaticus* colitis. In line with our data, a study by Longman *et al.* has revealed that colonic ILC3 from UC and CD patients leads to higher expression of IL-22 than in healthy individuals[215]. In addition, in innate colitis models such as the anti-CD40 model, IL-22 production by ILC3s was found to be pathogenic[216].

Together, the role of ILC3-derived IL-22 in the intestine cannot be easily labeled as protective or pathogenic without context. Though ILC3 production of IL-22 can be protective in promoting epithelial barrier integrity, inappropriate and prolonged activation of ILC3 can cause intestinal damage through excessive production of IL-22[155, 216, 217]. Overall, our data showed that ILC3s were the main producers of IL-22 in the *H.hepaticus* colitis model and this production of IL-22 is pathogenic as it leads to the OSMR expression on the IECs.

5.4 The role of IL-12 and IL-23 in the *H.h* colitis model

In human IBD, the expression of IL-12 is upregulated and correlates strongly with an increase in disease activity[218]. In animal models, such as the *H.h* colitis model, IL-23 is essential to manifest chronic intestinal inflammation[87]. Notably, IL-23 is vital in driving Th17 responses. Th17 cells have been recognized as essential drivers of intestinal inflammation. In mice, Th17 cells, which produce IL-17 and express RORγt, are the critical source for IL-22[149, 158, 177, 219]. While IL-23 is essential in Th17 cell expansion, IL-12 is vital in differentiating naive T cells to Th1 cells[50, 218]. Monoclonal antibodies targeting IL-12p40 are available in the clinics and were designed to inhibit both the IL-12 and IL-23 signaling pathways to treat IBD[220-222].

Our data showed that blocking IL-12p40 led to a significant reduction of IL-22, consequently reducing the OSMR in epithelial cells. Although speculative, this decrease

in the OSMR could be the reason for the decrease in the histopathology of the mice that received the anti-IL12p40 blocking antibody. Moreover, our data revealed that by modulating the continuous presence of IL-22 expression during inflammation, OSMR expression on the epithelium diminishes, leading to restorative effects.

5.5 The OSM-OSMR axis is pathogenic in intestinal inflammation

It is paradoxical but not surprising that OSM can play both pathogenic and protective roles in inflammatory conditions. The mechanism by which OSM mediates barrier dysfunction was initially unknown. Although Biegel *et al.* had shown that treatment of human colorectal cancer-derived IEC lines with OSM was necessary for regrowth/wound healing after injury; the *in vivo* mechanism had not been shown[114]. In addition, the lack of primary cells in their study made it difficult to determine whether their findings were translatable or related to transformed epithelial cells.

The strength of this Ph.D. study is that, for the first time, we could show mechanistically how OSM and OSMR promote epithelial cell destruction, which subsequently leads to inflammation. Many studies have made it evident that chemokines are essential for activating, recruiting, and retaining leukocytes along a chemotactic gradient[7, 10, 48]. For example, West *et al.* have shown that in IBD, as the level of OSM increases, so does leukocyte enhancement, contributing to a substantial infiltrate of immune cells. Our study showed for the first time that during inflammation, the OSMR is induced by IL-22. Then, OSM binds to its receptor and activates the STAT3 downstream pathway. Importantly, STAT3 has been shown to be essential for epithelial homeostasis and repair[189, 197, 223]. Although OSM activates many downstream pathways, it is a potent activator of STAT3[126, 132, 133]. Our data showed that when the OSMR is removed from the epithelial cells during inflammation, so does the proliferation of the IECS and phosphorylation of STAT3 (**Figure 25D/E**).

This activation of STAT3 by OSM on the epithelial cells subsequently leads to chemokine recruitment such as CCL2, CXCL5, CXCL9, and CXCL11. Intriguingly, our data showed

that CXCL5, a chemokine that has been reported to be involved in IBD pathogenesis, specifically in UC patients[224-226], is modulated by the OSM-OSMR axis during inflammation. We found that in the OSMR deficient mice (*Villin^{CreERT2} x Osmr$^{fl/fl}$*), CXCL5 was significantly lower compared to the OSMR sufficient mice. In addition, the OSMR-deficient mice had lower histopathology scores and lower neutrophil, macrophages, eosinophils, and T-cell accumulation than the OSMR-sufficient mice (*Villin^{CreERT2} x Osmr$^{fl/+}$*) (**Figure 25G**). It has been well-studied that CXCL5 is not only upregulated in UC patients but is expressed explicitly by colonic epithelial cells in these patients[227]. CXCL5 is responsible for neutrophil activation and recruitment in IBD patients[10, 48, 225].

Neutrophil infiltration strongly correlates with disease severity in UC patients[185]. During IBD, uncontrolled accumulation and persistence of neutrophils is associated with the degeneration of crypts and overt deterioration of the epithelium and further extensive mucosal erosion[185, 228]. This impedes the clearance of the gut leukocytes thereby, delaying the resolution of gut inflammation. Consistent with this, markers such as fecal calprotectin and neutrophil gelatinase-associated lipocalin (NGAL) are widely used as biomarkers for IBD[229-239] . Neutrophils mainly produce calprotectin, an abundant calcium-binding protein belonging to the S100 family, with S100A8 and S100A9 forming hetero-oligomers capable of binding zinc [232-237, 239]. Additionally, marked elevated calprotectin levels have been detected in IBD patients' feces, indicating a neutrophilic influx from the mucosal lining into the gut lumen during intestinal inflammation[232-237, 239]. Furthermore, lipocalin, initially described as a neutrophil protein, is produced by several cell types, including epithelial cells, which is particularly important in IBD[229-232]. During inflammation, lipocalin is secreted in high concentrations into the gut lumen[229-232]. Our data showed that removal of the OSMR from the epithelial cells during inflammation led to significantly lower fecal calprotectin and lipocalin detection (**Figure 13B/C**). In line with this observation, bulk RNA sequencing data from mice that received the anti-OSM blocking antibody during colitis showed various matrix metalloproteinases (MMPs) and genes related to neutrophil biology dependent on the presence of OSM (data not shown).

Interestingly, the effect of OSM and OSMR happens in a time-dependent manner. For example, removing the OSMR from the epithelial cells during inflammation in early-phase colitis did not lead to any significant changes in genes or protein expressions **(Figure 25**). Observational changes were only seen when colitis was established and maintained for 21 days. This indicates that therapeutically, time should be heavily considered when targeting OSM in IBD patients.

5.6 Limitations and future research opportunities

The strong therapeutic potential of the OSM-OSMR pathway brought forth by this study triggers further exploration of their involvement in other cell types context-dependently. Combinedly, the mouse and human data generated showed various similarities; however, it is pertinent to accentuate the limitations of this study. The problematic translatability of the various mouse genotypes and the colitis model used in this study are of particular importance. Though using mouse models to understand underlying mechanisms is advantageous, the diversity of the different IBD models causes an inadequate representation of the disease. For example, while in the *H.hepaticus*-induced colitis model, IL-22 is pathogenic, in models such as DSS colitis, IL-22 is protective. This hinders the translation of the findings to human IBD and makes it difficult to understand the OSM-OSMR pathway in the IECs. Our colonic epithelial organoids data showed that IL-22 induced the OSM receptor expression in humans and mice; However, we cannot certainly confirm that this follows the exact mechanisms as seen in mice, as there are considerable physiological differences. This limitation is fundamental and reflects the general problem with translational research.

Furthermore, although we could identify that IECs express the OSMR during inflammation, future work should focus on identifying which types of IECs expressed the OSMR. This question can be directly addressed in collaboration with a bioinformatician by doing a detailed analysis of the single-cell sequencing experiments in **figure 6.** Moreover, the molecular signatures induced on the IECs upon OSM stimulation should be further clarified. This can be clarified by next-generation sequencing of stimulated

mouse and human organoids. As the sequencing experiments of the stimulated organoids have already been carried out in this project, this question can be addressed quickly in the future. Identifying which epithelial cells express the receptor during inflammation and the effects of OSM on these cells will further shed light on our understanding of the underlying mechanisms driving the disease.

5.7 Concluding remarks

As mucosal OSM is strongly correlated with increased disease severity, it is undeniable that OSM is an important cytokine that should be evaluated for its therapeutic potential in IBD. However, based on this research, IL-22 is also essential, and it can be argued that its therapeutic potential in IBD should also be assessed. Although both OSM and IL-22 could be potential targets for IBD, it is tempting to speculate that they would not be ideal treatments for IBD. For example, as OSM acts as an inflammatory mediator in various contexts, its therapeutic utility has been investigated in systemic sclerosis. A randomized phase two study found that the anti-OSM monoclonal antibody (GSK2330811) was inadequate to ameliorate systemic sclerosis. The biological effects of the anti-OSM antibody in patients with systemic sclerosis were the same as in the placebo group[240]. Importantly, treatment with the anti-OSM antibody led to adverse effects such as a dose-related decrease in hemoglobin and platelet count[240]. Although these observations were made in patients with systemic sclerosis, it is vital to note the side effects of treating with an anti-OSM antibody and the further complications it can produce in IBD patients.

Furthermore, IL-22 would not be a therapy of choice, as a breakthrough study by Gronke *et al.* showed that IL-22 produced by ILC3s and γδ T cells was required to initiate DNA damage response (DDR) following DNA damage[241]. Since IBD patients are at increased risk of developing colorectal cancer[242, 243], inhibiting IL-22 would lead to more damage and further impairment in the DDR in IECs. Although speculative, treatment with an anti-OSMR antibody would be the ideal therapeutic option for regulating extra-intestinal manifestations of IBD. Currently, an anti-OSMR treatment known as

Vixarelimab is in the pipeline and shows promising results for treating prurigo nodularis, a chronic skin disease[244]. In addition, a phase two randomized, double-blinded study showed that the anti-OSMR antibody, vixarelimab, was well-tolerated by the participants, and no dose-limiting adverse effects were observed.

Overall, OSM and OSMR are over-expressed in IBD patients. The over-expression of the OSM and OSMR on intestinal stromal cells had been correlated with patients that are resistant to anti-TNF treatment[126, 132]. For the first time we were able to show that during chronic intestinal inflammation, the OSM-OSMR axis is also relevant in intestinal epithelial cells. We showed that IL-22 promoted the OSMR on the IECs, OSM is produced by leukocytes and subsequently binds to its receptor and activated the STAT3 downstream pathways. Consequently, chemokines such as CXCL5 and CXCL9 activate and recruit neutrophils, which strongly contribute to barrier defect and IBD severity (**Figure 26**). Therefore, this Ph.D. thesis further confirmed/ supported that OSM could be a predictive biomarker and OSMR should be considered as a potential therapeutic target for IBD.
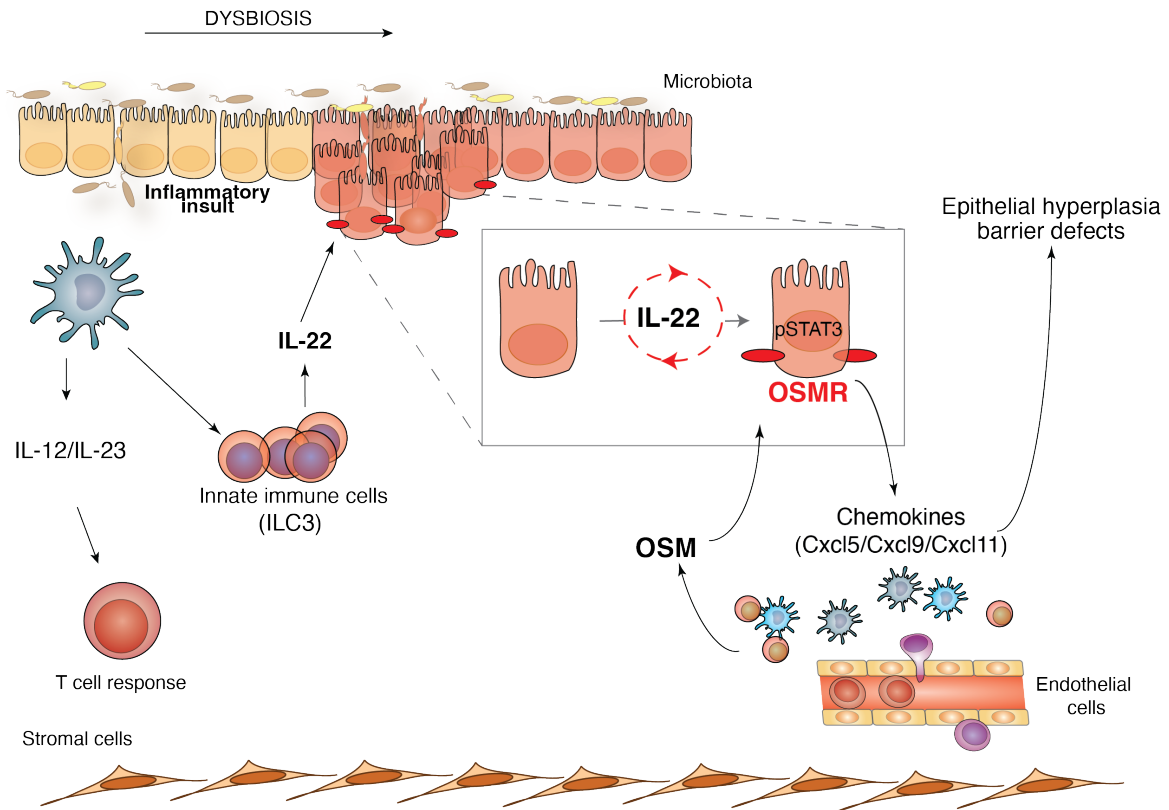
5.7 Graphical summary

Figure 26: Graphical depiction of OSMR expression on intestinal epithelial cells. *Upon inflammatory insults, gut leukocytes are recruited and lead to immune responses. IL-12/IL-23 leads to T-cell responses such as CD4+ T cells, while the innate immune system leads to ILC3 production. ILC3s produce IL-22, subsequently leading to the expression of the OSMR on IECs. IL-22 is important for both the induction and maintenance of the OSMR on the IECs. Next, OSM binds to its receptor and leads to STAT3 phosphorylation. This interaction leads to chemokine production, such as CXCL5, CXCL9, and CXCL11, which then amplifies the inflammatory responses that cause barrier defects, epithelial hyperplasia, and tissue remodeling.*

6 References

1.   Herrin BR, Cooper MD. Alternative adaptive immunity in jawless vertebrates. The Journal of Immunology. 2010;185(3):1367-74.

2.   Pancer Z, Cooper MD. The evolution of adaptive immunity. Annual review of immunology. 2006;24(1):497-518.

3.   Schenten D, Medzhitov R. The control of adaptive immune responses by the innate immune system. Advances in immunology. 2011;109:87-124.

4.   Denning TL, Bhatia AM, Kane AF, Patel RM, Denning PW. Pathogenesis of NEC: Role of the innate and adaptive immune response. Seminars in Perinatology. 2017;41(1):15-28.

5.   Parkin J, Cohen B. An overview of the immune system. The Lancet. 2001;357(9270):1777-89.

6.   Delves PJ, Roitt IM. The immune system. New England journal of medicine. 2000;343(1):37-49.

7.   Lea RG, Riley SC, Antipatis C, Hannah L, Ashworth CJ, Clark DA, Critchley HO. Cytokines and the regulation of apoptosis in reproductive tissues: a review. American Journal of Reproductive Immunology. 1999;42(2):100-9.

8.   Neurath MF. Cytokines in inflammatory bowel disease. Nature Reviews Immunology. 2014;14(5):329-42.

9.   Shao Y, Cheng Z, Li X, Chernaya V, Wang H, Yang X-F. Immunosuppressive/anti-inflammatory cytokines directly and indirectly inhibit endothelial dysfunction- a novel mechanism for maintaining vascular function. Journal of Hematology & Oncology. 2014;7(1).

10.   Turner MD, Nedjai B, Hurst T, Pennington DJ. Cytokines and chemokines: At the crossroads of cell signalling and inflammatory disease. Biochimica et Biophysica Acta (BBA)-Molecular Cell Research. 2014;1843(11):2563-82.

11.   Wojdasiewicz P, Poniatowski ŁA, Szukiewicz D. The role of inflammatory and anti-inflammatory cytokines in the pathogenesis of osteoarthritis. Mediators of inflammation. 2014;2014.

12.   Zhang J-M, An J. Cytokines, Inflammation, and Pain. International Anesthesiology Clinics. 2007;45(2):27-37.

13.   Hooper LV, Macpherson AJ. Immune adaptations that maintain homeostasis with the intestinal microbiota. Nature Reviews Immunology. 2010;10(3):159-69.

14.   Maloy KJ, Powrie F. Intestinal homeostasis and its breakdown in inflammatory bowel disease. Nature. 2011;474(7351):298-306.

15.   Mowat AM, Viney JL. The anatomical basis of intestinal immunity. Immunological reviews. 1997;156(1):145-66.

16.   Round JL, Mazmanian SK. The gut microbiota shapes intestinal immune responses during health and disease. Nature reviews immunology. 2009;9(5):313-23.

17.   Yu LC-H. Host-microbial interactions and regulation of intestinal epithelial barrier function: From physiology to pathology. World Journal of Gastrointestinal Pathophysiology. 2012;3(1):27.

18.   Mowat AM, Agace WW. Regional specialization within the intestinal immune system. Nature Reviews Immunology. 2014;14(10):667-85.

19.   Doherty MM, Charman WN. The mucosa of the small intestine. Clinical pharmacokinetics. 2002;41(4):235-53.

20.   Hall E, Simpson K. Diseases of the small intestine. Textbook of veterinary internal medicine: diseases of the dog and cat, Volumes 1 and 2. 2000(Ed. 5):1182-238.

21.   Azzouz LL, Sharma S. Physiology, large intestine. 2018.

22.   Clench MH, Mathias JR. The avian cecum: a review. The Wilson Bulletin. 1995:93-121.

23.   Smith HF. A review of the function and evolution of the cecal appendix. The Anatomical Record. 2022.

24.   Carrington EV, Scott SM. Physiology and function of the colon. Advanced Nutrition and Dietetics in Gastroenterology. 2014:28-32.

25.   Debongnie J, Phillips S. Capacity of the human colon to absorb fluid. Gastroenterology. 1978;74(4):698-703.

26.   Rescigno M. The intestinal epithelial barrier in the control of homeostasis and immunity. Trends in Immunology. 2011;32(6):256-64.

27.   Buettner M, Lochner M. Development and function of secondary and tertiary lymphoid organs in the small intestine and the colon. Frontiers in immunology. 2016;7:342.

28.   Hamada H, Hiroi T, Nishiyama Y, Takahashi H, Masunaga Y, Hachimura S, Kaminogawa S, Takahashi-Iwanaga H, Iwanaga T, Kiyono H. Identification of multiple isolated lymphoid follicles on the antimesenteric wall of the mouse small intestine. The Journal of Immunology. 2002;168(1):57-64.

29.   Eckburg PB, Bik EM, Bernstein CN, Purdom E, Dethlefsen L, Sargent M, Gill SR, Nelson KE, Relman DA. Diversity of the human intestinal microbial flora. Science. 2005;308(5728):1635-8.

30.   Parfrey LW, Walters WA, Knight R. Microbial eukaryotes in the human microbiome: ecology, evolution, and future directions. Frontiers in microbiology. 2011;2:153.

31.   Gill SR, Pop M, DeBoy RT, Eckburg PB, Turnbaugh PJ, Samuel BS, Gordon JI, Relman DA, Fraser-Liggett CM, Nelson KE. Metagenomic analysis of the human distal gut microbiome. Science. 2006;312(5778):1355-9.

32.   Kau AL, Ahern PP, Griffin NW, Goodman AL, Gordon JI. Human nutrition, the gut microbiome and the immune system. Nature. 2011;474(7351):327-36.

33.   Qin J, Li R, Raes J, Arumugam M, Burgdorf KS, Manichanh C, Nielsen T, Pons N, Levenez F, Yamada T. A human gut microbial gene catalogue established by metagenomic sequencing. Nature. 2010;464(7285):59-65.

34.   Gill N, Finlay BB. The gut microbiota: challenging immunology. Nature Reviews Immunology. 2011;11(10):636-7.

35.   Artis D. Epithelial-cell recognition of commensal bacteria and maintenance of immune homeostasis in the gut. Nature reviews immunology. 2008;8(6):411-20.

36.   Chung H, Pamp SJ, Hill JA, Surana NK, Edelman SM, Troy EB, Reading NC, Villablanca EJ, Wang S, Mora JR. Gut immune maturation depends on colonization with a host-specific microbiota. Cell. 2012;149(7):1578-93.

37.   Niess JH, Leithäuser F, Adler G, Reimann Jr. Commensal gut flora drives the expansion of proinflammatory CD4 T cells in the colonic lamina propria under normal and inflammatory conditions. The Journal of Immunology. 2008;180(1):559-68.

38.   Hansen JJ. Immune responses to intestinal microbes in inflammatory bowel diseases. Current allergy and asthma reports. 2015;15(10):1-8.

39.   Hooper LV, Littman DR, Macpherson AJ. Interactions between the microbiota and the immune system. Science. 2012;336(6086):1268-73.

40.   Podolsky DK. The current future understanding of inflammatory bowel disease. Best practice & research Clinical gastroenterology. 2002;16(6):933-43.

41.   Strober W, Fuss I, Mannon P. The fundamental basis of inflammatory bowel disease. Journal of Clinical Investigation. 2007;117(3):514-21.

42.   Fuss IJ, Heller F, Boirivant M, Leon F, Yoshida M, Fichtner-Feigl S, Yang Z, Exley M, Kitani A, Blumberg RS. Nonclassical CD1d-restricted NK T cells that produce IL-13 characterize an atypical Th2 response in ulcerative colitis. The Journal of clinical investigation. 2004;113(10):1490-7.

43.   Andoh A, Zhang Z, Inatomi O, Fujino S, Deguchi Y, Araki Y, Tsujikawa T, Kitoh K, Kim–Mitsuyama S, Takayanagi A. Interleukin-22, a member of the IL-10 subfamily, induces inflammatory responses in colonic subepithelial myofibroblasts. Gastroenterology. 2005;129(3):969-84.

44.   Baumgart DC, Carding SR. Inflammatory bowel disease: cause and immunobiology. The Lancet. 2007;369(9573):1627-40.

45.   Friedrich M, Pohin M, Powrie F. Cytokine Networks in the Pathophysiology of Inflammatory Bowel Disease. Immunity. 2019;50(4):992-1006.

46.   Lucey DR, Clerici M, Shearer GM. Type 1 and type 2 cytokine dysregulation in human infectious, neoplastic, and inflammatory diseases. Clinical microbiology reviews. 1996;9(4):532-62.

47.   Neurath MF, Travis SP. Mucosal healing in inflammatory bowel diseases: a systematic review. Gut. 2012;61(11):1619-35.

48.   Singh UP, Singh NP, Murphy EA, Price RL, Fayad R, Nagarkatti M, Nagarkatti PS. Chemokine and cytokine levels in inflammatory bowel disease patients. Cytokine. 2016;77:44-9.

49.   Tamboli CP. Dysbiosis in inflammatory bowel disease. Gut. 2004;53(1):1-4.

50.   Uhlig HH, McKenzie BS, Hue S, Thompson C, Joyce-Shaikh B, Stepankova R, Robinson N, Buonocore S, Tlaskalova-Hogenova H, Cua DJ, Powrie F. Differential Activity of IL-12 and IL-23 in Mucosal and Systemic Innate Immune Pathology. Immunity. 2006;25(2):309-18.

51.   Uhlig HH, Powrie F. Translating immunology into therapeutic concepts for inflammatory bowel disease. Annual review of immunology. 2018;36:755-81.

52.   Xavier RJ, Podolsky DK. Unravelling the pathogenesis of inflammatory bowel disease. Nature. 2007;448(7152):427-34.

53.   Bruewer M, Luegering A, Kucharzik T, Parkos CA, Madara JL, Hopkins AM, Nusrat A. Proinflammatory cytokines disrupt epithelial barrier function by apoptosis-independent mechanisms. The Journal of Immunology. 2003;171(11):6164-72.

54. Okamoto R, Watanabe M. Role of epithelial cells in the pathogenesis and treatment of inflammatory bowel disease. Journal of Gastroenterology. 2016;51(1):11-21.

55. Okamoto R, Watanabe M. Cellular and Molecular Mechanisms of the Epithelial Repair in IBD. Digestive Diseases and Sciences. 2005;50(S1):S34-S8.

56. Parikh K, Antanaviciute A, Fawkner-Corbett D, Jagielowicz M, Aulicino A, Lagerholm C, Davis S, Kinchen J, Chen HH, Alham NK. Colonic epithelial cell diversity in health and inflammatory bowel disease. Nature. 2019;567(7746):49-55.

57. Peterson LW, Artis D. Intestinal epithelial cells: regulators of barrier function and immune homeostasis. Nature Reviews Immunology. 2014;14(3):141-53.

58. Corridoni D, Chapman T, Antanaviciute A, Satsangi J, Simmons A. Inflammatory Bowel Disease Through the Lens of Single-cell RNA-seq Technologies. Inflammatory Bowel Diseases. 2020;26(11):1658-68.

59. Tang F, Barbacioru C, Wang Y, Nordman E, Lee C, Xu N, Wang X, Bodeau J, Tuch BB, Siddiqui A. mRNA-Seq whole-transcriptome analysis of a single cell. Nature methods. 2009;6(5):377-82.

60. Lee JC, Lyons PA, McKinney EF, Sowerby JM, Carr EJ, Bredin F, Rickman HM, Ratlamwala H, Hatton A, Rayner TF. Gene expression profiling of CD8+ T cells predicts prognosis in patients with Crohn disease and ulcerative colitis. The Journal of clinical investigation. 2011;121(10):4170-9.

61. Loftus Jr EV. Clinical epidemiology of inflammatory bowel disease: incidence, prevalence, and environmental influences. Gastroenterology. 2004;126(6):1504-17.

62. Lennard-Jones JE. Classification of Inflammatory Bowel Disease. Scandinavian Journal of Gastroenterology. 1989;24(sup170):2-6.

63. Jewell D. Aetiology and pathogenesis of ulcerative colitis and Crohn's disease. Postgraduate medical journal. 1989;65(768):718.

64. Tysk C, Lindberg E, Järnerot G, Floderus-Myrhed B. Ulcerative colitis and Crohn's disease in an unselected population of monozygotic and dizygotic twins. A study of heritability and the influence of smoking. Gut. 1988;29(7):990-6.

65. Shanahan F. Inflammatory bowel disease: Immunodiagnostics, immunotherapeutics, and ecotherapeutics. Gastroenterology. 2001;120(3):622-35.

66. Anderson CA, Boucher G, Lees CW, Franke A, D'Amato M, Taylor KD, Lee JC, Goyette P, Imielinski M, Latiano A. Meta-analysis identifies 29 additional ulcerative colitis risk loci, increasing the number of confirmed associations to 47. Nature genetics. 2011;43(3):246-52.

67.   Cleynen I, Boucher G, Jostins L, Schumm LP, Zeissig S, Ahmad T, Andersen V, Andrews JM, Annese V, Brand S, Brant SR, Cho JH, Daly MJ, Dubinsky M, Duerr RH, Ferguson LR, Franke A, Gearry RB, Goyette P, Hakonarson H, Halfvarson J, Hov JR, Huang H, Kennedy NA, Kupcinskas L, Lawrance IC, Lee JC, Satsangi J, Schreiber S, Théâtre E, Van Der Meulen-De Jong AE, Weersma RK, Wilson DC, Parkes M, Vermeire S, Rioux JD, Mansfield J, Silverberg MS, Radford-Smith G, McGovern DPB, Barrett JC, Lees CW. Inherited determinants of Crohn's disease and ulcerative colitis phenotypes: a genetic association study. The Lancet. 2016;387(10014):156-67.

68.   Data, 5 Donnelly Peter 5 15 AGSCCcswoaubBJCBCDDFCSA, 5 PCMCGBJMBMACAMMISCC, 33 UBSCAAPSJSJOWH, 36 BCCMWLRSMSDP. Genome-wide association study of ulcerative colitis identifies three new susceptibility loci, including the HNF4A region. Nature genetics. 2009;41(12):1330-4.

69.   Lees C, Barrett J, Parkes M, Satsangi J. New IBD genetics: common pathways with other diseases. Gut. 2011;60(12):1739-53.

70.   Thompson AI, Lees CW. Genetics of ulcerative colitis. Inflammatory bowel diseases. 2011;17(3):831-48.

71.   Allgayer H, Kruis W. Aminosalicylates: potential antineoplastic actions in colon cancer prevention. Scandinavian journal of gastroenterology. 2002;37(2):125-31.

72.   Baumgart DC, Sandborn WJ. Inflammatory bowel disease: clinical aspects and established and evolving therapies. The Lancet. 2007;369(9573):1641-57.

73.   Greenfield S, Punchard N, Teare J, Thompson R. The mode of action of the aminosalicylates in inflammatory bowel disease. Alimentary pharmacology & therapeutics. 1993;7(4):369-83.

74.   Ardizzone S, Cassinotti A, Duca P, Mazzali C, Penati C, Manes G, Marmo R, Massari A, Molteni P, Maconi G. Mucosal healing predicts late outcomes after the first course of corticosteroids for newly diagnosed ulcerative colitis. Clinical Gastroenterology and Hepatology. 2011;9(6):483-9. e3.

75.   Ramamoorthy S, Cidlowski JA. Corticosteroids: mechanisms of action in health and disease. Rheumatic Disease Clinics. 2016;42(1):15-31.

76.   Waljee AK, Wiitala WL, Govani S, Stidham R, Saini S, Hou J, Feagins LA, Khan N, Good CB, Vijan S. Corticosteroid use and complications in a US inflammatory bowel disease cohort. PLoS One. 2016;11(6):e0158017.

77.   Pithadia AB, Jain S. Treatment of inflammatory bowel disease (IBD). Pharmacological Reports. 2011;63(3):629-42.

78.   Van Dullemen HM, van Deventer SJ, Hommes DW, Bijl HA, Jansen J, Tytgat GN, Woody J. Treatment of Crohn's disease with anti-tumor necrosis factor chimeric monoclonal antibody (cA2). Gastroenterology. 1995;109(1):129-35.

79.   Marchiando AM, Shen L, Graham WV, Edelblum KL, Duckworth CA, Guan Y, Montrose MH, Turner JR, Watson AJ. The epithelial barrier is maintained by in vivo tight junction expansion during pathologic intestinal epithelial shedding. Gastroenterology. 2011;140(4):1208-18. e2.

80.   Parikh K, Antanaviciute A, Fawkner-Corbett D, Jagielowicz M, Aulicino A, Lagerholm C, Davis S, Kinchen J, Chen HH, Alham NK, Ashley N, Johnson E, Hublitz P, Bao L, Lukomska J, Andev RS, Björklund E, Kessler BM, Fischer R, Goldin R, Koohy H, Simmons A. Colonic epithelial cell diversity in health and inflammatory bowel disease. Nature. 2019;567(7746):49-55.

81.   Blumberg RS, Saubermann LJ, Strober W. Animal models of mucosal inflammation and their relation to human inflammatory bowel disease. Current opinion in immunology. 1999;11(6):648-56.

82.   Wirtz S, Neurath MF. Mouse models of inflammatory bowel disease. Advanced drug delivery reviews. 2007;59(11):1073-83.

83.   Fox JG, Ge Z, Whary MT, Erdman SE, Horwitz BH. Helicobacter hepaticus infection in mice: models for understanding lower bowel inflammation and cancer. Mucosal Immunology. 2011;4(1):22-30.

84.   Goyal N, Rana A, Ahlawat A, Bijjem KRV, Kumar P. Animal models of inflammatory bowel disease: a review. Inflammopharmacology. 2014;22(4):219-33.

85.   Chin EY, Dangler CA, Fox JG, Schauer DB. Helicobacter hepaticus Infection Triggers Inflammatory Bowel Disease in T Cell Receptor α   Mutant Mice. Comparative medicine. 2000;50(6):586-94.

86.   Erdman SE, Poutahidis T, Rogers AB, Tomszaki M, Horwitz B, Fox JG. Susceptibility of three strains of Rag2-deficient mice to Helicobacter hepaticus induced colitis and colorectal cancer. Gastroenterology. 2003;4(124):A340.

87.   Kullberg MC, Jankovic D, Feng CG, Hue S, Gorelick PL, McKenzie BS, Cua DJ, Powrie F, Cheever AW, Maloy KJ. IL-23 plays a key role in Helicobacter hepaticus–induced T cell–dependent colitis. The Journal of experimental medicine. 2006;203(11):2485-94.

88.   Young VB, Knox KA, Pratt JS, Cortez JS, Mansfield LS, Rogers AB, Fox JG, Schauer DB. In vitro and in vivo characterization of Helicobacter hepaticus cytolethal distending toxin mutants. Infection and immunity. 2004;72(5):2521-7.

89.   Fox J, Dewhirst F, Tully J, Paster B, Yan L, Taylor N, Collins Jr M, Gorelick P, Ward J. Helicobacter hepaticus sp. nov., a microaerophilic bacterium isolated from livers and intestinal mucosal scrapings from mice. Journal of clinical microbiology. 1994;32(5):1238-45.

90.   Ward JM, Fox JG, Anver MR, Haines DC, George CV, Collins Jr MJ, Gorelick PL, Nagashima K, Gonda MA, Gilden RV. Chronic active hepatitis and associated liver tumors in mice caused by a presistent bacterial infection with a novel Helicobacter species. JNCI: Journal of the National Cancer Institute. 1994;86(16):1222-7.

91.   Burich A, Hershberg R, Waggie K, Zeng W, Brabb T, Westrich G, Viney JL, Maggio-Price L. Helicobacter-induced inflammatory bowel disease in IL-10-and T cell-deficient mice. American Journal of Physiology-Gastrointestinal and Liver Physiology. 2001;281(3):G764-G78.

92.   Keubler LM, Buettner M, Häger C, Bleich A. A Multihit Model: Colitis Lessons from the Interleukin-10-deficient Mouse. Inflamm Bowel Dis. 2015;21(8):1967-75.

93.   Peloquin JM, Nguyen DD. The microbiota and inflammatory bowel disease: insights from animal models. Anaerobe. 2013;24:102-6.

94.   Hue S, Ahern P, Buonocore S, Kullberg MC, Cua DJ, McKenzie BS, Powrie F, Maloy KJ. Interleukin-23 drives innate and T cell–mediated intestinal inflammation. The Journal of experimental medicine. 2006;203(11):2473-83.

95.   Scharl M, Paul G, Weber A, Jung BC, Docherty MJ, Hausmann M, Rogler G, Barrett KE, McCole DF. Protection of Epithelial Barrier Function by the Crohn's Disease Associated Gene Protein Tyrosine Phosphatase N2. Gastroenterology. 2009;137(6):2030-40.e5.

96.   Johansson ME, Larsson JMH, Hansson GC. The two mucus layers of colon are organized by the MUC2 mucin, whereas the outer layer is a legislator of host–microbial interactions. Proceedings of the national academy of sciences. 2011;108(supplement_1):4659-65.

97.   Linden SK, Sutton P, Karlsson NG, Korolik V, McGuckin MA. Mucins in the mucosal barrier to infection. Mucosal Immunology. 2008;1(3):183-97.

98.   Pelaseyed T, Bergström JH, Gustafsson JK, Ermund A, Birchenough GM, Schütte A, van der Post S, Svensson F, Rodríguez-Piñeiro AM, Nyström EE. The mucus and mucins of the goblet cells and enterocytes provide the first defense line of the gastrointestinal tract and interact with the immune system. Immunological reviews. 2014;260(1):8-20.

99.   Koch S, Nusrat A. Dynamic regulation of epithelial cell fate and barrier function by intercellular junctions. Annals of the New York Academy of Sciences. 2009;1165(1):220-7.

100. Pelaseyed T, Bergström JH, Gustafsson JK, Ermund A, Birchenough GMH, Schütte A, Van Der Post S, Svensson F, Rodríguez-Piñeiro AM, Nyström EEL, Wising C, Johansson MEV, Hansson GC. The mucus and mucins of the goblet cells and enterocytes provide the first defense line of the gastrointestinal tract and interact with the immune system. Immunological Reviews. 2014;260(1):8-20.

101. Van der Sluis M, De Koning BA, De Bruijn AC, Velcich A, Meijerink JP, Van Goudoever JB, Büller HA, Dekker J, Van Seuningen I, Renes IB. Muc2-deficient mice spontaneously develop colitis, indicating that MUC2 is critical for colonic protection. Gastroenterology. 2006;131(1):117-29.

102. Velcich A, Yang W, Heyer J, Fragale A, Nicholas C, Viani S, Kucherlapati R, Lipkin M, Yang K, Augenlicht L. Colorectal cancer in mice genetically deficient in the mucin Muc2. Science. 2002;295(5560):1726-9.

103. Slifer ZM, Blikslager AT. The integral role of tight junction proteins in the repair of injured intestinal epithelium. International Journal of Molecular Sciences. 2020;21(3):972.

104. Gumbiner B, Lowenkopf T, Apatira D. Identification of a 160-kDa polypeptide that binds to the tight junction protein ZO-1. Proceedings of the National Academy of Sciences. 1991;88(8):3460-4.

105. Stevenson BR, Siliciano JD, Mooseker MS, Goodenough DA. Identification of ZO-1: a high molecular weight polypeptide associated with the tight junction (zonula occludens) in a variety of epithelia. The Journal of cell biology. 1986;103(3):755-66.

106. Okamoto R, Watanabe M. Molecular and clinical basis for the regeneration of human gastrointestinal epithelia. Journal of Gastroenterology. 2004;39(1):1-6.

107. McKaig BC, Makh SS, Hawkey CJ, Podolsky DK, Mahida YR. Normal human colonic subepithelial myofibroblasts enhance epithelial migration (restitution) via TGF-β3. American Journal of Physiology-Gastrointestinal and Liver Physiology. 1999;276(5):G1087-G93.

108. Sasaki H, Hirai K, Yamamoto H, Tanooka H, Sakamoto H, Iwamoto T, Takahashi T, Terada M, Ochiya T. HST-1/FGF-4 plays a critical role in crypt cell survival and facilitates epithelial cell restitution and proliferation. Oncogene. 2004;23(20):3681-8.

109. Zbar AP, Simopoulos C, Karayiannakis AJ. Cadherins: an integral role in inflammatory bowel disease and mucosal restitution. Journal of gastroenterology. 2004;39(5):413-21.

110. Rahmani S, Breyner NM, Su H-M, Verdu EF, Didar TF. Intestinal organoids: a new paradigm for engineering intestinal epithelium in vitro. Biomaterials. 2019;194:195-214.

111.   Sato T, Vries RG, Snippert HJ, Van De Wetering M, Barker N, Stange DE, Van Es JH, Abo A, Kujala P, Peters PJ. Single Lgr5 stem cells build crypt-villus structures in vitro without a mesenchymal niche. Nature. 2009;459(7244):262-5.

112.   Mahe MM, Aihara E, Schumacher MA, Zavros Y, Montrose MH, Helmrath MA, Sato T, Shroyer NF. Establishment of gastrointestinal epithelial organoids. Current protocols in mouse biology. 2013;3(4):217-40.

113.   Wallach TE, Bayrer JR. Intestinal Organoids: New Frontiers in the Study of Intestinal Disease and Physiology. Journal of Pediatric Gastroenterology & Nutrition. 2017;64(2):180-5.

114.   Puschhof J, Pleguezuelos-Manzano C, Martinez-Silgado A, Akkerman N, Saftien A, Boot C, De Waal A, Beumer J, Dutta D, Heo I, Clevers H. Intestinal organoid cocultures with microbes. Nature Protocols. 2021;16(10):4633-49.

115.   Wynn TA. Type 2 cytokines: mechanisms and therapeutic strategies. Nature Reviews Immunology. 2015;15(5):271-82.

116.   Sanchez-Muñoz F, Dominguez-Lopez A, Yamamoto-Furusho JK. Role of cytokines in inflammatory bowel disease. World Journal of Gastroenterology. 2008;14(27):4280.

117.   Cavaillon J-M. Pro-versus anti-inflammatory cytokines: myth or reality. CELLULAR AND MOLECULAR BIOLOGY-PARIS-WEGMANN-. 2001;47(4):695-702.

118.   Dinarello CA. Historical insights into cytokines. European Journal of Immunology. 2007;37(S1):S34-S45.

119.   McLeod JJ, Baker B, Ryan JJ. Mast cell production and response to IL-4 and IL-13. Cytokine. 2015;75(1):57-61.

120.   Marie C, Pitton C, Fitting C, Cavaillon J. Regulation by anti-inflammatory cytokines (IL-4, IL-10, IL-13, TGFβ) of interleukin-8 production by LPS-and/or TNFα-activated human polymorphonuclear cells. Mediators of inflammation. 1996;5(5):334-40.

121.   Francescone R, Hou V, Grivennikov SI. Cytokines, IBD, and Colitis-associated Cancer. Inflammatory Bowel Diseases. 2015;21(2):409-18.

122.   Cicchese JM, Evans S, Hult C, Joslyn LR, Wessler T, Millar JA, Marino S, Cilfone NA, Mattila JT, Linderman JJ, Kirschner DE. Dynamic balance of pro- and anti-inflammatory signals controls disease and limits pathology. Immunological Reviews. 2018;285(1):147-67.

123.   Richards CD. The enigmatic cytokine oncostatin m and roles in disease. International Scholarly Research Notices. 2013;2013.

124. Zarling JM, Shoyab M, Marquardt H, Hanson MB, Lioubin MN, Todaro GJ. Oncostatin M: a growth regulator produced by differentiated histiocytic lymphoma cells. Proceedings of the National Academy of Sciences. 1986;83(24):9739-43.

125. Hermanns HM. Oncostatin M and interleukin-31: cytokines, receptors, signal transduction and physiology. Cytokine & growth factor reviews. 2015;26(5):545-58.

126. West NR, Owens BM, Hegazy AN. The oncostatin M-stromal cell axis in health and disease. Scandinavian Journal of Immunology. 2018;88(3):e12694.

127. Stawski L, Trojanowska M. Oncostatin M and its role in fibrosis. Connective tissue research. 2019;60(1):40-9.

128. Jatiani SS, Baker SJ, Silverman LR, Reddy EP. Jak/STAT pathways in cytokine signaling and myeloproliferative disorders: approaches for targeted therapies. Genes & cancer. 2010;1(10):979-93.

129. Gearing DP, Comeau MR, Friend DJ, Gimpel SD, Thut CJ, McGourty J, Brasher KK, King JA, Gillis S, Mosley B. The IL-6 Signal Transducer, gp130: an Pncostatin M Receptor and Affinity Converter for the LIF Receptor. Science. 1992;255(5050):1434-7.

130. Liu J, Modrell B, Aruffo A, Scharnowske S, Shoyab M. Interactions between oncostatin M and the IL-6 signal transducer, gp130. Cytokine. 1994;6(3):272-8.

131. Mosley B, De Imus C, Friend D, Boiani N, Thoma B, Park LS, Cosman D. Dual oncostatin M (OSM) receptors: cloning and characterization of an alternative signaling subunit conferring OSM-specific receptor activation. Journal of Biological Chemistry. 1996;271(51):32635-43.

132. West NR, Hegazy AN, Owens BM, Bullers SJ, Linggi B, Buonocore S, Coccia M, Görtz D, This S, Stockenhuber K. Oncostatin M drives intestinal inflammation and predicts response to tumor necrosis factor–neutralizing therapy in patients with inflammatory bowel disease. Nature medicine. 2017;23(5):579-89.

133. Beigel F, Friedrich M, Probst C, Sotlar K, Göke B, Diegelmann J, Brand S. Oncostatin M mediates STAT3-dependent intestinal epithelial restitution via increased cell proliferation, decreased apoptosis and upregulation of SERPIN family members. PLoS One. 2014;9(4):e93498.

134. Ouyang W, O'Garra A. IL-10 family cytokines IL-10 and IL-22: from basic science to clinical translation. Immunity. 2019;50(4):871-91.

135. Nikoopour E, Bellemore SM, Singh B. IL-22, cell regeneration and autoimmunity. Cytokine. 2015;74(1):35-42.

136. Pestka S, Krause CD, Sarkar D, Walter MR, Shi Y, Fisher PB. Interleukin-10 and related cytokines and receptors. Annual review of immunology. 2004;22(1):929-79.

137.   Sanjabi S, Zenewicz LA, Kamanaka M, Flavell RA. Anti-inflammatory and pro-inflammatory roles of TGF-β, IL-10, and IL-22 in immunity and autoimmunity. Current Opinion in Pharmacology. 2009;9(4):447-53.

138.   Zenewicz LA, Flavell RA. Recent advances in IL-22 biology. International immunology. 2011;23(3):159-63.

139.   Keir ME, Yi T, Lu TT, Ghilardi N. The role of IL-22 in intestinal health and disease. Journal of Experimental Medicine. 2020;217(3).

140.   Li L-J. Role of interleukin-22 in inflammatory bowel disease. World Journal of Gastroenterology. 2014;20(48):18177.

141.   Mizoguchi A, Yano A, Himuro H, Ezaki Y, Sadanaga T, Mizoguchi E. Clinical importance of IL-22 cascade in IBD. Journal of gastroenterology. 2018;53(4):465-74.

142.   Seiderer J, Brand S. IL-22: a two-headed cytokine in IBD? Inflammatory bowel diseases. 2009;15(3):473-4.

143.   Sonnenberg GF, Fouser LA, Artis D. Border patrol: regulation of immunity, inflammation and tissue homeostasis at barrier surfaces by IL-22. Nature immunology. 2011;12(5):383-90.

144.   Xie M-H, Aggarwal S, Ho W-H, Foster J, Zhang Z, Stinson J, Wood WI, Goddard AD, Gurney AL. Interleukin (IL)-22, a novel human cytokine that signals through the interferon receptor-related proteins CRF2–4 and IL-22R. Journal of Biological Chemistry. 2000;275(40):31335-9.

145.   Hughes T, Becknell B, Freud AG, McClory S, Briercheck E, Yu J, Mao C, Giovenzana C, Nuovo G, Wei L. Interleukin-1β selectively expands and sustains interleukin-22+ immature human natural killer cells in secondary lymphoid tissue. Immunity. 2010;32(6):803-14.

146.   Rutz S, Noubade R, Eidenschenk C, Ota N, Zeng W, Zheng Y, Hackney J, Ding J, Singh H, Ouyang W. Transcription factor c-Maf mediates the TGF-β-dependent suppression of IL-22 production in TH17 cells. Nature immunology. 2011;12(12):1238-45.

147.   Lejeune D, Dumoutier L, Constantinescu S, Kruijer W, Schuringa JJ, Renauld J-C. Interleukin-22 (IL-22) activates the JAK/STAT, ERK, JNK, and p38 MAP kinase pathways in a rat hepatoma cell line: pathways that are shared with and distinct from IL-10. Journal of Biological Chemistry. 2002;277(37):33676-82.

148.   Sonnenberg GF, Fouser LA, Artis D. Functional biology of the IL-22-IL-22R pathway in regulating immunity and inflammation at barrier surfaces. Advances in immunology. 2010;107:1-29.

149. Rutz S, Eidenschenk C, Ouyang W. IL-22, not simply a Th17 cytokine. Immunological reviews. 2013;252(1):116-32.

150. Parks OB, Pociask DA, Hodzic Z, Kolls JK, Good M. Interleukin-22 signaling in the regulation of intestinal health and disease. Frontiers in cell and developmental biology. 2016;3:85.

151. Bellemore SM. The role of IL-22 produced by Th17 cells in Type 1 Diabetes. 2013.

152. Zenewicz LA. IL-22 binding protein (IL-22BP) in the regulation of IL-22 biology. Frontiers in Immunology. 2021;12:766586.

153. Mizoguchi A. Healing of intestinal inflammation by IL-22. Inflammatory bowel diseases. 2012;18(9):1777-84.

154. Sekikawa A, Fukui H, Suzuki K, Karibe T, Fujii S, Ichikawa K, Tomita S, Imura J, Shiratori K, Chiba T. Involvement of the IL-22/REG Iα axis in ulcerative colitis. Laboratory Investigation. 2010;90(3):496-505.

155. Zenewicz LA, Flavell RA. IL-22 and inflammation: Leukin' through a glass onion. European Journal of Immunology. 2008;38(12):3265-8.

156. Xuan X, Zhang L, Tian C, Wu T, Ye H, Cao J, Chen F, Liang Y, Yang H, Huang C. Interleukin-22 and connective tissue diseases: emerging role in pathogenesis and therapy. Cell & Bioscience. 2021;11(1):1-11.

157. Zenewicz LA, Yancopoulos GD, Valenzuela DM, Murphy AJ, Karow M, Flavell RA. Interleukin-22 but not interleukin-17 provides protection to hepatocytes during acute liver inflammation. Immunity. 2007;27(4):647-59.

158. Ma H-L, Liang S, Li J, Napierata L, Brown T, Benoit S, Senices M, Gill D, Dunussi-Joannopoulos K, Collins M. IL-22 is required for Th17 cell–mediated pathology in a mouse model of psoriasis-like skin inflammation. The Journal of clinical investigation. 2008;118(2):597-607.

159. Atuma C. Strugala V, Allen A, Holm L. The adherent gastrointestinal mucus gel layer: thickness and physical state in vivo Am J Physiol Gastrointest Liver Physiol. 2001;280:G922-G9.

160. Brand S, Beigel F, Olszak T, Zitzmann K, Eichhorst SrT, Otte J-M, Diepolder H, Marquardt A, Jagla W, Popp A. IL-22 is increased in active Crohn's disease and promotes proinflammatory gene expression and intestinal epithelial cell migration. American Journal of Physiology-Gastrointestinal and Liver Physiology. 2006;290(4):G827-G38.

161.	Powrie F, Leach MW, Mauze S, Menon S, Caddle LB, Coffman RL. Inhibition of Thl responses prevents inflammatory bowel disease in scid mice reconstituted with CD45RBhi CD4+ T cells. Immunity. 1994;1(7):553-62.

162.	Zenewicz LA, Yancopoulos GD, Valenzuela DM, Murphy AJ, Stevens S, Flavell RA. Innate and Adaptive Interleukin-22 Protects Mice from Inflammatory Bowel Disease. Immunity. 2008;29(6):947-57.

163.	Eken A, Singh AK, Treuting PM, Oukka M. IL-23R+ innate lymphoid cells induce colitis via interleukin-22-dependent mechanism. Mucosal Immunology. 2014;7(1):143-54.

164.	Jiang R, Sun B. IL-22 signaling in the tumor microenvironment. Tumor Microenvironment: Springer; 2021. p. 81-8.

165.	Morrison PJ, Ballantyne SJ, Macdonald SJ, Moore JW, Jenkins D, Wright JF, Fouser LA, Kullberg MC. Differential Requirements for IL-17A and IL-22 in Cecal versus Colonic Inflammation Induced by Helicobacter hepaticus. Am J Pathol. 2015;185(12):3290-303.

166.	Madisen L, Zwingman TA, Sunkin SM, Oh SW, Zariwala HA, Gu H, Ng LL, Palmiter RD, Hawrylycz MJ, Jones AR. A robust and high-throughput Cre reporting and characterization system for the whole mouse brain. Nature neuroscience. 2010;13(1):133-40.

167.	El Marjou F, Janssen KP, Hung-Junn Chang B, Li M, Hindie V, Chan L, Louvard D, Chambon P, Metzger D, Robine S. Tissue-specific and inducible Cre-mediated recombination in the gut epithelium. genesis. 2004;39(3):186-93.

168.	Zheng B, Zhang Z, Black CM, de Crombrugghe B, Denton CP. Ligand-dependent genetic recombination in fibroblasts: a potentially powerful technique for investigating gene function in fibrosis. The American journal of pathology. 2002;160(5):1609-17.

169.	Chen M. Yokomizo t, Zeigler BM et al. Runx1 is required for the endothelial to haematopoietic cell transition but not thereafter nature. 2009;457(7231):887Y91.

170.	Shinkai Y, Lam K-P, Oltz EM, Stewart V, Mendelsohn M, Charron J, Datta M, Young F, Stall AM, Alt FW. RAG-2-deficient mice lack mature lymphocytes owing to inability to initiate V (D) J rearrangement. Cell. 1992;68(5):855-67.

171.	Choi GB, Yim YS, Wong H, Kim S, Kim H, Kim SV, Hoeffer CA, Littman DR, Huh JR. The maternal interleukin-17a pathway in mice promotes autism-like phenotypes in offspring. Science. 2016;351(6276):933-9.

172.	Eberl G, Marmon S, Sunshine M-J, Rennert PD, Choi Y, Littman DR. An essential function for the nuclear receptor RORγt in the generation of fetal lymphoid tissue inducer cells. Nature immunology. 2004;5(1):64-73.

173.   Madison BB, Dunbar L, Qiao XT, Braunstein K, Braunstein E, Gumucio DL. Cis elements of the villin gene control expression in restricted domains of the vertical (crypt) and horizontal (duodenum, cecum) axes of the intestine. Journal of Biological Chemistry. 2002;277(36):33275-83.

174.   Moh A, Iwamoto Y, Chai G-X, Zhang SS-m, Kano A, Yang DD, Zhang W, Wang J, Jacoby JJ, Gao B. Role of STAT3 in liver regeneration: survival, DNA synthesis, inflammatory reaction and liver mass recovery. Laboratory investigation. 2007;87(10):1018-28.

175.   Durbin JE, Hackenmiller R, Simon MC, Levy DE. Targeted disruption of the mouse Stat1 gene results in compromised innate immunity to viral disease. Cell. 1996;84(3):443-50.

176.   Zheng M, Horne W, McAleer JP, Pociask D, Eddens T, Good M, Gao B, Kolls JK. Therapeutic role of interleukin 22 in experimental intra-abdominal Klebsiella pneumoniae infection in mice. Infection and immunity. 2016;84(3):782-9.

177.   Zheng Y, Danilenko DM, Valdez P, Kasman I, Eastham-Anderson J, Wu J, Ouyang W. Interleukin-22, a TH17 cytokine, mediates IL-23-induced dermal inflammation and acanthosis. Nature. 2007;445(7128):648-51.

178.   Sohal DS, Nghiem M, Crackower MA, Witt SA, Kimball TR, Tymitz KM, Penninger JM, Molkentin JD. Temporally regulated and tissue-specific gene manipulations in the adult and embryonic heart using a tamoxifen-inducible Cre protein. Circulation research. 2001;89(1):20-5.

179.   Izcue A, Hue S, Buonocore S, Arancibia-Cárcamo CV, Ahern PP, Iwakura Y, Maloy KJ, Powrie F. Interleukin-23 restrains regulatory T cell activity to drive T cell-dependent colitis. Immunity. 2008;28(4):559-70.

180.   Sato T, Stange DE, Ferrante M, Vries RG, Van Es JH, Van Den Brink S, Van Houdt WJ, Pronk A, Van Gorp J, Siersema PD. Long-term expansion of epithelial organoids from human colon, adenoma, adenocarcinoma, and Barrett's epithelium. Gastroenterology. 2011;141(5):1762-72.

181.   Picelli S, Björklund ÅK, Faridani OR, Sagasser S, Winberg G, Sandberg R. Smart-seq2 for sensitive full-length transcriptome profiling in single cells. Nature methods. 2013;10(11):1096-8.

182.   Picelli S, Faridani OR, Björklund ÅK, Winberg G, Sagasser S, Sandberg R. Full-length RNA-seq from single cells using Smart-seq2. Nature protocols. 2014;9(1):171-81.

183.   Venereau E, Diveu C, Grimaud L, Ravon E, Froger J, Preisser L, Danger Y, Maillasson M, Garrigue-Antar L, Jacques Y, Chevalier S, Gascan H. Definition and characterization of an inhibitor for interleukin-31. J Biol Chem. 2010;285(20):14955-63.

184.   Wang F, Flanagan J, Su N, Wang L-C, Bui S, Nielson A, Wu X, Vo H-T, Ma X-J, Luo Y. RNAscope: a novel in situ RNA analysis platform for formalin-fixed, paraffin-embedded tissues. The Journal of molecular diagnostics. 2012;14(1):22-9.

185.   Fournier B, Parkos C. The role of neutrophils during intestinal inflammation. Mucosal immunology. 2012;5(4):354-66.

186.   Geremia A, Biancheri P, Allan P, Corazza GR, Di Sabatino A. Innate and adaptive immunity in inflammatory bowel disease. Autoimmunity reviews. 2014;13(1):3-10.

187.   Regner EH, Ohri N, Stahly A, Gerich ME, Fennimore BP, Ir D, Jubair WK, Görg C, Siebert J, Robertson CE. Functional intraepithelial lymphocyte changes in inflammatory bowel disease and spondyloarthritis have disease specific correlations with intestinal microbiota. Arthritis Research & Therapy. 2018;20:1-13.

188.   Strober W, Fuss I, Mannon P. The fundamental basis of inflammatory bowel disease. The Journal of clinical investigation. 2007;117(3):514-21.

189.   Pickert G, Neufert C, Leppkes M, Zheng Y, Wittkopf N, Warntjen M, Lehr H-A, Hirth S, Weigmann B, Wirtz S. STAT3 links IL-22 signaling in intestinal epithelial cells to mucosal wound healing. Journal of Experimental Medicine. 2009;206(7):1465-72.

190.   Sugimoto K, Ogawa A, Mizoguchi E, Shimomura Y, Andoh A, Bhan AK, Blumberg RS, Xavier RJ, Mizoguchi A. IL-22 ameliorates intestinal inflammation in a mouse model of ulcerative colitis. The Journal of clinical investigation. 2008;118(2):534-44.

191.   Zhu Q, Korenfeld D, Suarez-Fueyo A, Graham S, Jin L, Punit S, Duffy R, Puri M, Caruso A, Hu C. Epithelial dysfunction is prevented by IL-22 treatment in a Citrobacter rodentium-induced colitis model that shares similarities with inflammatory bowel disease. Mucosal Immunology. 2022:1-12.

192.   Zindl CL, Lai J-F, Lee YK, Maynard CL, Harbour SN, Ouyang W, Chaplin DD, Weaver CT. IL-22–producing neutrophils contribute to antimicrobial defense and restitution of colonic epithelial integrity during colitis. Proceedings of the National Academy of Sciences. 2013;110(31):12768-73.

193.   Saxton RA, Henneberg LT, Calafiore M, Su L, Jude KM, Hanash AM, Garcia KC. The tissue protective functions of interleukin-22 can be decoupled from pro-inflammatory actions through structure-based design. Immunity. 2021;54(4):660-72.e9.

194.   Denning TL, Bhatia AM, Kane AF, Patel RM, Denning PW, editors. Pathogenesis of NEC: Role of the innate and adaptive immune response. Seminars in perinatology; 2017: Elsevier.

195.   Medzhitov R, Janeway Jr CA. Innate immunity: impact on the adaptive immune response. Current opinion in immunology. 1997;9(1):4-9.

196. Geremia A, Arancibia-Cárcamo CV, Fleming MP, Rust N, Singh B, Mortensen NJ, Travis SP, Powrie F. IL-23–responsive innate lymphoid cells are increased in inflammatory bowel disease. Journal of Experimental Medicine. 2011;208(6):1127-33.

197. Nagalakshmi ML, Rascle A, Zurawski S, Menon S, de Waal Malefyt R. Interleukin-22 activates STAT3 and induces IL-10 by colon epithelial cells. International immunopharmacology. 2004;4(5):679-91.

198. Sovran B, Loonen LM, Lu P, Hugenholtz F, Belzer C, Stolte EH, Boekschoten MV, van Baarlen P, Kleerebezem M, De Vos P. IL-22-STAT3 pathway plays a key role in the maintenance of ileal homeostasis in mice lacking secreted mucus barrier. Inflammatory bowel diseases. 2015;21(3):531-42.

199. Dignass AU. Mechanisms and modulation of intestinal epithelial repair. Inflammatory bowel diseases. 2001;7(1):68-77.

200. Pothoven KL, Schleimer RP. The barrier hypothesis and Oncostatin M: Restoration of epithelial barrier function as a novel therapeutic strategy for the treatment of type 2 inflammatory disease. Tissue Barriers. 2017;5(3):e1341367.

201. Thoreson R, Cullen JJ. Pathophysiology of inflammatory bowel disease: an overview. Surgical Clinics of North America. 2007;87(3):575-85.

202. Turpin W, Lee S-H, Garay JAR, Madsen KL, Meddings JB, Bedrani L, Power N, Espin-Garcia O, Xu W, Smith MI. Increased intestinal permeability is associated with later development of Crohn's disease. Gastroenterology. 2020;159(6):2092-100. e5.

203. Kuo W-T, Zuo L, Odenwald MA, Madha S, Singh G, Gurniak CB, Abraham C, Turner JR. The Tight Junction Protein ZO-1 Is Dispensable for Barrier Function but Critical for Effective Mucosal Repair. Gastroenterology. 2021;161(6):1924-39.

204. Pavlidis P, Tsakmaki A, Pantazi E, Li K, Cozzetto D, Digby-Bell J, Yang F, Lo JW, Alberts E, Sa ACC. Interleukin-22 regulates neutrophil recruitment in ulcerative colitis and is associated with resistance to ustekinumab therapy. Nature Communications. 2022;13(1):5820.

205. Blumberg RS, Strober W. Prospects for research in inflammatory bowel disease. Jama. 2001;285(5):643-7.

206. Musch E, Andus T, Kruis W, Raedler A, Spehlmann M, Schreiber S, Krakamp B, Malek M, Malchow H, Zavada F. Interferon-β-1a for the treatment of steroid-refractory ulcerative colitis: a randomized, double-blind, placebo-controlled trial. Clinical Gastroenterology and Hepatology. 2005;3(6):581-6.

207. Tilg H, Ulmer H, Kaser A, Weiss G. Role of IL-10 for induction of anemia during inflammation. The Journal of immunology. 2002;169(4):2204-9.

208. Herrlinger KR, Witthoeft T, Raedler A, Bokemeyer B, Krummenerl T, Schulzke J-D, Boerner N, Kueppers B, Emmrich J, Mescheder A. Randomized, double blind controlled trial of subcutaneous recombinant human interleukin-11 versus prednisolone in active Crohn's disease. Official journal of the American College of Gastroenterology| ACG. 2006;101(4):793-7.

209. Birchenough GM, Johansson ME, Gustafsson JK, Bergström JH, Hansson G. New developments in goblet cell mucus secretion and function. Mucosal immunology. 2015;8(4):712-9.

210. Sanos SL, Bui VL, Mortha A, Oberle K, Heners C, Johner C, Diefenbach A. RORγt and commensal microflora are required for the differentiation of mucosal interleukin 22–producing NKp46+ cells. Nature immunology. 2009;10(1):83-91.

211. Satoh-Takayama N, Vosshenrich CA, Lesjean-Pottier S, Sawa S, Lochner M, Rattis F, Mention J-J, Thiam K, Cerf-Bensussan N, Mandelboim O. Microbial flora drives interleukin 22 production in intestinal NKp46+ cells that provide innate mucosal immune defense. Immunity. 2008;29(6):958-70.

212. Kamanaka M, Huber S, Zenewicz LA, Gagliani N, Rathinam C, O'Connor Jr W, Wan YY, Nakae S, Iwakura Y, Hao L. Memory/effector (CD45RBlo) CD4 T cells are controlled directly by IL-10 and cause IL-22–dependent intestinal pathology. Journal of Experimental Medicine. 2011;208(5):1027-40.

213. Cella M, Fuchs A, Vermi W, Facchetti F, Otero K, Lennerz JK, Doherty JM, Mills JC, Colonna M. A human natural killer cell subset provides an innate source of IL-22 for mucosal immunity. Nature. 2009;457(7230):722-5.

214. Crellin NK, Trifari S, Kaplan CD, Cupedo T, Spits H. Human NKp44+ IL-22+ cells and LTi-like cells constitute a stable RORC+ lineage distinct from conventional natural killer cells. Journal of Experimental Medicine. 2010;207(2):281-90.

215. Longman RS, Diehl GE, Victorio DA, Huh JR, Galan C, Miraldi ER, Swaminath A, Bonneau R, Scherl EJ, Littman DR. CX3CR1+ mononuclear phagocytes support colitis-associated innate lymphoid cell production of IL-22. Journal of Experimental Medicine. 2014;211(8):1571-83.

216. Eken A, Singh A, Treuting P, Oukka M. IL-23R+ innate lymphoid cells induce colitis via interleukin-22-dependent mechanism. Mucosal immunology. 2014;7(1):143-54.

217. Zeng B, Shi S, Ashworth G, Dong C, Liu J, Xing F. ILC3 function as a double-edged sword in inflammatory bowel diseases. Cell Death & Disease. 2019;10(4).

218. Christ AD, Stevens AC, Koeppen H, Walsh S, Omata F, Devergne O, Birkenbach M, Blumberg RS. An interleukin 12-related cytokine is up-regulated in ulcerative colitis but not in Crohn's disease. Gastroenterology. 1998;115(2):307-13.

219.	Veldhoen M, Hirota K, Westendorf AM, Buer J, Dumoutier L, Renauld J-C, Stockinger B. The aryl hydrocarbon receptor links TH17-cell-mediated autoimmunity to environmental toxins. Nature. 2008;453(7191):106-9.

220.	Camoglio L, Juffermans NP, Peppelenbosch M, Velde AAt, Kate FJt, Deventer SJv, Kopf M. Contrasting roles of IL-12p40 and IL-12p35 in the development of hapten-induced colitis. European journal of immunology. 2002;32(1):261-9.

221.	Castro-Mejia J, Jakesevic M, Krych Ł, Nielsen DS, Hansen LH, Sondergaard BC, Kvist PH, Hansen AK, Holm TL. Treatment with a monoclonal anti-IL-12p40 antibody induces substantial gut microbiota changes in an experimental colitis model. Gastroenterology Research and Practice. 2016;2016.

222.	Kim D-J, Kim K-S, Song M-Y, Seo S-H, Kim S-J, Yang B-G, Jang M-H, Sung Y-C. Delivery of IL-12p40 ameliorates DSS-induced colitis by suppressing IL-17A expression and inflammation in the intestinal mucosa. Clinical immunology. 2012;144(3):190-9.

223.	Yang XO, Panopoulos AD, Nurieva R, Chang SH, Wang D, Watowich SS, Dong C. STAT3 regulates cytokine-mediated generation of inflammatory helper T cells. Journal of Biological Chemistry. 2007;282(13):9358-63.

224.	Cai M, Chen S, Hu W. MicroRNA-141 is involved in ulcerative colitis pathogenesis via aiming at CXCL5. Journal of Interferon & Cytokine Research. 2017;37(9):415-20.

225.	Koltsova EK, Ley K. The Mysterious Ways of the Chemokine CXCL5. Immunity. 2010;33(1):7-9.

226.	Lin Y, Cheng L, Liu Y, Wang Y, Wang Q, Wang H, Shi G, Li J, Wang Q, Yang Q. Intestinal epithelium-derived BATF3 promotes colitis-associated colon cancer through facilitating CXCL5-mediated neutrophils recruitment. Mucosal Immunology. 2021;14(1):187-98.

227.	Koukos G, Polytarchou C, Kaplan JL, Oikonomopoulos A, Ziring D, Hommes DW, Wahed R, Kokkotou E, Pothoulakis C, Winter HS. A microRNA signature in pediatric ulcerative colitis: deregulation of the miR-4284/CXCL5 pathway in the intestinal epithelium. Inflammatory bowel diseases. 2015;21(5):996-1005.

228.	Muthas D, Reznichenko A, Balendran CA, Böttcher G, Clausen IG, Kärrman Mårdh C, Ottosson T, Uddin M, MacDonald TT, Danese S. Neutrophils in ulcerative colitis: a review of selected biomarkers and their potential therapeutic implications. Scandinavian journal of gastroenterology. 2017;52(2):125-35.

229.	Janas RM, Ochocińska A, Śnitko R, Dudka D, Kierkuś J, Teisseyre M, Najberg E. Neutrophil gelatinase-associated lipocalin in blood in children with inflammatory bowel disease. Journal of Gastroenterology and Hepatology. 2014;29(11):1883-9.

230. Oikonomou K, Kapsoritakis A, Theodoridou C, Karangelis D, Germenis A, Stefanidis I, Potamianos S. Neutrophil gelatinase-associated lipocalin (NGAL) in inflammatory bowel disease: association with pathophysiology of inflammation, established markers, and disease activity. Journal of gastroenterology. 2012;47:519-30.

231. Thorsvik S, Damås JK, Granlund Av, Flo TH, Bergh K, Østvik AE, Sandvik AK. Fecal neutrophil gelatinase-associated lipocalin as a biomarker for inflammatory bowel disease. Journal of gastroenterology and hepatology. 2017;32(1):128-35.

232. Zollner A, Schmiderer A, Reider SJ, Oberhuber G, Pfister A, Texler B, Watschinger C, Koch R, Effenberger M, Raine T. Faecal biomarkers in inflammatory bowel diseases: calprotectin versus lipocalin-2—a comparative study. Journal of Crohn's and Colitis. 2021;15(1):43-54.

233. Ayling RM, Kok K. Fecal calprotectin. Advances in clinical chemistry. 2018;87:161-90.

234. Bjarnason I. The use of fecal calprotectin in inflammatory bowel disease. Gastroenterology & hepatology. 2017;13(1):53.

235. Bunn SK, Bisset WM, Main MJ, Gray ES, Olson S, Golden BE. Fecal calprotectin: validation as a noninvasive measure of bowel inflammation in childhood inflammatory bowel disease. Journal of pediatric gastroenterology and nutrition. 2001;33(1):14-22.

236. Costa F, Mumolo M, Ceccarelli L, Bellini M, Romano M, Sterpi C, Ricchiuti A, Marchi S, Bottai M. Calprotectin is a stronger predictive marker of relapse in ulcerative colitis than in Crohn's disease. Gut. 2005;54(3):364-8.

237. Khaki-Khatibi F, Qujeq D, Kashifard M, Moein S, Maniati M, Vaghari-Tabari M. Calprotectin in inflammatory bowel disease. Clinica chimica acta. 2020;510:556-65.

238. Konikoff MR, Denson LA. Role of fecal calprotectin as a biomarker of intestinal inflammation in inflammatory bowel disease. Inflammatory bowel diseases. 2006;12(6):524-34.

239. Walsham NE, Sherwood RA. Fecal calprotectin in inflammatory bowel disease. Clinical and experimental gastroenterology. 2016:21-9.

240. Denton CP, del Galdo F, Khanna D, Vonk MC, Chung L, Johnson SR, Varga J, Furst DE, Temple J, Zecchin C, Csomor E, Lee A, Wisniacki N, Flint SM, Reid J. Biological and clinical insights from a randomized phase 2 study of an anti-oncostatin M monoclonal antibody in systemic sclerosis. Rheumatology. 2022;62(1):234-42.

241. Gronke K, Hernández PP, Zimmermann J, Klose CSN, Kofoed-Branzk M, Guendel F, Witkowski M, Tizian C, Amann L, Schumacher F, Glatt H, Triantafyllopoulou A, Diefenbach A. Interleukin-22 protects intestinal stem cells against genotoxic stress. Nature. 2019;566(7743):249-53.

242.   Axelrad JE, Lichtiger S, Yajnik V. Inflammatory bowel disease and cancer: The role of inflammation, immunosuppression, and cancer treatment. World J Gastroenterol. 2016;22(20):4794-801.

243.   Ullman TA, Itzkowitz SH. Intestinal inflammation and cancer. Gastroenterology. 2011;140(6):1807-16. e1.

244.   Sofen H, Bissonnette R, Yosipovitch G, Silverberg JI, Tyring S, Loo WJ, Zook M, Lee M, Zou L, Jiang G-L. Efficacy and safety of vixarelimab, a human monoclonal oncostatin M receptor β antibody, in moderate-to-severe prurigo nodularis: a randomised, double-blind, placebo-controlled, phase 2a study. eClinicalMedicine. 2023;57.

7 Appendix

7.1 Statutory Declaration

"I, Roodline, Cineus, by personally signing this document in lieu of an oath, hereby affirm that I prepared the submitted dissertation on the topic "The Oncostatin M receptor expression in epithelial cells promotes intestinal inflammation" "Die Expression des Oncostatin-M-Rezeptors in Epithelzellen fördert die Entzündung des Darms", independently and without the support of third parties, and that I used no other sources and aids than those stated.

All parts which are based on the publications or presentations of other authors, either in letter or in spirit, are specified as such in accordance with the citing guidelines. The sections on methodology (in particular regarding practical work, laboratory regulations, statistical processing) and results (in particular regarding figures, charts and tables) are exclusively my responsibility.

Furthermore, I declare that I have correctly marked all of the data, the analyses, and the conclusions generated from data obtained in collaboration with other persons, and that I have correctly marked my own contribution and the contributions of other persons (cf. declaration of contribution). I have correctly marked all texts or parts of texts that were generated in collaboration with other persons.

My contributions to any publications to this dissertation correspond to those stated in the below joint declaration made together with the supervisor. All publications created within the scope of the dissertation comply with the guidelines of the ICMJE (International Committee of Medical Journal Editors; www.icmje.org) on authorship. In addition, I declare that I shall comply with the regulations of Charité – Universitätsmedizin Berlin on ensuring good scientific practice.

I declare that I have not yet submitted this dissertation in identical or similar form to another Faculty.

The significance of this statutory declaration and the consequences of a false statutory declaration under criminal law (Sections 156, 161 of the German Criminal Code) are known to me."

_____   _____
Date   Signature

7.2 Curriculum vitae

My curriculum vitae does not appear in the electronic version of my paper for the reasons of data protection.

7.3 Publication list of all publications

List of publications during the period of my doctoral thesis

Arash Haghikia, Friederike Zimmermann, Paul Schumann, Andrzej Jasina, Johann Roessler, David Schmidt, Philipp Heinze, Johannes Kaisler, Vanasa Nageswaran, Annette Aigner, Uta Ceglarek, **Roodline Cineus**, Ahmed N Hegazy, Emiel P C van der Vorst, Yvonne Döring, Christopher M Strauch, Ina Nemet, Valentina Tremaroli, Chinmay Dwibedi, Nicolle Kränkel, David M Leistner, Markus M Heimesaat, Stefan Bereswill, Geraldine Rauch, Ute Seeland, Oliver Soehnlein, Dominik N Müller, Ralf Gold, Fredrik Bäckhed, Stanley L Hazen, Aiden Haghikia, Ulf Landmesser, Propionate attenuates atherosclerosis by immune-dependent regulation of intestinal cholesterol metabolism, European Heart Journal, Volume 43, Issue 6, 7 February 2022, Pages 518–533, https://doi.org/10.1093/eurheartj/ehab644

7.4 Acknowledgements

7.5 Certificate of the accredited statistician

CHARITÉ

CharitéCentrum für Human- und Gesundheitswissenschaften

Charité | Campus Charité Mitte | 10117 Berlin

Institut für Biometrie und klinische Epidemiologie

Direktor: Prof. Dr. Frank Konietschke

Postanschrift:
Charitéplatz 1 | 10117 Berlin
Besucher*innenanschrift:
Sauerbruchweg 3 | 10117 Berlin

Tel. +49 (0)30 450 562171
https://biometrie.charite.de

Name, Vorname:
Cineus, Roodline
Emailadresse:
roodline.cineus@charite.de
Matrikelnummer:
147116
Promotionsbetreuer*in:
Prof. Dr. med. Dr. rer. nat. Ahmed Hegazy
Promotionsinstitution:
Klinik für Gastroenterologie, Infektiologie und Rheumatologie

Bescheinigung

Hiermit bescheinige ich, dass *Roodline Cineus* innerhalb der Service Unit Biometrie des Instituts für Biometrie und klinische Epidemiologie (iBikE) bei mir eine statistische Beratung zu einem Promotionsvorhaben in Anspruch genommen hat. Folgende Beratungstermine wurden wahrgenommen:

- 03.02 2023

Folgende wesentliche Ratschläge hinsichtlich einer sinnvollen Auswertung und Interpretation der Daten wurden während der Beratung erteilt:

- Erklärung der verwendeten statistischen Testverfahren verbessern und präzisieren

- Für die Analyse eines Parameter einer Verteilung (wie z.B. des Mittelwerts) sollte das dazu passende statistische Verfahren verwendet werden

- Allgemeine Hinweise für eine konsistente Darstellung der Ergebnisse

Diese Bescheinigung garantiert nicht die richtige Umsetzung der in der Beratung gemachten Vorschläge, die korrekte Durchführung der empfohlenen statistischen Verfahren und die richtige Darstellung und Interpretation der Ergebnisse. Die Verantwortung hierfür obliegt allein dem Promovierenden. Das iBikE übernimmt hierfür keine Haftung.

Datum: 3. Februar 2023

Unterschrift Berater*in